General Disclaimer

One or more of the Following Statements may affect this Document

NASA

Technical Memorandum 83883

Experimental and Theoretical Studies of Interstellar Grains

Joseph A. Nuth

DECEMBER 1981

National Aeronautics and
Space Administration

Goddard Space Flight Center
Greenbelt, Maryland 20771

APPROVAL SHEET

Title of Dissertation: An Experimental and Theoretical Study of
Interstellar Grains

Name of Candidate: Joseph Andrew Nuth III
Doctor of Philosophy, 1982

Dissertation and Abstract Approved: _____

Isidore Adler
Professor of Chemistry
Geochemistry Program
Department of Chemistry

Date Approved : _____

CURRICULUM VITAE

Name: Joseph Andrew Nuth III.

Permanent Address: 4316 Rowalt Drive Apartment # 202

College Park, MD. 20740.

Degree and date to be conferred: Ph.D. , 1982.

Date of birth: ▮▮▮▮▮▮▮▮▮

Place of birth: ▮▮▮▮▮▮▮▮▮▮▮▮,

Secondary education: Loyola High School, Towson, Md. (1971)

Collegiate institutions attended	Dates	Degree/Date	Major
University of Maryland	1971-1975	B.S. 1975	Astronomy.
University of Maryland	1971-1975	B.S. 1975	Chemistry.
University of Maryland	1975-1977	M.S. 1977	Geochemistry.
University of Maryland	1978-1982	Ph..D. 1982	Geochemistry.

Professional Publications:

J.A. Nuth, J.Photoochem., 11, 121 (1979).

J.A. Nuth and B. Donn, Astrophys.J., 247, 925 (1981).

B. Donn, J. Hecht, R. Khanna, J. Nuth, D. Stranz, A.B. Anderson,
Surf.Sci., 106, 546 (1981).

J.A. Nuth and S. Glicker, J.Quant.Spectrosc.Rad.Trans., (accepted).

J. Hecht and J.A. Nuth, Astrophys.J., (submitted).

Professional positions held:

Summer, 1975 Research Assistant Department of Physics and Astronomy.

1975 - 1977 Teaching Assistant Department of Chemistry.

1978 - 1981 Research Assistant Department of Physics and Astronomy.

1981 NASA/NRC Resident Research Associate Laboratory for
Extraterrestrial Physics, Goddard Space Flight Center

Greenbelt, Maryland.

ABSTRACT

Title of Dissertation: Experimental a. j Theoretical Studies of

Interstellar G ains

Joseph Andrew Nuth III

Dissertation directed by: Dr. Isidore Adler, Professor

Geochemistry Program, Chemistry Department

Steady state vibrational populations of SiO and CO in dilute black body radiation fields have been calculated as a function of total pressure, kinetic temperature and chemical composition of the gas. Approximate calculations for polyatomic molecules have also been presented. Vibrational disequilibrium becomes increasingly significant as total pressure and radiation density decrease. Many regions of postulated grain formation are found to be far from thermal equilibrium before the onset of nucleation. Calculations based upon classical nucleation theory or equilibrium thermodynamics are expected to be of dubious value in such regions.

Laboratory measurements of the extinction of small iron and magnetite grains were made from 105nm to 830nm and found to be consistent with predictions based upon published optical constants.

This implies that small iron particles are not responsible for the 220nm interstellar extinction feature. A feature which begins near 160nm in the extinction spectrum of HD44179 is identified as due to water ice.

Measurements have been made of the critical partial pressure of SiO (P_c) necessary to initiate avalanche nucleation in the SiO-H_2 system as a function of temperature (750K<T<1000K). The condensate produced by this process is Si_2O_3 rather than SiO_2. Analysis of P_c versus T using classical nucleation theory yields a value of 500 ergs/cm^2 for the surface free energy of the initial clusters. Despite the fact that this value is in reasonable agreement with those from the literature, numerous inconsistencies in the analysis are noted. It is shown that classical nucleation theory is not applicable to this system.

Measurements of P_c vs T for the Mg-SiO-H_2 system have been obtained (750K<T<1015K). These are compared to similar measurements for the SiO-H_2 system. The presence of magnesium lowers the nucleation barrier for T<925K but does not effect condensation at higher temperatures. Infrared spectra of both the initial condensate and samples annealed in vacuo at 1000K are presented and compared with infrared observations of OH26.5+0.6. Much of the previously ignored fine structure in both the 10 and 20 micron features could be modeled by laboratory produced amorphous silicate smokes.

EXPERIMENTAL AND THEORETICAL STUDIES

OF

INTERSTELLAR GRAINS

by
Joseph Andrew Nuth III

Dissertation submitted to the Faculty of the Graduate School
of the University of Maryland in partial fulfillment
of the requirements for the degree of
Doctor of Philosophy
1982

ACKNOWLEDGEMENTS

TABLE OF CONTENTS

CHAPTER   PAGE

LIST OF TABLES

LIST OF FIGURES

Introduction

The chemical composition of interstellar dust has been the subject of debate for more than forty years. Within the past twenty five years however, our conception of the interstellar medium has undergone a drastic change. This environment was previously seen as a benign, quiet oasis in which solids could leisurely nucleate and grow. Once formed, a grain was believed to persist for eons.

We now know that the interstellar medium is an extremely hostile environment. It is permeated by cosmic, X and γ rays; bathed in both hard and soft ultraviolet radiation; heated and mixed by shock waves from supernova explosions and intercloud collisions. Such processes bring about the destruction of many of the previously proposed grain materials much faster than the rates at which they could be reformed. In fact, because of the extremely low density of condensible material and the hostility of the environment, it is doubtful that any type of grain could form in the general interstellar medium.

Our view of the chemical composition of interstellar solids, once believed to consist of ices of water, methane and ammonia, has undergone a similar transformation. Grains must now be composed of materials capable of withstanding high particle and radiation fluxes for long periods of time. Metals, metal oxides, graphite, metal carbides and silicates all fulfill such criteria and are therefore the

preferred materials to model interstellar dust. Nevertheless, even though ices are no longer expected to be the major constituents of interstellar grains, they might still be important in the more sheltered regions of the interstellar medium.

This model of interstellar materials is supported to some extent by measurements of the depletion patterns of the elements in the interstellar medium (Field, 1974; Trivedi and Larimer, 1981). In such studies, the absolute absorption strength in a resonance line of an element is used to calculate its abundance along the line of sight to a specific star. These abundances are then compared to the 'cosmic' abundance of the element and its depletion factor is determined. Although there are numerous observational and theoretical difficulties in such determinations, the average cosmic depletion pattern indicates that refractory elements such as Si, Mg, Ni, Fe, Ca, Al and Cr are more depleted than less refractory species such as S, O, N, Na, Zn or P. Elements found to be depleted from the gas phase are most probably incorporated into interstellar grains.

Although models based on the measured depletion patterns can predict the average elemental composition of interstellar solids, such models are not able to predict the chemical structure of such material. A complete model of interstellar grains requires an understanding of the processes by which they are formed and subsequently modified in typical astrophysical environments. Such a model necessarily requires that the structure of the major grain components be well characterized.

A successful attack upon this problem must therefore incorporate at least three lines of research. First, it is necessary to understand the physical environment in which nucleation processes occur. Second, it requires the laboratory production of materials which emulate the observed properties of interstellar grains. Finally, it is essential to understand the nucleation process itself, especially for the refractory materials which are the most likely components of the dust.

Chapter 1 briefly reviews the astronomical literature which pertains to the formation, composition or structure of interstellar grains. Chapter 2 reviews previous laboratory measurements of materials proposed as models for the dust. This chapter also contains a brief outline of classical nucleation theory and the manner in which it has been applied to astrophysical systems.

The results of theoretical calculations to determine the steady state populations of SiO and CO in dilute black body radiation fields as a function of the total pressure, chemical composition and kinetic temperature of the ambient gas are reported in Chapter 3. An approximate calculation applicable to polyatomic molecules is also described in this chapter. Chapter 4 describes the production of small iron and magnetite grains. Both of these materials are expected to be present in the interstellar medium. The optical extinction spectra of these grains was studied from 195nm to 830 nm and compared to astronomical observations.

3

Chapter 5 describes measurement of the temperature dependence of the critical pressure of SiO necessary to initiate spontaneous nucleation in a pure $SiO-H_2$ system. These measurements are then used as the basis upon which to analyze the temperature dependence of the onset of avalanche nucleation in a $Mg-SiO-H_2$ system, described in Chapter 6. Chapter 6 reports studies of the infrared spectra of amorphous magnesium silicates and Si_2O_3 as a function of annealing time at 1000K in vacuo. These materials were produced under carefully controlled conditions in the laboratory. The implications of these studies for the formation of interstellar silicates in the atmospneres of oxygen rich stars are discussed, as are the observational consequences of this assumption.

References

Field, G.B., 1974, Ap.J., 187, 453

Trivedi, B.M.P. and Larimer, J.W., 1981, Ap.J., 248, 563

Chapter 1   Astronomical Observations

The astronomical literature relating to interstellar grains has been extensively reviewed on numerous occasions. The review of Savage and Mathis (1979) lists many of the books and review articles which have appeared before 1979. This chapter will be divided into four sections. In the first section I will review the various spectral features observed in the interstellar extinction curve from the far infrared to the extreme ultraviolet. In the second I will review the information extracted from scattering and polarization measurements. In the third section I will discuss the types of grain models which have been proposed to explain these observations. In the last section I will review the information available in the literature on regions considered to be important sources of grains. I will also discuss the mechanisms by which these grains could be modified or destroyed.

I. Spectral Features of the Interstellar Extinction Curve

One of the oldest and most useful sources of information about the properties of interstellar grains is the interstellar extinction curve. Table 1 lists values for the average extinction of

Table 1

An Average Interstellar Extinction Curve

Color	λ(microns)	λ^{-1}(microns^{-1})	E(λ-V)/E(B-V)	A_λ/E(B-V)
	∞	0.00	-3.10	0.00
L	3.4	0.29	-2.94	0.16
K	2.2	0.45	-2.72	0.38
J	1.25	0.80	-2.23	0.87
I	0.90	1.11	-1.60	1.50
R	0.70	1.43	-0.78	2.32
V	0.55	1.82	0.00	3.10
B	0.44	2.27	1.00	4.10
	0.40	2.50	1.30	4.40
	0.344	2.91	1.80	4.90
	0.274	3.65	3.10	6.20
	0.250	4.00	4.19	7.29
	0.240	4.17	4.90	8.00
	0.230	4.35	5.77	8.87
	0.219	4.57	6.57	9.67
	0.210	4.76	6.23	9.33
	0.200	5.00	5.52	8.62
	0.190	5.26	4.90	8.00
	0.180	5.56	4.65	7.75
	0.170	5.88	4.77	7.87
	0.160	6.25	5.02	8.12
	0.149	6.71	5.05	8.15
	0.139	7.18	5.39	8.49
	0.125	8.00	6.55	9.65
	0.118	8.50	7.45	10.55
	0.111	9.00	8.45	11.55
	0.105	9.50	9.80	12.90
	0.100	10.00	11.30	14.40

interstellar material as a function of wavelength. This table is taken from the review of Savage and Mathis (1979). It must be noted however that this average curve is by no means universally invariant. Indeed there are many stars which are known to possess anomolous extinction (see for instance Sitko, Savage and Meade, 1981 or Snow and Seab, 1980). Some of these curves are discussed at greater length in Chapter 4 of this work.

Table 2 lists most of the known spectral features of the interstellar extinction curve, the material currently held to be responsible for the feature and the region or regions in which it is observed. Much of this information is available in the reviews of Huffman (1977) or Merrill (1979). In what follows I will briefly discuss what is 'known' about each feature in this table. I shall begin with those in the infrared and proceed through the electromagnetic spectrum into the ultraviolet.

a. Infrared Extinction

The far infrared region ($\lambda > 30\mu m$) is the "last frontier of astronomical spectroscopy "(Huffman, 1977). Observations must be taken at very high altitudes in order to avoid much of the interference due to atmospheric water vapor. Because the field is relatively young, most of the spectra available in the literature are taken at only low resolution. These indicate that the thermal emission from dust grains surrounding hot sources falls off roughly as λ^{-1}. This implies either

Table 2
Major Features of the Interstellar Extinction Curve

Feature	Carrier	Where Observed
Increase in extinction ($\lambda < 130$nm)	Silicates	1
Increase in Extinction ($\lambda = 159$nm)	Water Ice	HD44179
Extinction Maximum (220nm)	Graphite	1,4
Change in Slope ($\lambda \sim 410$nm)	Large Particles	1
Diffuse Bands (Table 2b)	(impurities ?)	1
Very Broad Structure	Magnetite	1
Mid-Infrared Signatures	(See Table 2a)	
45 micron Absorption	Water Ice	KL Nebula
Far-Infrared Falloff (Intensity $\propto \lambda^{-1}$)	'Dirty' Silicates Magnetite	3

Legend
1. General Interstellar Medium
2. Molecular Clouds/Compact HII Regions
3. Oxygen Rich Stars
4. Carbon Rich Stars
5. Planetary Nebulae
6. Eruptive Stars
7. Misc. Galactic Sources
8. Galactic Nuclei

that the grains have emissivities which are higher than expected in
the infrared or that they are much better absorbers than expected on
the basis of a silicate model. Such enhanced emission might be due to
the presence of impurities within the grain (Aannestad,1975) or to the
presence of 'giant' grains (Rowan-Robinson, 1976). It should be noted
that Day (1976, 1981) has produced amorphous silicates, the extinction
of which falls off as $\lambda^{-1.8}$.

Both the sensitivity and resolution of far infrared detectors is
rapidly improving. This has resulted in the recent detection of a
feature at 45μm attributed to water ice (Erickson et al, 1980;
Papoular et al, 1978). I should note however that this feature has
only been detected in the KL Nebula in Orion, the region with the
strongest known 3.07μm ice feature.

Mid infrared (2μm< λ < 30μm) spectra of many classes of objects
have been available at medium to high resolution for about the last
five years in the short wavelength end of this range (λ < 13μm). High
resolution studies at longer wavelengths are published much less
frequently. This has resulted in the identification of numerous
features at λ < 13μm and almost none above (see Table 2a). An
excellent review of the known infrared features from an observational
point of view was presented by Merrill (1979) at the Workshop on
Thermodynamics and Kinetics of Dust Formation in the Space Medium.
This was augmented by a review of the properties of unidentified
infrared features (Willner et al, 1979) presented at the same meeting.

9

Table 2a

Mid-Infrared Spectral Features

Band Center (Width) (microns)	Seen In [*]	Carrier	Where Observed
3.1	A	Water Ice	2
3.3(0.5)/3.4	E	(C-H ?)	2,5,7,8
3.4	A	(C-H ?)	(1),2
3.5	E	(poly H_2CO ?)	3
6.0	A	?	2
6.2(0.3)	E	(water of hydration ?)	2,5,7,8
6.8	A	?	2
7.7(0.8)	E	?	2,5,7,8
8.6(0.3)	E	?	2,5,7,8
11.2(0.4)	E	?	2,5,7,8
9.7(3.0)/18(3.0)	AE	Silicates	1,2,3,(5),(6),7,8
11.2(1.7)	AE	Silicon Carbide	4,(5)
Continuum	AE	C,Metals,Metal Carbides	1,4,5,6,7

[*] A (Seen in Absorption)   E (Seen in Emission)

Legend

1. General Interstellar Medium
2. Molecular Clouds/Compact HII Regions
3. Oxygen Rich Stars
4. Carbon Rich Stars
5. Planetary Nebulae
6. Eruptive Stars
7. Misc. Galactic Sources
8. Galactic Nuclei

The most widely held beliefs are that amorphous silicates are responsible for the features observed at 9.7 and 18 microns, silicon carbide is responsible for the feature at 11.2 microns and water ice is responsible for the feature at 3.1 microns. These beliefs are by no means universal. The most controversial identification of this group is probably the identification of the 9.7 and 18 micron features as due to silicates. Millar and Duley (1978) have proposed a model based on combinations of diatomic oxides such as SiO, MgO, NiO and FeO which is plausible from a spectroscopic point of view. The model is also quite interesting in that it attempts to provide, simultaneously, a mechanism for the selective depletion of the elements and for the prominent extinction feature observed near 220nm. It does not attempt to explain how such grains form. This could be a major problem since Day and Donn (1978) have shown that co-condensation of Mg and SiO produces amorphous silicates rather than separate oxides. This will be discussed in more detail in section III.

An alternative hypothesis, which has received much more notoriety than acceptance, is that these features are produced by organic materials (Hoyle and Wickramasinghe, 1977a,b). Much of the recent controversy which surrounds this proposal has centered around the identification of a feature at 3.4μm which could possibly be due to the C-H stretching vibration in hydrocarbons (Wickramasinghe and Allen, 1980). The merits of this model will be discussed further in section III.

As can be seen by inspection of Table 2a, there are many unexplained features which can be associated with various grain populations. Observations indicate that the features at 6.0 and 6.8 microns could be due to a single species of grains while those at 3.1/3.4, 6.2, 7.7, 8.6 and 11.3 microns could arise in a second population (Merrill, 1979). Because the 6.0 and 6.8 micron features are only observed in compact infrared sources in molecular clouds, the material responsible for them is probably destroyed in more hostile environments. This has led to the speculation that these features might be due to to hydrocarbons. Specifically, the 6.8 micron feature could arise from carbonyl groups in various chemical environments while the 6.0 micron feature could be due to the bending modes of CH_2 (Willner et al, 1979). The mechanism which produces the associated peaks at 3.4, 6.2, 7.7, 8.6 and 11.2 microns (which are only observed in emission) is still quite controversial. Willner et al (1979) believe that a fluorescence mechanism could account for the observations but note that the process would need to be very efficient. (For example, each UV photon in NGC 7027 would need to produce 3 IR photons.) Dwek et al (1980) have shown that these features could be produced by the thermal emission of hot dust. The composition of the constituent or constituents responsible for these features is still unknown (Aitken, 1980).

Finally, there is a featureless component observed in the infrared spectra of numerous sources which might be due to the presence of metallic grains, graphite, amorphous carbon or a metal carbide. This is especially interesting since such a spectrum is

characteristic of that observed in novae (Ney and Hatfield, 1978; Sato et al, 1978) where it is thought that one might actually be observing grain formation. This will be further discussed in section IV.

b. Visible Extinction

The visible portion of the interstellar extinction spectrum is characterized by a λ^{-1} dependence. This fact has long been known to indicate that the size of the grains responsible for the visible extinction is on the order of the wavelength of visible light, since the extinction of larger grains would be independent of wavelength, while that of smaller grains should vary as λ^{-4}. Of much more interest is the presence of at least 39 diffuse bands (Table 2b) which occur between 685nm and 440nm. A thorough review of the observations was presented by Herbig (1975) at IAU Symposium # 31 while a brief overview can be obtained from the work of Martin (1978) or Huffman (1977).

If these features actually originate in grains - and this is still a matter of debate - then the carriers must be much smaller than average since typical sized grains should show an asymmetric profile. Because the strength of these features does not seem to be correlated with the strength of the far ultraviolet extinction but does show some correlation with the feature observed at 220nm, the bands may arise in carbon grains. Measurements of the wavelength dependence of the polarization have failed to detect any structure, thus strengthening

13

Table 2b

The Diffuse Interstellar Bands

Wavelength(nm)	Central Depth(%)	Full Width at Half Depth(Å)
442.80	16.0	20.0
450.18	6.5	3.0
472.60	5.0	5.0
475.49	3.0	5.6
476.30	5.0	5.3
477.97	3.5	1.8
488.20	6.0	17.0
536.20	2.5	4.4
540.43	5.5	1.0
542.00	2.0	11.0
544.90	4.5	14.0
548.731	6.0	4.4
549.38	5.0	0.8
553.50	2.5	23.0
554.46	3.5	0.8
570.512	7.5	3.5
577.83	6.0	17.0
578.041	37.0	2.6
579.496	22.0	1.3
579.703	22.0	1.3
584.41	3.2	4.5
584.979	9.5	1.0
601.09	4.0	4.2
604.20	2.0	14.0
611.30	5.0	0.85
617.71	7.0	30.0
619.595	14.0	0.70
620.306	16.0	2.3
620.649	16.0	2.3
626.977	17.0	1.4
628.391	38.0	3.8
631.40	4.0	19.0
635.35	3.0	3.1
637.68	5.7	1.5
637.93	16.0	0.86
642.57	4.0	1.1
659.74	3.0	0.6
661.363	34.0	1.1
666.071	...	...

the case for graphite carriers at least for the bands at 443nm, 578nm and 628.3nm (Martin, 1978). More recent work by Wu, York and Snow (1980) using observations obtained from the ANS satellite on a sample of 110 hot stars has reached the same general conclusions if one does not accept the hypothesis that all small grains are responsible for the increase in the far ultraviolet extinction. In particular it seems quite possible that much of the increase in the far ultraviolet extinction is caused by small silicate particles while a seperate population of small graphite particles could exist which might carry the diffuse bands (as surface impurities ?).

Another puzzling feature of the visible extinction is the relatively recent discovery of the VBS (Very Broad Structure). The VBS is between 50 and 100 nm wide, peaks around 455nm and shows a minimum near 570nm (Hayes and Rex, 1977; Hayes et al, 1973; Rex, 1974). Based on laboratory spectra of a colloidal magnetite suspension and on spectra of magnetite from the Orgueil Meteorite, both of which are quite similar to the VBS, Huffman (1977) has concluded that magnetite grains could be present in the interstellar medium. More recently, van Breda and Whittet (1981) have shown that the VBS appears to be a widespread feature of the general interstellar extinction. Moreover, they find that a change in the shape of these features could be indicative of a chemical change on the surface of the grains.

The remaining feature in the visible portion of the extinction curve is a 'knee' or change in slope at about 400nm. This could be

due to a population of larger grains (Huffman, 1977). Other characteristics of this grain population remain unknown and of little apparent interest.

c. Ultraviolet Extinction

The ultraviolet extinction spectrum of material in the line of sight to most stars studied to date shows a peak at 217.5nm + 2.5nm. This is almost universally attributed to the plasma resonance peak in small graphite particles (approximately 20nm in radius). Much of the recent discussion has centered around the possible effect of an ice coating on the observable properties of such particles (see Hecht, 1981). Duley, Millar and Williams (1979) however have presented an alternative model to produce this feature from a mixture of diatomic oxide grains. This model will be discussed in section III.

Within the last year or so, spectra have been obtained which either do not show the peak near 220nm (Sitko, Savage and Meade, 1981; Snow and Seab, 1980) or which show a peak that is unusually weak (Seab, Snow and Joseph, 1981; Witt, Bohlin and Stecker, 1981; Witt and Cottrell, 1980). Most regions which exhibit anomalous behavior near 220nm appear to be dense clouds where the graphite grains responsible for the feature might either be selectively destroyed by some unknown mechanism or accrete mantles to mask it. This problem is discussed in more detail in Chapter 5 where we show that magnetite grains could account for many of the observed features of such regions. We also

16

show that in at least one case, that of HD44179, a substantial ice mantle over a core of magnetite grains can reproduce the published ultraviolet spectrum. To the best of our knowledge this is the first reported identification of the water ice ultraviolet absorption edge in interstellar material. This is the feature listed at 159nm in Table 2.

Following the 220nm peak, the average interstellar extinction decreases and reaches a minimum between 180nm and 155nm. This is followed by an increase in the far ultraviolet extinction which continues to at least 100nm. A distribution of small silicate grains is generally thought to cause this increase (Mathis, Rumple and Nordsieck, 1977) since it has been shown that the strength of the 220nm feature is not well correlated with it (Wu, York and Snow, 1980) but that the strength of the 9.7 micron silicate feature is (Savage and Mathis, 1979)

II. Data from Scattering and Polarization Studies

Independent measurement of the scattering properties of interstellar grains, if the total extinction cross section is already known, can put quite severe limits on the composition and size distribution of the grain population. Such measurements have been attempted for the dust in reflection nebulae and the dust responsible for the Diffuse Galactic Light (DGL). Unfortunately, such data is

extremely difficult to interpret due either to uncertainty in the geometry of the source (or stellar radiation field), uncertainty in the dust distribution within the nebula (or within the galaxy) and uncertainties inherent in the theory of light scattering. This last is because the phase function used to interpret most observations (Henyey and Greenstein, 1941) depends on only two parameters; a, the albedo of the particle and g, the average value of the cosine of the scattering angle. Within certain limits, almost any value of one parameter can give a satisfactory fit to the observations if a suitable adjustment of the other parameter is made. This is further complicated by doubts concerning the applicability of this function based both on laboratory measurements (Zerull, 1976; Chylek, Grams and Pinnick, 1976) and on Mie theory (see Savage and Mathis, 1979).

Linear polarization measurements of dust in circumstellar shells, dense clouds and the interstellar medium yields information on the size distributions of these grain populations as well as some constraints on the composition of the material which causes the polarization. Measurements of the circular polarization yield more certain compositional constraints on the carrier of the polarization as well as information about the probable changes in grain alignment along the line of sight. We can thus study either the variation of the galactic magnetic field or the mechanism of grain alignment provided that a suitable model for the other is assumed. Polarization measurements across individual spectral features can be used to determine if the feature is contained in the same population of grains

responsible for the overall polarization and thus can help to further define and delineate specific grain populations.

The following sections will discuss measurements of the Diffuse Galactic Light, reflection nebulae, linear and circular polarization and measurements of the polarization across individual spectral features. Much of this information is taken from the reviews of Huffman (1977) and Savage and Mathis (1979) although more recent observations have been added where these either contradict or extend previous interpretations.

a. Scattering Measurements

There are many problems inherent in the measurement of the DGL. In the visible, the DGL is faint compared to radiation due to direct starlight and to the Zodiacal light (scattering of <u>sunlight</u> from <u>interplanetary</u> grains - see IAU Symposium #90). At 530nm, the average value of the ratio of the DGL to starlight to Zodiacal Light is one to three to six respectively (Roach and Megill, 1961). The ratio of DGL to starlight increases to about 1 to 2.5 near the galactic equator (Witt, 1968). Unfortunately, there is an uncertainty of at least 20% in the brightness of the average stellar radiation field. The uncertainty of the magnitude of the Zodiacal Light is also large when compared to the intensity of the DGL. Uncertainties in the stellar radiation field increase at increased galactic latitudes (Savage and Mathis, 1979).

In the ultraviolet, problems associated with the Zodiacal Light are less important due to the relative weakness of the solar spectrum. Unfortunately, models of the stellar ultraviolet radiation field are much less reliable than those in the visible. Furthermore, since most of the ultraviolet flux is provided by fairly bright stars which have a rather irregular distribution within the galaxy (Henry, 1977) such models are more difficult to construct.

Despite such difficulties, some useful information can be extracted from measurements of the intensity of the DGL as a function of galactic latitude. In the visible, the grains must be relatively efficient scatterers (a > 0.4); the most probable value for a is 0.7 ± 0.1 (Savage and Mathis, 1979). The value of g is less certain (and cannot be determined indepenuently of a; the most probable value of g in the visible is 0.7 ± 0.2 (Savage and Mathis, 1979). In the ultraviolet, Lillie and Witt (1976) found that $0.6 \leq g \leq 0.9$ over the spectral range $150nm \leq \lambda \leq 420nm$. They also concluded that a(λ>300nm) = 0.7 ± 1, a($\sim$220nm) = 0.35 ± 0.05 and that a(155nm) = 0.6 ± 0.05. This indicates first, that the grains are strongly forward scattering, second, that the extinction peak observed at 220nm is at least partially due to absorption and third, that tne albedo of interstellar grains increases in the far ultraviolet. Huffman (1977) finds tnis last conclusion rather disturbing since it indicates increased scattering efficiency combined with decreased absorption at far ultraviolet wavelengths. Most solids show increased absorption at

20

these energies. These results have however been confirmed by Henry
(1981) who finds a > 0.5 and g > 0.7 in the far ultraviolet.

Nevertheless, recent studies of the surface brightness of the
Merope Nebula (Andriesse et al, 1977) indicate that g = 0.25 in the
far ultraviolet (Witt, 1977). Similar conclusions were drawn from
observations of the Orion Reflection Nebulosity (Witt and Lillie,
1978). Because it is hard to find a single population of grains which
will have a forward directed (g > 0 ?) phase function in the visible
and simultaneously produce more isotropic scattering in the far
ultraviolet, Witt (1979) has proposed that there is a second
population of grains which cause the far ultraviolet scattering.
These particles should be extremely small so that they scatter
essentially as Rayleigh particles. Because of the observed increase
in the far ultraviolet extinction, the number density of these grains
would need to be extremely high compared to the density of the grain
population responsible for the visible extinction.

The most serious problems associated with the study of reflection
nebulae are related to the determination of the geometry of the system
(Jura, 1977, 1979). Such problems include the possible variation in
dust density and grain size throughout the nebula, as well as the more
familiar problems associated with the exact determination of the
relative positions of the cloud, observer and illuminating star. An
additional problem in such studies is the possibility that the dust in
these nebulae is not representative of the general population of
interstellar grains. Therefore, although there is some evidence that

the far ultraviolet phase function of interstellar grains appears to be more isotropic than in the visible, this evidence is by no means conclusive. Because of the inherent uncertainties in the value of g, it is impossible to reach any definite conclusions about the real value of a in the far ultraviolet.

b. Polarization Measurements

The variation of linear polarization as a function of galactic coordinates has been well described in the astronomical literature (see Mathewson and Ford, 1970; Coyne, Gehrels and Serkowski, 1974; Serkowski, Mathewson and Ford, 1975). Variations in the position angle of the polarization can be explained by variations in the galactic magnetic field and in the alignment efficiency of the polarizing material. Variation of the strength of polarization as a function of wavelength can only be explained with respect to the optical properties of the grains themselves. The wavelength at which the strength of the polarization reaches a maximun (λmax) varies from about 410nm in the Cygnus OB-2 association up to about 800nm in dense regions such as Orion, Scorpius and Ophiuchus (Savage and Mathis, 1979). This is commonly attributed to variation in the average size of the grains. Denser regions such as Orion might tend to have larger grains due to the accretion of mantles or the effects of coagulation (see section IV) and thus λmax would tend to occur at longer wavelengths. A region such as the Cygnus OB-2 Association could be characterized by a smaller average grain size if many of the larger

22

grains have been eliminated due to the extremely high radiative flux
of the region. The average value of λmax is approximately 550nm
(Savage and Mathis, 1979).

Despite the rather large variations in both the observed strength
and wavelength dependence of interstellar polarization, the normalized
polarization ($P(\lambda)$/Pmax) can be fit by a function which, for most
regions, depends solely on the ratio of λ/λmax (Equation 1) where K

$$P(\lambda)/Pmax = exp\{-K \ln^2(\lambda/\lambda max)\} \qquad (1)$$

usually is set equal to 1.15. A more recent study by Wilking et al.
(1980) which measured the wavelength dependence of the polarization
from 300nm to 1000nm indicates that K should actually depend on λmax
i.e. K=1.7λmax, due to the observed narrowing of the normalized
polarization curve in regions characterized by large values of λmax.
This is thought to reflect a change in the size distribution of the
grain populations of such regions rather than in the optical constants
of the average grain material.

Equation 1 (with K = 1.15) adequately describes most observations
of regions of small and large average grain sizes. Therefore, the
optical constants of the material responsible for the polarization
must remain relatively constant from the blue into the near infrared
(Martin, 1974). This appears to rule out graphite as the carrier of
polarization but allows such dielectric materials as ices, silicates
and silicon carbide.

In the near infrared ($\lambda < 1600$nm), equation (1) does not
adequately describe the degree of polarization observed toward young
molecular cloud sources. Quite often the maximum polarization at
these wavelengths is much higher than expected. In fact, large
variations are observed within the same molecular cloud complex. This
indicates that the excess polarization arises close to the infrared
source rather than in the intervening interstellar medium. Dyck and
Lonsdale (1981) feel that the most plausible explanation for this
phenomenon is that the excess polarization arises from within the
cloud itself by radiation which passes through a medium of aligned
grains.

In such sources it is impossible to measure $P(\lambda)$ at shorter
wavelengths due to the heavily reddened nature of the cloud. However,
measurements of the angle of polarization within the source can be
compared to the angle measured in the visible for nearby OB stars. If
the angles are correlated, then the excess polarization of the cloud
is due to alignment of the grains by the galactic magnetic field. The
strength of the field within these clouds however is expected to be
much greater than average due to the compression of the magnetic field
lines by the collapsing cloud. Such a correlation has been found
(Dyck and Lonsdale, 1979) although the evidence is certainly not
overwhelming. The observations indicate that the grains in both
sources are aligned by the same mechanism - the action of the galactic
magnetic field. A corrolary is that trapped magnetic field lines can
play a significant role in the evolution of such dense regions.

24

In the visible, measurements of the circular polarization have been used to place some helpful constraints on the composition of the polarizing material. It is well known that the wavelength dependence of circular polarization for a dielectric changes sign at some wavelength, λc. If the imaginary part of the optical constant (k) is near 0, then $\lambda c = \lambda max$, the wavelength at which the linear polarization reaches a maximum (Martin, 1980). As k increases, λc becomes larger than λmax. Because the index of refraction of metals is independent of wavelength, circular polarization produced by metallic particles does not necessarily change sign; although if it does then $\lambda c \ll \lambda max$ (Savage and Mathis, 1979). Because the quantity $(\lambda c - \lambda max)$ is also quite sensitive to the value of n, it is possible for λc to be approximately equal to λmax even if $k \neq 0$, if n is also wavelength dependent. This situation does occur in the case of magnetite grains (Shapiro, 1975).

Observations of the circular polarization in numerous sources were made by Martin and Angel (1976). In all cases they found that $\lambda c = \lambda max$. Therefore the material responsible for tne polarization in these objects must be a dielectric. Similar studies have been carried out by other workers (see for instance McMillan and Tapia, 1977). Such studies rule out graphite as the carrier of the interstellar polarization.

Measurement of the wavelength dependence of the polarization across specific spectral features can not only help to clarify the

interrelationships between the various features but can also yield an upper limit to their band strengths. Observational measurements of the wavelength dependence of the polarization across the 10 micron feature in the BN source and in the galactic center have shown that the volume absorption coefficient of the material responsible for this feature must be less than 3×10^3 and 7×10^3 respectively (Martin, 1978 p.202). This tends to confirm the amorphous nature of this material since more ordered minerals (such as quartz) tend to have higher volume absorption coefficients (Martin, 1975; Capps, 1976; Capps and Knacke, 1976).

On the other hand, polarization measurements across the diffuse bands at 443nm, 578nm and 628.3nm indicate that the grains which carry these features are not aligned (Martin and Angel, 1975). These features therefore do not arise in the same population of grains responsible for the silicate feature at 10 microns. If the diffuse bands arise in the same population of small graphite grains thought responsible for the feature at 220nm, then there should be no pronounced wavelength dependence across this region. Measurements have indeed shown that the variation of $P(\lambda)/Pmax$ across the 220nm feature is adequately predicted by Equation 1 (Gehrels, 1974). In this manner, a systematic survey of the wavelength dependence of the polarization across all observed absorption features could be exteremly benificial. It would be quite interesting for instance, if it were discovered that there were two populations of diffuse bands, one of which arises in aligned grains, the other in nonaligned carriers.

III Models of the Chemical Composition of Interstellar Grains

There are at least three different approaches from which grain models have been constructed. Thermodynamic models have been proposed to predict the composition of the grains formed in the atmospheres of stars (Gilman, 1969; Fix, 1969a,b, 1971), circumstellar shells (Hackwell, 1971), the presolar nebula (Grossman,1972; Larimer and Grossman, 1974) and the ejecta from supernovae (Lattimer, Schramm and Grossman, 1978; Lattimer and Grossman, 1978). Calculations based on nucleation theory have been performed to predict the rate of condensation and final size distribution of thermodynamically predicted materials in regions of astronomical interest. These models exemplify a relatively pure theoretical approach. They start with basic theory, make some simplifying assumptions about the chemical composition, temperature and pressure history of the region considered and thereby calculate the properties of the condensate. To the extent that the theoretical framework employed and the assumptions made correspond to reality, the conclusions drawn from such work are valid. The thermodynamic approach will be discussed in this section. Discussion of models based on nucleation theory will be postponed until the theory is reviewed in Chapter 2.

A second approach to the problem is purely empirical. In models of this sort, an attempt is made to synthesize the observed properties of interstellar grains by appropriate combinations of 'well known' materials. Such models include the work of Mathis and co-workers

27

(Mathis, Rumple and Nordsieck, 1977 - hereafter MRN; Mathis, 1979;
Mathis and Wallenhorst, 1981) who attempt to obtain quantitative
matches to observations of the interstellar extinction in the range
110nm < λ < 1000nm using mixtures of graphite, enstatite, olivine,
silicon carbide, iron and magnetite grains. Also included are the
less quantitative models of Duley and co-workers (i.e. Duley, Millar
and Williams, 1979), Hoyle and Wickramasinghe (1977, 1979) and that of
Hong and Greenberg (1980). Such models will be described below.

A third approach is to attempt the laboratory production of
materials similar to those expected to be formed under astrophysical
conditions. Such work has been undertaken by Donn and co-workers
(i.e. Day and Donn, 1978; Donn et al, 1981) who have condensed an
amorphous magnesium silicate from the vapor. The infrared spectrum of
this material resembles the 10-20 micron spectra of oxygen rich
regions. Matrix isolation studies of the intermediates in this
reaction have been carried out in an attempt to understand the
mechanism by which such species condense (Khanna, Stranz and Donn,
1980). More refined vapor phase experiments of the nucleation of
$SiO-H_2$ and $Mg-SiO-H_2$ systems have recently been completed (see
Chapters 5 and 6 of this dissertation). The experimental approach has
also been taken by Greenberg and colleagues (Hagen, Allamandola and
Greenberg, 1979; Allamandola, Greenberg and Norman, 1979) who
concentrate on the processing of ice mixtures by ultraviolet
radiation. Such materials form a host of organic compounds which
could possibly account for the unidentified infrared emission features
discussed earlier and might also help to explain the formation of some

28

of the more complex organic molecules observed in dense clouds. This approach will be discussed in the second review chapter which will emphasize laboratory investigations related to the study of grains.

a. Thermodynamic Models

The thermodynamic approach is by far the most straightforward means of predicting the composition of interstellar materials, although a few rather important initial assumptions must obviously be made. First, one must assume that the system under study is indeed in thermodynamic equilibrium. Second, one must assume that the thermodynamic data for all species of importance have been included in the calculations. Third, one must assume a particular temperature - pressure history for the system of interest. Fourth, one must assume an initial composition appropriate to the region under consideration. Finally, one usually assumes that the equilibrium approximation breaks down to some degree in order that some of the earlier condensates are preserved through later metamorphoses. One now merely begins at an appropriately high temperature, so that all of the species are initially in the gas phase, and allows the temperature to fall until the first solid condenses.

As an example, let us consider the condensation of corundum (Al_2O_3) from the vapor. Equation (2) is a consequence of the usual

$$K_{eq} = P^2(Al) \times P^3(O) \qquad (2)$$

29

definition of the equilibrium constant for the reaction of a gas and solid. Similarly, K_{eq} equals $\exp(-\Delta G/kT)$. It is usually assumed that the gas is well mixed so that by keeping track of the total pressure of the major species (usually H atoms) and defining a quantity ψ such that it represents the fractional abundance of an element in the gas phase, equation (2) can be rewritten as

$$\exp[(T\Delta S - \Delta H)/kT] = \psi^2_{Al}\psi^3_O(N_H kT)^5 \qquad (3)$$

in which the measured thermodynamic quantities ΔH and ΔS have been substituted for ΔG and $N_H kT$ has been used for P_H. N_H is defined as the number density of H atoms. When the left hand side of Equation (3) becomes equal to the right hand side, Al_2O_3 grains are said to condense from the vapor.

When condensation occurs, one usually assumes that the reaction procedes to completion, i.e. continues until one of the grain constituents becomes virtually depleted from the gas phase. The composition of the remaining vapor is then recalculated and the system is again allowed to cool until the next solid species becomes stable. This process is continued either until the vapor is completely condensed or until one decides that the assumption of thermodynamic equilibrium has broken down sufficiently that further computations are meaningless. It should be noted that these calculations can (and often do) include provisions for the reaction of previously condensed material with either gaseous or even other solid components within the

system. Thus iron grains, which condense at a relatively high temperature, could be converted to magnetite at lower temperatures, corundum could be transformed to anorthite, etc.

Thermodynamic models can be said to have had some measure of success. Gilman (1969) predicted that the condensates from oxygen rich M stars should contain an appreciable fraction of silicates. Silicate-like absorption at 10 microns was subsequently observed. Hoyle and Wickramasinghe (1962) examined the problem for carbon rich stars and predicted the formation of graphite. This was subsequently observed in early ultraviolet rocket studies (Stecher, 1969) as the prominent feature at 220nm. Grossman has had some success in formulating a model based upon the thermodynamic approach which explains the high temperature mineral assemblages found in carbonaceous chondrites. Such models therefore serve as excellent starting points from which to study condensing systems since they provide a framework around which existing data can be organized and future experimentation planned.

Unfortunately, some of the basic assumptions of the thermodynamic approach have been questioned (Donn, 1976) on the grounds that, in a system of approximately cosmic composition, kinetic considerations tend to preclude the formation of some of the more complex species predicted by thermodynamics. Moreover, Blander and Katz (1967) have shown that differing degrees of vapor supersaturation are required before species predicted by thermodynamic models would nucleate, if indeed they actually were to form from the vapor at all. This would

31

disrupt the predicted condensation sequence and could profoundly alter the predicted composition of species formed at lower temperatures since the composition of the vapor could be drastically different.

More recently, it has been shown that the vibrational temperatures of molecules in the relatively low pressure environments suggested as sources of grain condensation are significantly lower than the gas kinetic temperature (Nuth and Donn, 1981; Chapter 3). It has previously been shown that the temperatures of small grains in such regions could also be significantly lower than that of the gas (Arrhenius and De, 1973; De, 1978). It therefore seems highly unlikely that most of the regions thought to produce grains (see section IV) are in thermodynamic equilibrium.

b. Empirical Approaches

Observational measurements of the extinction and polarization properties of interstellar dust are available from the far infrared to the extreme ultraviolet (see section I). If one makes a few assumptions as to the types of grains which might form in various astrophysical environments then an attempt can be made to fit these observations by appropriate distributions of such grains. The most comprehensive and quantitative treatment of this type has been carried out by Mathis and co-workers. Each of the other models discussed below attempts to explain only a relatively restricted set of observations and even these are usually treated only qualitatively.

32

Mathis, Rumple and Nordsieck (1977) - MRN- used Mie theory to calculate the absolute extinction efficiency as a function of wavelength for various mixtures and size distributions of proposed grain materials. These size distributions were constrained such that the total ratio of an individual element to hydrogen could not exceed cosmic abundances. The mixtures studied consisted of graphite, olivine, enstatite, iron, silicon carbide and magnetite taken individually and in combination (up to three at a time). The calculated extinction as a function of wavelength was then compared to the interstellar extinction curve by means of a least squares analysis. This analysis was weighted so as to force the fit to conform to the observed width and position of the 220nm feature.

They found that any mixture which gave a satisfactory fit to the observed extinction had to contain graphite grains. However, graphite alone did not yield a good fit. The best fit for a binary mixture contained graphite and olivine. This was followed by graphite plus (in order) enstatite, silicon carbide, magnetite and iron. Even the worst of these combinations (graphite plus iron) however, was not poor enough to be excluded by the calculations. Given this fact, it is not surprising that the best ternary mixture contained graphite, olivine and enstatite and that enstatite contributed less than 10% to the total extinction.

MRN did not build in a preconceived size distribution, but rather allowed the total number of grains in a series of "bins" to vary

independently until the best possible fit had been achieved. They found however that the final distribution obtained for any component of a mixture which gave an acceptable fit to the observations could be described by a power law distribution of the form $n(a) \propto a^{-q}$ where $3.3 < q < 3.6$. It was suggested that such a distribution of grain sizes could possibly result from stochastic processes in the region of grain formation. This was subsequently investigated by Biermann and Harwit (1980) who conclude that this is indeed the case.

MRN also found upper and lower size cutoffs for their distribution. For graphite, particle radii varied from about 5nm to near 1000nm while radii of other components remained between 25nm and 250nm. These limits were not rigidly established however since larger particles of any composition contribute only 'gray' extinction, while smaller particles are in the Rayleigh regime so that the extinction per gram is virtually independent of particle size.

Although MRN calculated the average polarization for their mixtures as a function of wavelength, they found that λ_{max} occurred at much too short a wavelength to agree with observation. Mathis (1979) later made a more thorough calculation of the wavelength dependence of the polarization. He assumed that the same grain mixture which accounted for the extinction measurements could also be used to explain the degree of polarization. Observational evidence cited earlier (Gehrels, 1974) indicates that the material responsible for the 220nm feature (graphite in the MRN mixture) does not contribute to the polarization. Mathis (1979) therefore assumed that only

34

dielectric materials such as silicon carbide (n ≈ 2.5) and silicates
(n ≈ 1.6) will be important. He argues that a distribution of
infinite cylinders, whose radii follow a power law distribution of the
form $n(a) \propto a^{-2.5}$, will yield the equivalent extinction <u>per unit</u>
<u>length</u> as a MRN distribution of spheres ($n(a) \propto a^{-3.5}$) of the same
material.

Using these assumptions he shows that the above distribution of
cylinders - roughly equivalent to a MRN distribution of elongated
particles - yields excellent agreement with Serkowski's Law (Eq. 1).
Furthermore, the variation of λmax can be accounted for by a
reasonable variation of the upper and lower limits of the radii in the
size distribution used in the calculations. In addition, Mathis
(1979) finds that the smallest dielectric particles required to fit
the extinction data are not likely to be aligned since this would tend
to shift λmax too far into the ultraviolet. He postulates that, as
larger particles grow, small iron or magnetite particles could be
incorporated into the grain which would tend to increase the alignment
efficiency of the larger particles. He therefore demonstrates that a
MRN mixture not only provides an excellent fit to the average observed
extinction curve from 110nm < λ < 1000nm, but simultaneously provides
an equally satisfactory explanation for the observed wavelength
dependence of the polarization.

In a later paper, Mathis and Wallenhorst (1981) extend the model
into the near infrared and also attempt to fit observations of
anomalous extinction seen towards highly reddened regions. In the

first application, they show that the same indices of refraction and size distributions used to fit the visible-ultraviolet observations also yield satisfactory agreement with the color ratio $(I-L)/(B-V)$ for both the average interstellar extinction and for that of ρ Ophiuchus (a highly reddened region).

In the second application, progressively peculiar extinctions are examined as a function of the reddening parameter R_V ($R_V \equiv A_V/E(B-V)$). It is shown that as this parameter increases, the resultant extinction curves can be explained by a continuous increase in particle size. It is demonstrated that first, small silicates are eliminated. As the density of the cloud increases, the upper size limit of the silicate population increases as well. At the highest values of R_V the small graphite component of the mixture begins to disappear. These systematic results could also be caused by an increasingly flatter particle size distribution as R_V increases, which first effects silicates and only begins to perturb the graphite distribution at the highest densities. It may be possible to distinguish between these alternatives by a careful investigation of the wavelength dependence of the polarization as a function of R_V using the techniques of Mathis (1979). Such data could aid in the development of models of the coagulative growth of grains in denser astrophysical environments.

Although the model of Mathis and coworkers is quite satisfactory, it is not the only model available in the literature. We shall now briefly review some of the alternatives.

Duley and coworkers have advocated a model of interstellar solids based upon the properties of diatomic oxides (see Millar and Duley, 1978; Duley, Millar and Williams, 1979; Millar and Duley, 1980). In these models, the 10 micron 'silicate' feature is produced by SiO while the feature at 18 microns is produced by a combination of MgO and FeO. Duley (1980a) claims that variations in the refractive index of the silicon oxide series SiO_x ($1 \leq x \leq 2$) might be responsible for the variation observed in λmax of dense clouds, rather than the usually assumed variation in average grain size. In addition, Duley (1978) has also shown that mixed oxide grains should be either superparamagnetic or weakly ferromagnetic and therefore quite easily aligned by the Davis-Greenstein mechanism.

Although Duley and coworkers have used this model to account for everything from the interstellar chemistry of sulfur (Duley, Millar and Williams, 1980) to the selective depletion of the elements (Duley and Millar, 1978; Duley, 1980b) to the origin of the diffuse interstellar bands (Duley and McCullough, 1977), few of their predictions or calculations are quantitative. Furthermore, they almost always fail to discuss inconsistencies between their model and observations.

As an example, their model predicts that the 10 and 20 micron features are produced by the same population of grains responsible for the feature at 220nm. Observational evidence cited earlier suggests that these features arise in seperate grain populations. Their model also suggests that SiO, MgO and FeO will condense into small mixed

37

grains without alteration of the spectroscopic properties of the individual oxides. Experimental evidence (Day and Donn, 1978) suggests the opposite, even at cryogenic temperatures (Khanna, Strantz and Donn, 1980). Millar and Duley (1980) discuss the fact that the spectral characteristics of alternative models for the 10 and 20 micron features - namely the amorphous silicate of Day and Donn (1978)- might change at the temperatures observed in circumstellar shells (=1000K) yet they fail to discuss the behavior of their proposed mixture at such temperatures. As a final example, Duley and McCullough (1977) have shown that benzene ions adsorbed on protosilicates could be responsible for the diffuse band at 443nm, yet benzene has never been observed in the interstellar medium. Indeed no aromatic hydrocarbon has ever been observed in any astrophysical source (Myers, Thaddeus and Link, 1980; Mann and Williams, 1980).

In summary, although many of the ideas of this group, discussed in the aforementioned papers, might have at least some merit, sufficient justification is seldom given for the assumptions used to derive their conclusions. This obviously detracts from the value of their work.

An organic composition has been proposed by Hoyle and coworkers as a 'single component' model of the interstellar dust. A model based on the infrared spectrum of polysaccharides was first proposed to explain observations of the infrared features normally attributed to both silicates and to water ice (Hoyle and Wickramasinghe, 1977a; Hoyle, Olvasen and Wickramasinghe, 1978). These papers did not

attempt to explain how such a grain could be produced, nor did they address the obvious problem of how such a grain was to survive in the relatively hostile environment of the interstellar medium. Such a model predicts a correlation between the 3.07 and 10 micron features since both are hypothesized to arise in the same population of grains. This correlation is not observed. Although the feature at 10 microns is observed in a wide variety of sources, the feature at 3.07 microns is only observed in fairly dense clouds (see Table 2a).

This model now seems to have been abandoned in favor of a biochemical origin for interstellar grains (Hoyle and Wickramasinghe, 1979). In this model, the feature at 220nm is attributed to biochemical chromophores (Hoyle and Wickramasinghe, 1977b, 1978; Wickramasinghe, Hoyle and Nandy, 1977). Bacteria are held responsible for the visible extinction while viruses account for the far ultraviolet observations (see Fig.3 of Hoyle and Wickramasinghe, 1979). In a more recent article (Hoyle and Wickramasinghe, 1981), the infrared spectra of E.coli, yeast and E.coli annealed at 300°C are compared to observations of the unidentified 3.4 micron feature. Although the observed spectrum is reproduced by such materials, the authors again fail to adequately discuss the origin and survival of such 'grains'. It is interesting to note that the authors do discuss the fact that the cosmic ray bombardment of such species could produce free radicals which could then account for some additional infrared features. They fail to note however, that such bombardment should easily kill their grain population.

To summarize, although some correspondence to the observed properties of interstellar materials can be reproduced by a model based on organic constituents, the model is far from satisfactory for the reasons noted above. In addition, it is known that both oxygen and carbon rich stars expell condensible atoms and molecules into the interstellar medium and that these elements are observed to be depleted from the gas phase (MRN). A model which fails to utilize such materials must be at least partially in error.

Greenberg has been actively engaged in the study of interstellar materials for more than twenty years. Recently, Hong and Greenberg (1980) published a unified model of interstellar grains which attempts to establish a quantitative relationship between grain size and alignment efficiency subject to cosmic abundance constraints. They fit the observational extinction and polarization measurements using a bimodal grain size distribution. Relatively large core-mantle grains are needed to fit the visible-infrared extinction and polarization data while smaller, bare silicate (0.01micron) and graphite (0.013micron) grains account for the ultraviolet observations. Although single sized cores are assumed, the size distribution of the core-mantle grains is expected to follow Equation (4), where a, a_c and

$$n(a,a_i) = n_0 \exp\{-5((a-a_c)/a_i)^3\} \qquad (4)$$

n are respectively, the total particle radius, the core radius and a normalization constant. The parameter a_i acts to cut off the size distribution for small particles.

Overall, these authors do not attempt to obtain results which are as quantitative as those of Mathis and coworkers cited above. Hong and Greenberg (1980) conclude that some enhancement of the Davis-Greenstein grain alignment mechanism is necessary in order to adequately fit observational constraints. Mathis (1979), on the other hand, finds that he does not even need the full degree of alignment produced by this means to accurately model the polarization of a wide variety of sources. As Hong and Greenberg (1980) do not comment on any of the findings of Mathis and coworkers, it is hard to judge the validity of their conclusions. This model does predict that the grains responsible for the visible extinction do have fairly thick mantles of primarily CNO composition. The volume ratio of core/mantle material is approximately 0.1 in this model. It seems that even highly irradiated mantles should produce some infrared features which would be observable over very long pathlengths if such mantles actually account for as much as 90% of the mass of interstellar grains. Laboratory measurements of the quantitative absorption coefficients of highly irradiated ices are needed before such an observational test of this model could be performed.

IV. The Formation, Growth and Destruction of Interstellar Grains.

In this section I will review the observational evidence relating to the formation, growth and destruction of interstellar grains. I

will therefore first consider astrophysical regions where dust is observed to form. Next I will discuss regions in which grain formation has been hypothesized. Finally, I will briefly review the processes thought responsible for grain growth, mantle formation and grain destruction. The mechanism of grain formation will not be discussed in this section but rather will be deferred until Chapter 2.

a. Observed Regions of Dust Formation

Dust has been observed to form in only two astrophysical environments, the envelopes of cool stars and the ejecta from novae. I should note however that there exists some controversey in the interpretation of the observational data used to infer the condensation of grains in novae on a rapid timescale. Grain formation in circumstellar shells is much less controversial. Several studies of this phenomonon will be summarized below which illustrate the range of stellar types, mass loss rates and observations reported in the literature.

Circumstellar Condensation: Hagen (1978) studied the circumstellar gas and dust shells of M giants and supergiants. She combined detailed radiative transfer models with high resolution optical spectra to derive the column densities of circumstellar material from observed line asymmetries. She also used the observed infrared energy distributions to derive the column density of circumstellar dust from the height of the 10 micron silicate feature using a model which

includes the effect. of self absorption by the dust. From a comparison of the μ s to dust ratio she concluded that almost all of the metals in the shells of stars of M6 or later are locked into grains.

Although the inner radii of the circumstellar shells are not well determined, she concluded that they must begin quite close to the photosphere (within $\approx 2R_*$). Particle densities are calculated to be in the range 10^7 to 10^8 atoms/cc (Pressure $\approx 10^{-10}$ atm). Mass loss rates for the stars in her sample were in the range 10^{-8} to 10^{-6} solar masses per year. Although the effect of radiation pressure on the grains nucleated in the atmospheres of cool stars has been proposed as the mechanism which drives mass loss, Hagen (1978) concluded that grain formation is the consequence of mass loss rather than the reverse. It is unfortunate that gas temperatures within the shells could not be determined from her observations. It is worth noting however that the two stars in her sample which were observed to contain a significant metallic fraction in the gas phase - α Sco and α Her - both have hot companions. This would imply that the circumstellar material in these stars is hotter and that either grain formation in such regions is inhibited or that grains formed in the shell of the cool star are evaporated by the hotter companion.

Andriesse, Donn and Viotti (1978) have studied the condensation of dust around the high luminosity star n Carinae. They derive a stellar mass loss rate of 7.5×10^{-2} solar masses per year assuming constant outflow since approximately 1840. Condensation begins when

the gas cools from photospheric temperatures ($\approx$ 50,000K) to those of order $\sim$1000K. The decrease in the visual light curve beginning in $\sim$1856, when combined with the expansion velocity in the shell of 10^6m/s roughly corresponds to the time at which the initially ejected envelope material would have reached the inner radius of the observed dust shell and gas kinetic temperatures would have been between 1000K and 2000K. Unfortunately, particle densities at this radius would have decreased to approximately 10^6 atoms/cc (Pressure $\approx 10^{-12}$atm). Nucleation at such low densities is extremely difficult without the invocation of massive density enhancements (of order 10^6) due to turbulence, magnetic confinement, etc.

The observed infrared spectrum of the dust can be modeled by an amorphous silicate material, heated by stellar radiation, which re-emits in the infrared. There is little doubt that this dust must have condensed in the stellar outflow. The size of the grains is postulated to be $\sim$1 micron. If this is true, then significant grain growth must have occurred after the initial nucleation process. Because the region of nucleation and subsequent grain growth must of necessity occur at a radius much greater than that of the stellar photosphere, a more careful study of the region interior to the dust shell might be possible. This is in contrast to the situation in cool M stars where grain formation occurs very close to the photosphere. Such a study might detect molecular precursers to the observed solids and could possibly yield valuable information on the kinetic and vibrational temperatures of these molecules in the region of grain formation.

Forrest et al. (1978) have studied the infrared spectrum of the variable star OH 26.5 + 0.6 over a period of two years in the wavelength range 2 microns < λ < 40 microns. The shell around this star is thought to produce more than 70 magnitudes of visual extinction. The underlying source is thought to be an M type variable star. The spectrum of the shell shows prominent 18 and 20 micron absorption features and is therefore thought to consist of silicates. The mass loss rate for this star is estimated to be $\sim 10^{-5}$ solar masses per year. It is probably an extreme example of mass loss in late stars and most likely belongs to an evolutionary stage which occurs after that studied by Hagen (1978). The infrared spectrum of this source is presented in Chapter 6 along with a discussion of the interpretation of the residuals in the broader 10 and 20 micron peaks in terms of laboratory produced amorphous silica, Si_2O_3 and magnesium silicates.

Hackwell, Gehrz and Grasdalen (1978) observed a sudden infrared brightening in the Wolf-Rayet star HD 193793 between November 1976 and June 1977 at $\lambda = 2.3$ microns and $\lambda = 10$ microns. This was followed by a decline in intensity at $\lambda = 2.3$, 3.6 and 4.9 microns and a slow brightening at $\lambda > 8$ microns. This was interpreted as the condensation of an optically thin dust shell from material ejected by the star in 1976 at a velocity of approximately 2.7×10^6 m/s. The infrared spectrum of this object does not show a 10 micron feature and the dust is therefore thought to be either iron or graphite. Detailed characteristics of the grain spectrum are insufficient to accurately

model condensation in this system although an attempt has been made to obtain a measure of the mass loss from the star. This is estimated to be $\sim 10^{-4}$ solar masses if the grains are iron and $\sim 10^{-6}$ solar masses if they are graphite. The temperature of the photosphere of this star is $\approx 30,000K$.

Condensation in this system is thought to occur in waves - unlike the continuous outflows seen in the sources discussed above. The authors believe that the infrared brightening of this star, observed in 1970, was due to an ejection of material which occurred in 1969 while that observed in 1977 was due to an outburst in 1976. If this star is periodic, then another ejection is due in 1982-83 and should be followed by an infrared brightening in 1983-84. A search for infrared, optical and ultraviolet emission (or absorption) by the molecular precursors to the expected grains - possibly SiC, FeC, C_2, C_3, etc. could prove to be quite informative.

Koorneef and Sitko (1979) have shown that the wavelength dependence of the extinction toward HD 193793 could be explained by a population of relatively small graphite grains which originated in the stellar wind and were slowed by the interstellar medium at a distance of $\sim 10^{17}$ cm from the star. This further supports the contention of Hackwell, Gehrz and Grasdalen (1978) that grain formation can occur periodically in this star.

In summary, numerous examples of grain formation exist in a variety of stellar types. These range from stars with photospheric

temperatures significantly in excess of 10^4K to those with temperatures of only a few times 10^3. Some stars condense silicate dust while others nucleate iron or graphite grains. We observe dust formation in stars which eject as little as 10^{-8} solar masses per year as well as in sources which might expell as much as 10^{-2} solar masses per year. Mass loss occurs continuously in some stars and as discrete episodes in others. The dust envelope can be optically thin or can produce enough extinction to completely mask the underlying star. No one star can be said to typify those which produce grains. Each must be treated seperately. Yet each environment in which the nucleation process can be demonstrated to occur furthers our knowledge of the process in general, since each seperate case must be treated in any comprehensive theory of grain formation.

Condensation in Novae: Observations of dust formation in novae were reported by Hyland and Neugebauer (1970) and Geisel, Kleinman and Low (1970) for Nova Serpentis 1970. Visual observations showed a gradual decline in the luminosity of the nova until ∿ day 60 when a drastic reduction in intensity began. Simultaneously, infrared observers noted a sharp increase in infrared emission. The most straightforward interpretation of these observations is that, between days 60 and 70, an optically thick dust shell formed from the material in the outflowing nova ejecta. This shell absorbed the stellar visual and ultraviolet radiation and reradiated the energy in the infrared.

This pattern has been repeated for several more recent novae, e.g. Nova Vulpeculae 1976 (Ney and Hatfield,1978), Nova Serpentis 1978

47

(Szkody, et al., 1979; Gehrz, et al., 1980a) and Nova Cygni 1978
(Gehrz et al., 1980b). It should be noted that not all nova form
dust. An example of this later type is probably Nova Cygni 1975
(Gallagher and Ney, 1976) which was followed for ~1 year after visual
maximum and which showed no evidence for dust condensation.

Several models have been proposed to explain (Clayton, 1979;
Clayton and Hoyle, 1976; Clayton and Wickramasinghe, 1976) or to
predict (Gallagher, 1977) the conditions under which dust will form in
novae. In this latter work, Gallagher (1977) contends that if
ionization of the ejected material becomes significant before
conditions suitable for dust condensation have developed, then dust
will not form. He derives an empirical relationship for the time (in
days) after maximum light at which grain formation will begin
(Equation 5) as a function of the luminosity (L) of the nova and

$$t_d = (320/v)(L/L_{sun})^{1/2} \qquad (5)$$

the expansion velocity (v) of the ejecta in km/s. By setting t_d equal
to t_i (the time at which significant ionization developes in the
envelope) he predicts that novae with luminosities greater than about
$5 \times 10^4 L_{sun}$ will not produce dust. Nova Cygni 1975 is cited as an
example of this class of outburst.

Although thermal radiation from dust grains surrounding novae is
almost certain to be responsible for the observed infrared flux, it is
not universally accepted that these grains form in the nova outburst

then under study. It has been suggested that pre-existing grains, already surrounding the nova before the outburst, could be heated by the intense ultraviolet radiation field which is known to increase with time after maximum light. In particular, Bode and Evans (1980) have proposed models for Novae Serpentis 1970 and Aquilae 1975 in which the decrease in visible radiation is a simple consequence of the shift of the bulk of the radiative energy into the ultraviolet as the outer layers of the nova become optically thin and the hotter surface of the underlying white dwarf become exposed. Because they postulate that the pre-existing grains have a larger absorption cross section for these ultraviolet photons, the emergence of such intense ultraviolet emission rapidly heats the surrounding material and thus causes the observed infrared emission.

Bode and Evans suggest that a distribution of ~ 0.01 micron graphite particles - left over from previous outbursts - could account for the observations. This seems quite plausible both since graphite has an increased absorption cross section in the ultraviolet near 80nm and 220nm and since such small grains would tend to remain within a nova system for relatively long periods of time (Bode and Evans, 1980). A similar interpretation of Nova Cygnus 1978 has recently been published (Strickland et al., 1981) in which the pre-existing dust is thought to have been heated by the absorption of photons in ultraviolet resonance lines rather than from the emerging ultraviolet continuum of the white dwarf. The observed infrared flux requires that only about 30 % of the resonant radiation be absorbed. The

calculations of Strickland et al. (1981) indicate that such a high efficiency is not unreasonable.

Although Strickland et al. (1981) estimate that this absorption has a relatively small effect on the ratios of the various resonance lines in the emergent spectrum of the nova, their model would seem more convincing if they could show an example of a line ratio for which this was not the case. Since graphite grains show enhanced absorption at 80nm and 220nm, a resonance line near one of these wavelengths should show a considerable decrease in intensity when compared to one between these peaks. Although it is impossible to measure line intensities for astronomical objects at 80nm, it may be possible to observe this effect near 220nm.

b. Proposed Regions of Grain Formation

It has been observationally established that grains form in the atmospheres of cool stars - and even in the outflow from other stellar sources at considerably higher temperatures. Additional regions of grain formation - for which no observational evidence exists - have also been proposed. Supernovae have been discussed as an important source of material enriched in certain short-lived radioisotopes. T-Tauri stars and/or primitive solar nebulae could be responsible for the establishment of the observed grain size spectrum. Planetary nebulae might be important sources of interstellar grains. Each of these regions will be briefly discussed in the following paragraphs.

Infrared observations of planetary nebulae have revealed the
presence of features usually attributed to dust formed in both carbon
and oxygen rich systems (Aitken et al., 1979). Therefore some
fraction of interstellar silicate and graphite grains probably formed
in planetaries of the appropriate composition at some evolutionary
stage. Unfortunately, the chemical composition of the material
ejected from a proto planetary nebula is the subject of some debate
(Zuckerman, 1980). The dynamics of the ejecta and the conditions
under which the observed grains may have formed are even less certain.
Natta and Panagia (1981) have observed that the grains appear to be
concentrated in the central regions of the nebulae. This would
indicate either that older grains (those farther from the star) have
been partially destroyed or that the concentration of grain forming
material was more abundant in the inner regions of the envelope when
it was ejected by the parent star. There is other observational
evidence however, which indicates that grains may be destroyed in the
interior regions of planetaries (Harrington, 1981).

It should be noted that the observed profile of the silicate
feature in NGC 7027 is not that typified by the signature of the
Trapezium - the archtypical 'silicate'. Rather it appears to have
sharper features - such as those observed in mineral spectra - than is
usually seen in astronomical sources (Jones et al., 1980). This could
be the result of an annealing process on materials originally of a
more amorphous nature, possibly even similar to the grains freshly
nucleated in the atmospheres of cool stars. Of course, the

possibility always exists that the pressures in the original ejected envelope were high enough that some more crystalline species may have formed. One definite conclusion is that the mechanism by which the grains observed in planetaries nucleated and evolved will remain unknown until much more information becomes available on the evolution of planetary nebulae themselves.

T-Tauri stars are known to exhibit rather extensive dust shells. These probably consist of dust originally contained within the cloud before it had collapsed (Finn and Simon, 1977; Harvey, Thronson and Gatley, 1979). These stars are therefore not an important source of the total mass of grains in the interstellar medium. They may however serve as an extremely important contributor to the observed grain size spectrum. Specifically, Burke and Silk (1976) propose that processes such as grain melting, shattering and nucleation can occur in the proto stellar envelope of a newly formed star. These smaller grains could subsequently be reinjected into the interstellar medium via radiation pressure or in the T-Tauri 'wind'. This mechanism might provide a larger number of small grains from the same total mass.

No convincing observational evidence has ever been presented which indicates that grains form in the ejecta from supernovae. In fact, supernovae shocks are usually considered to be a prime destruction mechanism of even highly refractory grain cores (Salpeter, 1977). Anomalies discovered in the refractory chondrules of carbonaceous chondrites do however indicate that some of the material which formed the solar nebula was enriched in supernova produced

isotopes (Cameron and Truran, 1977). This discovery has prompted some
researchers to calculate thermodynamic condensation sequences for
supernovae ejecta (Lattimer, Schramm and Grossman, 1978; Lattimer and
Grossman, 1978). Such a system is, of course, in a state of extreme
disequilibrium (Nuth and Donn, 1981; Chapter 3) and results which rely
on the attainment of such equilibria are therefore extremely dubious.
A more likely scenario for the observed isotopic enrichment would be
the gradual depletion of the gas phase refractories onto interstellar
grain cores which had survived the supernova blast wave. These
composite grains could have subsequently undergone reprocessing in the
primitive solar nebula.

c. Regions of Mantle Formation and Grain Growth

As discussed in section III, there exist regions of higher than
normal density which exhibit anomolous ultraviolet extinction. Mathis
and Wallenhorst (1981) have shown that a normal distribution of
typical interstellar dust grains which becomes deficient in small
particles can reproduce the observed extinction of some regions, while
others require that the number density of larger grains increases.
Although it is possible to preferentially eliminate smaller grains by
evaporation (McCall, 1979; Breger, Gehrz and Hackwell, 1981), such a
process can not explain regions of unusually large grains (Mathis and
Wallenhorst, 1981).

Three processes could possibly be responsible for such observations; simple grain growth, mantle formation and grain coagulation. It is possible that all three processes contribute to the formation of larger grains to some extent. The process which dominates in any particular region would, of course, depend upon the conditions in the region.

Whittet and Blades (1980) have concluded that grains in the ρ Ophiuchus cloud do not grow by the accretion of volatile mantles since the infrared extinction spectrum of the material in this cloud shows no sign of features at 3.1 or 3.4 microns (water ice and C-H stretch, respectively). This is in contrast to the conclusion reached by Cohen (1977) who found that abundance constraints, coupled with the increase in the average size of the particles necessary to explain the polarization observations in such dense clouds, required the condensation of CNO rich mantles. She did show however, that the gas phase abundances of even fairly volatile metals (i.e. Na and Ca) in such clouds was much less than in the average interstellar medium. She concluded that an increase in the mass of absorbing material was necessary to explain her observations and therefore ruled out grain coagulation as the mechanism of grain growth.

Unfortunately, Jura (1980) has suggested that a model of the extinction towards ρ Ophiuchus can be based upon coagulation since the visual opacity per gram is unusually low towards this star (Bohlin, Savage and Drake, 1978). This is felt to result from an increase in the average size of the graphite component of the 'average' grain

54

population by about a factor of three. In Jura's (1980) model silicate grains do not coagulate.

This behavior is in contrast to the behavior suggested by the analysis of Mathis and Wallenhorst (1981), i.e. that small graphite grains only begin to 'disappear' after both the upper and lower size limits of the silicate distribution have increased. Since it has been shown observationally that graphite grains do not contribute to the polarization of such sources, it is difficult to imagine that the growth of these grains will increase the value of λ_{max}. Jura (1979) does not comment on either of these problems.

Jura (1979) does however mention the fact that the timescale for coagulation may be on the order of $\sim 10^{14}$ s. This timescale is comparable to the lifetimes of the clouds themselves. If the grains in such clouds are charged (Watson, 1972; Jura, 1976; Draine, 1978) then the timescale for coagulation could increase substantially. Such an increase would mean that coagulation is unimportant for all but the most ancient or compact clouds.

In summary, grain growth resulting from the adsorption of gas phase metals and metal oxides as well as that resulting from the formation of volatile mantles are likely to be important mechanisms by which the average grain size in dense clouds increases. It is important to note that processing of volatile mantles by stellar ultraviolet radiation might result in a significant reduction in the strength of the infrared signature of such materials at 3.1 and 3.4

microns (Sagan and Khare, 1979). This might indicate that 'old' mantles would be very difficult to observe even when present as a quite substantial percentage of the dust, and could thus explain the failure of Whittet and Blades (1980) to detect the expected signature of a 'volatile' component. In contrast, grain coagulation is not likely to be an important mechanism for the production of larger grains in any but the densest and most ancient clouds.

d. Grain Destruction Mechanisms

Several mechanisms have been proposed which could contribute to the destruction of interstellar grains. In addition to the possible reprocessing of grains during star formation (Section III), sputtering, grain-grain collisions, photodesorption, evaporation and grain surface reactions/chemical sputtering may all affect the grain composition and size distribution.

Sputtering in both high and low velocity shocks is expected to be the most effective mechanism for the destruction of refractory grains. These shocks occur primarily as a result of supernova explosions and intercloud collisions. Grain sputtering can also occur in H II regions, planetary nebulae and the intercloud medium. Cowie (1978) has shown that sputtering can be extremely effective even for relatively low velocity shocks (40-50km/s). In his model, destruction occurs when a shock travels perpendicular to the magnetic field of the cloud. Charged grains are accelerated about these compressed field

56

lines and sputtered by He and CNO atoms. In higher velocity shocks (80-100km/s) a significant fraction of silicate or graphite grains could be destroyed. Shull (1978), in a similar study, has reached essentially the same conclusions.

Barlow (1978a) has developed empirical formulae to predict both the sputtering threshold energy and the sputtering yield based upon extensive review of the experimental data. He concludes that supernova produced shockwaves are likely to be the most important single mechanism for the destruction of grains. Sputtering by cosmic ray particles is not found to be effective.

Both Shull (1977, 1978a) and Havnes (1980) have studied the effect of intercloud collisions upon the average grain population. Shull (1977) considers the results of hydromagnetic shocks produced in low velocity collisions (20-50km/s). He finds that between 3-10% of the dust can be destroyed even in shocks in which the fractional ionization of the gas remains low. Destruction results from the differential acceleration of the grains within the cloud and subsequent grain-grain collisions. Havnes (1980) considers the onset of a two stream instability in the shocked region whereby grains less than ~100nm in diameter are brought to rest with respect to the gas on a short timescale while those of larger diameter continue at approximately the original velocity of the cloud. The net result is the formation of two grain populations which stream relative to one

57

another within the same cloud. Grain-grain collisions therefore can become sufficiently frequent and energetic to cause significant grain destruction.

Other processes, of little importance to the average grains in the interstellar medium, can however become important within certain astrophysical environments. Draine and Salpeter (1979) have studied the fate of dust embedded within a hot plasma (10^4-10^9K). Although sputtering is important at higher densities, at high temperatures ($T>10^5$K) ion field emission can become a significant process by which grain material is returned to the gas phase. In dense clouds, chemical reactions at grain surfaces - which lead to the production of volatile oxides or hydrides - can erode and eventually destroy small grains (Barlow, 1978b). Dust in compact ($N_H>10^5$ atoms/cc) H II regions can be destroyed by reactive sputtering with H, N and O atoms (Draine, 1979) although the process is not very effective at lower densities. Photodesorption is an important destructive process only for weakly bound van der Waals mantle materials (Barlow, 1978b) although it does help to eject the products produced by grain surface reactions. Photodesorption is, however, an effective mechanism for the prevention of mantle formation. It may also help to explain the depletion patterns of the non-metallic elements in diffuse clouds (Barlow, 1978c).

V. <u>Summary</u>

Refractory interstellar grains are produced as a result of mass loss in a wide variety of stellar sources. These grains are then modified by processes in the interstellar medium which include sputtering, ion emission, grain-grain collisions and mantle growth. The average resultant grain population can be characterized as a mixture of several components which must include graphite (or Carbyne?) but can also include "silicates", silicon carbide, iron and magnetite. The size distribution of the average population is likely to be of the form $n(a) \propto a^{-q}$ for $q = 3.5$ and a between 5 and 1000nm.

It is possible to distinguish at least two grain populations from measurements of the wavelength dependence of polarization. One is a population of small graphite grains which may serve as the carrier of the diffuse bands (at least those at 443nm, 578nm and 628.3nm.) and which are not aligned by the galactic magnetic field. The other is a population of 'silicate' grains which may be associated with small iron or magnetite grains and which is responsible for the polarization of starlight. A third population of grains may consist of extremely small silicates which are not aligned and which are responsible for the isotropic scattering observed in the far ultraviolet. A fourth population of grains is found in dense clouds and is characterized by a shift towards larger average grain size. This shift may be caused by the condensation of either refractory or volatile mantles but might also be the result of coagulation.

Dust, freshly nucleated in the outflows of certain stellar sources, may be characterized as a fifth population since such material represents solids as yet unmodified by processes in the interstellar medium. The infrared spectrum of one such region is discussed in Chapter 6 of this dissertation in relation to the laboratory spectra of annealed Mg-SiO smokes. It is demonstrated that similar annealing processes may occur after the initial ejection and nucleation of solids in the envelopes of such regions and that these may be observable with available infrared spectrometers.

It is probably possible to define distinguishing characteristics to categorize grain populations found in specific astronomical regions such as T-Tauri stars, planetary nebulae or H II regions. Careful laboratory studies to determine the effects of the various processes which are thought to be important in the interstellar medium and in the sources themselves, upon the materials expected to account for the majority of the solids in such regions, might result in a better understanding of the relative importance of these effects and of the most probable history of the material within the region. A review of such experimental efforts will be presented in Chapter 2. My own efforts along these lines will be presented in Chapters 4, 5 and 6 of this dissertation.

References

Aannestad, P., 1975, Ap.J., 200, 30

Aitken, D.K., 1980, in Infrared Astronomy, Wynn-Williams and
Cruikshank, eds. (D.Reidel, Boston) p.207

Aitken, D.K., Roche, P.F., Spenser, P.M. and Jones, B., 1979, Ap.J.,
233, 925

Allamandola, L.J., Greenberg, J.M. and Norman, C.A., 1979, Astron.
Astrophys., 77, 66

Andriesse, C.D., Donn, B.D., and Viotti, T., 1978, MNRAS, 135, 771

Andriesse, C.D., Piersma, Th.R. and Witt, A.N., 1977, Astron.
Astrophys., 54, 841

Arrhenius, G. and De, B., 1973, Meteoritics, 8, 297

Barlow, M.J., 1978a, MNRAS, 183, 367

Barlow, M.J., 1978b, MNRAS, 183, 397

Barlow, M.J., 1978c, MNRAS, 183, 417

Biermann, P. and Harwit, M., 1980, Ap.J., 241, L105

Blander, M. and Katz, J., 1967, Geochim. et Cosmochim. Acta, 31, 1025

Bode, M.F. and Evans, A., 1980, Astron.Astrophys., 89, 158

Bohlin, R.C., Savage, B.D. and Drake, J.F., 1978, Ap.J., 224, 132

Breger, M., Gehrz, R.D. and Hackwell, J.A., 1981, Ap.J., 248, 963

Burke, J.R. and Silk, J., 1976, Ap.J., 210, 341

Cameron, A.G.W. and Truran, J.W., 1977, Icarus, 30, 447

Capps, R.W., 1976, Ph.D. Thesis, Univ. of Arizona

Capps, R.W. and Knacke, R.F., 1976, Ap.J., 210, 76

Chylek, P., Grams, G.W. and Pinnick, R.G., 1976, Science, 193, 480

Clayton, D.D., 1979, Astrophys. Space Sci., 65, 179

Clayton, D.D. and Hoyle, F., 1976, Ap.J., 203, 490

Clayton, D.D. and Wickramasinghe, N.C., Astrophys. Space Sci., 42, 463

Cohen, J.G., 1977, Ap.J., 214, 86

Cowie, L.L., 1978, Ap.J., 225, 887

Coyne, G.V., Gehrels, T. and Serkowski, K., 1974, Astron.J., 79, 581

Day, K.L., 1976, Ap.J., 210, 614

Day, K.L., 1981, Ap.J., 246, 110

Day, D.L. and Donn, B., 1978, Ap.J., 222, L45

De, B., 1978, in Proc. 8th Lun. Sci. Conf. (Pergammon, New York) p.79

Donn, B., 1976, Mem.Soc.Roy.Sci.Liege, Ser.6, Tome 9, 499

Donn, B., Hecht, J., Khanna, R., Nuth, J., Stranz, D. and Anderson,
    A.B., 1981, Surf.Sci., 106, 546

Draine, B.T., 1978, Ap.J.Suppl., 36, 595

Draine, B.T., 1979, Ap.J., 230, 106

Draine, B.T. and Salpeter, E.E., 1979, 231, 77

Duley, W.W., 1978, Ap.J., 219, L129

Duley, W.W., 1980a, Ap.J., 240, 950

Duley, W.W., 1980b, Ap.J., 240, L47

Duley, W.W. and McCullough, 1977, Ap.J., 211, L145

Duley, W.W. and Millar, T.J., 1978, Ap.J., 220, 124

Duley, W.W., Millar, T.J. and Williams, D.A., 1979, Astrophys. Space
    Sci., 65, 69

Duley, W.W., Millar, T.J. and Williams, D.A., 1980, MNRAS, 192, 945

Dwek, E., Sellgren, K., Soifer, B.T. and Werner, M.W., 1980, Ap.J.,
    238, 140

Dyck, H.M. and Lonsdale, C.J., 1979, Astron.J., 84, 1339

Dyck, H.M. and Loncdale, C.J., 1981, in Infrared Astronomy,
    Wynn-Williams and Cruikshank eds. (D.Reidel, Boston) p. 223

Erickson, E.F., Knacke, R.F., Tokunaga, A.T. and Haas, M.R., 1981, Ap.J., 245, 148

Finn, G.D. and Simon, T., 1977, Ap.J., 212, 472

Fix, J.D., 1969a, MNRAS, 146, 37

Fix, J.D., 1969b, MNRAS, 146, 51

Fix, J.D., 1971, in Proc. of the Conf. on the Evol. of Late-Type Stars, Lockwood and Dyck eds. (KPNO Press, Tucson)

Forrest, W.J., et al., 1978, Ap.J., 219, 114

Gallagher, J.S., 1977, Astron.J., 82, 209

Gallagher, J.S. and Ney, E.P., 1976, Ap.J., 204, L35

Geisel, S.L., Kleinman, D.E. and Low, F.J., 1970, Ap.J., 161, L101

Gehrels, T., 1974, Astron.J., 79, 590

Gehrz, R.D., Grasdalen, G.L., Hackwell, J.A. and Ney, E.P., 1980a, Ap.J., 237, 855

Gehrz, R.D., Hackwell, J.A., Grasdalen, G.L. Ney, E.P., Neugebauer, G. and Sellgren, K., 1980b, Ap.J., 239, 570

Gilman, R.C., 1969, Ap.J., 155, L185

Grossman, L., 1972, Geochim. et Cosmochim. Acta, 36, 597

Hackwell, J.A., 1971, Ph.D. Thesis, University College, London

Hackwell, J.A., Gehrz, R.D. and Grasdalen, G.L., 1979, Ap.J., 234, 133

Hagen, W., 1978, Ap.J.Suppl., 38, 1

Hagen, W., Allamandola, L.J. and Greenberg, J.M., 1979, Astrophys. Space Sci., 65, 215

Harrington, P., 1981 (Personal Communication)

Harvey, P.M., Thronson, H.A. and Gatley, I., 1979, Ap.J., 231, 115

Havnes, O., 1980, Astron. Astrophys., 90, 106

Hayes, D.S., Mavko, G.E., Radick, R.R., Rex, K.H. and Greenberg, J.M., 1973, in Interstellar Dust and Related Topics, Greenberg and van de Hulst eds. (D.Reidel, Boston) p. 73

Hayes, D.S. and Rex, K.H., 1977, PASP, 89, 929

Hecht, J., 1981, Ap.J., 246, 794

Henry, R.C., 1977, Ap.J.Suppl., 33, 451

Henry, R.C., 1981, Ap.J., 244, L69

Henyey, L.G. and Greenstein, J.L., 1941, Ap.J., 93, 70

Herbig, G.H., 1975, Ap.J., 196, 129

Hong, S.S. and Greenberg, J.M., 1980, Astron. Astrophys., 88, 194

Hoyle, F., Olvasen, A.H. and Wickramasinghe, N.C., 1978, Nature, 271, 229

Hoyle, F. and Wickramasinghe, N.C., 1962, MNRAS, 124, 417

Hoyle, F. and Wickramasinghe, N.C., 1977a, Nature, 266, 241

Hoyle, F. and Wickramasinghe, N.C., 1977b, Nature, 268, 610

Hoyle, F. and Wickramasinghe, N.C., 1978, Nature, 270, 323

Hoyle, F. and Wickramasinghe, N.C., 1979, Astrophys. Space Sci., 65, 241

Hoyle, F. and Wickramasinghe, N.C., 1981, preprint # 71

Huffman, D.R., 1977, Adv. in Phys., 26, 129

Hyland, A.R. and Neugebauer, G., 1970, Ap.J., 160, L177

Jones, B., Merrill, K.M., Stein, W. and Willner, S.P., 1980, Ap.J., 242, 141

Jura, M., 1976, Ap.J., 204, 12

Jura, M., 1977, Ap.J., 218, 749

Jura, M., 1979, Ap.J., 231, 732

Jura, M., 1980, Ap.J., 235, 63

Khanna, R.K., Stranz, D.D. and Donn, B., 1980, J.Chem.Phys., 74, 2108

Koornneef, J. and Sitko, M.L., 1979, Ap.J., 234, 129

Larimer, J.W. and Grossman, L., 1974, Rev.Geophys.Space Phys., 12, 71

Lattimer, J.M. and Grossman, L., 1978, Moon and Planets, 19, 169

Lattimer, J.M., Schramm, D.N. and Grossman, L., 1978, Ap.J., 219, 230

Lillie, C.F. and Witt, A.N., 1976, Ap.J., 208, 64

McCall, M.L., 1981, MNRAS, 194, 485

McMillan, R.S. and Tapia, S., 1977, Ap.J., 212, 714

Mann, A.P.C. and Williams, D.A., 1980, Nature, 283, 721

Martin, P.G., 1974, Ap.J., 187, 461

Martin, P.G., 1975, Ap.J., 201, 373

Martin, P.G. and Angel, J.R.P., 1975, Ap.J., 195, 379

Martin, P.G. and Angel, J.R.P., 1976, Ap.J., 207, 126

Martin, P.G., 1978, Cosmic Dust: Its Impact on Astronomy (Oxford Univ. Press, Oxford)

Mathis, J.S., 1979, Ap.J., 232, 747

Mathis, J.S., Rumpl, W. and Nordsieck, K.H., 1977, Ap.J., 217, 425

Mathis, J.S. and Wallenhorst, S.G., 1981, Ap.J. 244, 483

Mathewson, D.S. and Ford, V.L., 1970, Mem.Roy.Ast.Soc., 74, 139

Merrill, K.M., 1979, Astrophys. Space Sci., 65, 199

Millar, T.J. and Duley, W.W., 1978, MNRAS, 183, 177

Millar, T.J. and Duley, W.W., 1980, MNRAS, 191, 641

Myers, P.C., Thaddeus, P. and Linke, R.A., 1980, Ap.J., 241, 155

Natta, A. and Panagia, N., 1981, Ap.J., 248, 189

Ney, E.P. and Hatfield, B.F., 1978, Ap.J., 219, L111

Nuth, J.A. and Donn, B., 1981, Ap.J., 247, 925

Popoular, R., Lena, P., Marten, A., Rouan, D. and Wijnbergen, J.,
     1978, Nature, 276, 593

Rex, K.H., 1974, Ph.D. Thesis, Rennsselaer Polytechnic Institute

Roach, F.E. and Megill, L.R., 1961, Ap.J., 133, 228

Rowan-Robinson, J., 1976, in Far Infrared Astronomy, Rowan-Robinson
     ed. (Pergammon, Oxford)

Sagan, C. and Khare, B.N., 1979, Astrophys. Space Sci., 65, 309

Salpeter, E.E., 1977, Ann.Rev.Astr.Astrophys., 15, 267

Sato, S., et al., 1978, PAS Japan, 30, 419

Savage, B.D. and Mathis, J.S., 1979, Ann.Rev.Astr.Astrophys., 17, 73

Seab, C.G., Snow, T.P. and Joseph, C.L., 1981, Ap.J., 246, 788

Serkowski, K., Matthewson, D.S. and Ford, V.L., 1975, Ap.J., 196, 261

Shull, J.M., 1977, Ap.J., 215, 805

Shull, J.M., 1978, Ap.J., 226, 858

Sitko, M.L., Savage, B.D. and Meade, M.R., 1981, Ap.J., 246, 161

Snow, T.P. and Seab, C.G., 1980, Ap.J., 242, L83

Stecher, T.P., 1969, Ap.J., 157, L125

Strickland, D.J., Penn, C.J., Seaton, M.J., Snijders, M.A.J. and
     Storey, P.J., 1981, MNRAS, 197, 107

Szkody, P., Dyck, H.M., Capps, R.W., Bechlin, E.E. and Cruikshank,
     D.P., 1979, Astron.J., 84, 1359

van Breda, I.G. and Whittet, D.C.B., 1981, MNRAS, 195, 79

Watson, W.D., 1972, Ap.J., 176, 103

Whittet, D.C.B. and Blades, J.C., 1980, MNRAS, 191, 309

Wickramasinghe, D.T. and Allen, D.A., Nature, 287, 518

Wickramasinghe, N.C., Hoyle, F. and Nandy, K., 1977, Astrophys. Space
     Sci., 47, L9

Wilking, B.A., Lebofski, M.J., Martin, P.G., Rieke, G.H. and Kemp, J.C., 1980, Ap.J., 235, 905

Willner, S.P., Puetter, R.C., Russell, R.W. and Soifer, B.T., Astrophys. Space Sci., 65, 95

Witt, A.N., 1968, Ap.J., 152, 59

Witt, A.N., 1977, PASP, 89, 750

Witt, A.N., 1979, Astrophys. Space Sci., 65, 21

Witt, A.N., Bohlin, R.C. and Stecher, T.P., 1981, Ap.J., 244, 199

Witt, A.N. and Cottrell, M.J., 1980, Ap.J., 235, 899

Witt, A.N. and Lillie, C.F., 1978, Ap.J., 222, 909

Wu, C.C., York, D. and Snow, T.P., 1981, Astron.J., 86, 755

Zerull, R., 1976, in Interplanetary Dust and Zodiacal Light, Elsasser and Fechtig eds. (Springer, Berlin) p. 130

Zuckerman, B., 1980, Ann.Rev.Astron.Astrophys., 18, 263

Chapter 2.

Experimental and Theoretical Studies of Interstellar Grains

Laboratory studies which relate to interstellar grains can be roughly divided into two classes. In the first class of experiments the primary aim of the research is the production of laboratory analogs of suspected interstellar materials. This is usually done in order to reproduce certain specific observations - such as the shape or position of an absorption or emission feature - and thus to 'identify' the component responsible. The second class of experiments are those which attempt to define the conditions under which grains might form. Currently, most models of grain formation are based on the classical theory of homogeneous nucleation.

This chapter is divided into four main sections. In the first, I review experimental studies which were primarily intended to 'identify' interstellar materials. In the second, I review classical nucleation theory and briefly discuss its limitations and possible alternative formulations. In the third, I discuss the application of this theory to the problem of the formation of interstellar grains. In the fourth section I review the experimental data applicable to such systems and the implications of this data for the models of grain formation currently in the literature.

68

I. Laboratory Analogs to Interstellar Dust

Until relatively recently the only "experimental" evidence related to the chemical composition of interstellar grains was obtained from the study of meteorites. Special emphasis was placed upon information gleaned from the study of carbonaceous chondrites, since these are thought to be the most 'primitive' class of meteorites and therefore the most representative of interstellar solids (Cameron, 1973).

Unfortunately, the temperature and pressure at which meteoritic materials were originally compacted is not well determined. The region of the solar nebula in which these processes may have occurred as well as the previous history of the material before coagulation into meteor parent bodies is even more speculative. The processes by which these parent bodies are ruptured and the effects of such catastrophic events on the structure of the material can only·be guessed. To understate the problem, meteoritic specimens were not produced under well controlled laboratory conditions.

Within the past 10 years, the study of possible analogs to interstellar materials has become more fashionable. Such studies will be divided for convenience into four general classes. The first class of studies attempts to use common materials as a basis for the identification of observed spectral features. Such work often reports

the measurement of the spectral features of a mineral - sometimes as a function of temperature, grain size or radiation damage. The second class of experiment reports the effects of heat, radiation, or electrical discharge upon the spectrum of organic - or at least carbon rich - materials. The third type of study measures the optical properties of glasses or materials produced by the sputtering or rapid evaporation/condensation of refractory materials. The fourth category of experiment includes those studies which produce smokes. It should be noted that these categories are completely arbitrary and that there may exist considerable overlap between experiments in seperate classes.

a. Mineral Analogs to Interstellar Dust

The thermodynamic calculations of Gilman (1969) predicted the formation of olivine grains in the envelopes of cool stars. An absorption feature at 10 microns was subsequently detected at low resolution in such sources and olivine became the mineral of choice with which to model circumstellar dust. High resolution spectra for $8 < \lambda < 13$ microns however do not confirm the presence of olivine in circumstellar enveloper. The observed feature lacks the sharp fine structure characteristic of mineral spectra. The search therefore began for a material which had a relatively featureless 10 micron band and which might also be a natural constituent of astrophysical environments.

Day (1974, 1976a,b) described a laboratory synthesized amorphous magnesium silicate which has an infrared absorption spectrum resembling that of circumstellar 'silicates'. The material was prepared as a gel from an aqueous solution and its infrared spectrum recorded as a function of annealing temperature. Annealing in a vacuum transforms the spectrum of this material from one which resembles that of interstellar dust to one identical to forsterite (the magnesium end member of the olivine solid solution series). It is interesting to note that when Day (1974) heated a sample of the matrix of the Murchinson Meteorite (a type II carbonaceous chondrite), the infrared spectrum of which also resembles that of the interstellar feature, he obtained a spectrum which exhibited many of the prominent olivine signatures.

Zaikowski, Knacke and Porco (1975) have suggested a phyllosilicate model of interstellar grains based primarily on studies of type I carbonaceous chondrites. Their analyses confirm that phyllosilicates are the dominant silicate minerals of such meteorites and that the infrared spectra of several phyllosilicates (i.e. montmorillonite or chlorite) resemble, to first approximation, the spectra of astronomical sources.

Unfortunately, associated peaks near 3 and 6 microns, produced by hydroxyl groups within such minerals, are not correlated with the band strength of the 10 micron feature as would be predicted by such a model. In addition, the direct condensation of such complex species from the vapor - needed to explain circumstellar observations -

71

should prove to be extremely difficult. However it is easy to imagine the formation of such materials from pre-existing amorphous silicates in regions of higher pressure such as the primitive solar nebula.

Knacke and Krätchmer (1980), in a study of the infrared spectra of carbonaceous chondrites, found that hydrated phyllosilicates might account for a long wavelength wing found in the 3.07 micron water ice absorption feature. The hydration of amorphous silicates, on a small scale, might be possible given the degree of reprocessing expected for the average interstellar grain. However, alternate explanations for the observed shape of this feature exist and will be discussed in the next subsection.

Because high temperature condensates such as olivine and enstatite are predicted to form in circumstellar environments, it has been suggested that the irradiation of such materials by energetic particles could alter their spectra sufficiently to match that observed in the interstellar medium (Wickramasinghe, 1971). Dybwad (1971) investigated the effects the irradiation of silicate minerals by KeV energy protons while Day (1977) used 1-2 MeV protons. Neither found any significant alteration of the spectra even for radiation doses which were factors of 10-100 higher than those expected for typical grains.

Krätchmer and Huffman (1979) have measured the optical constants of an extremely disordered olivine sample produced by the exposure of a polished, natural olivine to a dose of 5×10^{16} (1.5 MeV Neon ions)

cm^{-2}. The dielectric functions for the wavelength range 8 microns < λ < 30 microns have been determined from an analysis of the specular reflectance of the sample. The extinction produced by Rayleigh particles of this composition were calculated using Mie Theory. Extinction measurements for an amorphous olivine smoke were also taken and found to agree with calculations. Because the radiation dosage used to produce the amorphous olivine was much higher than that expected over the lifetime of typical interstellar grains, nothing could be concluded about the formation of such amorphous materials. Krätchmer and Huffman (1979) did conclude however that the material responsible for the 10 and 20 micron features could be an amorphous 'olivine'.

I have already noted that the best model for the visible and ultraviolet extinction and polarization measurements (Mathis and coworkers- see chapter 1) is based upon the optical properties of well known terrestrial materials. Such information has been available in the literature for many years for most of the less complex and more prominent mineral species.

b. Organic Polymers and Ices

As discussed in section III of Chapter 1, Hoyle and coworkers have suggested that the observed infrared spectra of astronomical sources could be explained in terms of models based upon the laboratory spectra of polysaccharides (Hoyle and Wickramasinghe, 1977)

or biochemical compounds (Hoyle and Wickramasinghe, 1981). Their
visible-ultraviolet extinction model is based upon laboratory
measurements of the optical properties of viruses, bacteria and
biochemical chromophores (Hoyle and Wickramasinghe, 1979). Much of
the current controversy surrounding this model revolves about the
recent detection of a 3.4 micron feature in the spectrum of IRS-7
(Wickramasinghe and Allen, 1980). While Duley and Williams (1979,
1981) interpret the feature as the signature of C-H functional groups
formed on the surface of interstellar graphite grains, Hoyle (1981)
prefers to interpret this feature as indicative of interstellar
microbes.

Little more need be said about such models except to point out
that they are obvious examples of what happens when the
'identification' of a grain material rests solely upon the shape of
its spectrum. Although this is indeed an important constraint, one
must also consider such factors as the relative stability of the
material in the regions in which it has been observed and the
mechanism by which such materials might form.

Studies of two other types of carbon based polymers have been
performed in the laboratory. Khare and Sagen (1971, 1973, 1979 and
references therein) have produced a relatively stable organic polymer
by electric discharge through, and ultraviolet irradiation of,
mixtures of fairly simple starting materials (i.e. CH_4, NH_3, H_2O, H_2S,
etc.) The properties of this material vary from run to run but may
nevertheless represent a small fraction of interstellar material.

This component could be produced as mantled grains approach the edges of interstellar clouds and thus become exposed to the interstellar radiation field.

Carbynes are solid allotropes of carbon formed from alternating triple and single C-C bonds. Whittaker and Wolten (1972) have synthesized carbynes at temperatures in excess of 2600K in the laboratory and Whittaker (1978, 1979) subsequently found several types of carbynes in samples of six terrestrial graphites. Carbynes have also been identified in meteorites (Hayatsu et al., 1980) where they have been shown to be carriers of primordial noble gas (Whittaker et al., 1980). Hayatsu et al. (1980) have demonstrated the formation of carbynes from the disproportionation of CO in the presence of a chromite catalyst at temperatures of only 300-400C. Webster (1980) has suggested that carbynes may be the primary condensate in the atmospheres of carbon stars. For this reason, it is important to obtain the ultraviolet extinction spectra of these materials. Such experiments are currently in the planning stage (Hecht, 1981).

A study of the condensation of water at the low temperatures expected in dense interstellar clouds indicates that an amorphous ice is formed (Leger et al.,1979). The spectrum of this amorphous solid more closely resembles the observed shape of the 3.1 micron feature than does a more crystalline species. This study also indicates that the band strength of the 3.1 micron feature in amorphous ice is only ~2/3 of that in crystalline ice.

Greenberg and coworkers (Hagen, Allamandola and Greenberg, 1979; Allamandola, Greenberg and Norman, 1979) have recently described experimental studies of the low temperature ($\sim$12-42K) photolysis of simple CO, CH_4, H_2O and NH_3 mixtures. The purpose of the experiments was to investigate the products formed by such processes in the mantles of interstellar grains by the action of ultraviolet radiation. The observed products were analysed as a function of the length of photolysis by infrared, visible and ultraviolet spectroscopy. In addition, the mass spectra of selected residues were obtained after the system had been brought up to room temperature. It was found that some of these residues were stable to temperatures as high as 550-600K.

Hagan et al. also found that a large number of molecules and radicals observed in the interstellar medium can be produced by such processes. It was also shown that grain mantles which contain such species also contain a large quantity of stored chemical energy. This energy could be released in relatively low velocity grain-grain collisions and result in the evaporation of the mantle and the release of a significant number of complex organic molecules. Such processes might be the primary mechanism by which the more complex organic species, which are observed in dense clouds, are produced.

Finally, it was shown that ultraviolet irradiation of CO/H_2O mixtures results in a feature at 3.1 microns which closely resembles the shape of the observed band attributed to water ice in the spectrum of the KL Nebula. It is not known (by this author) if this results

76

from a breakdown of the H_2O ice structure or from a chemical reaction with CO. Studies of the effect of the irradiation of other mixtures upon the shape of this feature are reported to be in progress (Hagen, Allamandola and Greenberg, 1979).

c. Sputtering and Laser/Flash Evaporated Condensates.

Lord (1968) vaporized powders of iron oxide, magnesium oxide, aluminum oxide and dunite with a flash discharge lamp but was unable to either chemically or structurally identify his condensation products which formed as mirrors as well as whiskers and spherules on the glass walls of his system. Because he was unable to control the composition of the vapor, could not achieve a homogeneous vapo· hase and could not control the rate of condensation, he abandoned the project.

Blander et al. (1969) used a laser to vaporize basalt targets and found (not surprisingly) that the recondensed material was enriched in volatiles while the residual basalt became enriched in refractory oxides. Meyer (1971) controllably condensed a vapor produced by the sputtering of silicate targets in an argon glow discharge onto substrates at known temperatures. Silicon, magnesium and iron were found to be depleted relative to calcium and aluminum at substrate temperatures above 500C while the Ca/Al ratio was found to remain unchanged over a wide temperature span (100C < T < 850C). He therefore proposed that although the bulk chemistry of chondritic

77

meteorites might be related to a high temperature condensation process in a relatively homogeneous solar nebula, individual chondrites are unlikely to be primordial gas phase condensates because of their variable Ca/Al ratios.

Stephens and Kothari (1978) have used a pulsed laser to evaporate samples of astrophysical interest such as olivine, pyroxene, alumina, carbon, etc. The samples recondensed in the laser plume, usually at pressures in excess of one atmosphere in an Ar, O_2 or H_2 buffer gas. Silicates vaporized in O_2 as well as calcium carbonate and carbon vaporized in Ar or H_2 recondensed into glassy spheres 20-30nm in diameter. Alumina and silicon carbide recondensed into crystalline grains. It is interesting to note that the condensates formed in their system always formed chainlike necklace structures.

Stephens and Russell (1979) used the system described above to produce samples of glassy olivine and enstatite from natural samples. The infrared spectra (4 microns $< \lambda <$ 14 microns) of these amorphous glasses were then compared to samples of the same composition which had been ground to similar dimensions. These spectra were also compared to the observed spectrum of the Trapezium. It is shown that although the spectra of the amorphous glasses are narrower than the observed profile of the Trapezium, variations in the composition of the grains or gradients in the source temperature of the dust cloud could broaden the laboratory profile to match the observations. This is not true of the ground samples which are shown to exhibit considerable structure thin the 10 micron band.

78

Stephens (1980) used the same apparatus to measure the extinction of small, vapor condensed silicate, carbon and silicon carbide particles in the range 130nm < λ < 800nm. Although the silicate and carbon particles produced in this study were amorphous, silicon carbide condensed in the low temperature (β) crystal form. The most interesting finding of this study was that amorphous or glassy carbon particles of mean radii 13nm and 6nm produced extinction peaks at 250 and 235 nm respectively. Graphitic carbon (or possibly carbynes) must therefore be responsible for the observed extinction peak at 220nm.

Day (1979) has reactively sputtered cathodes of $MgSi$ and Mg_2Si compositions in an Ar/O_2 atmosphere to produce amorphous films of $MgSiO_3$ and Mg_2SiO_4 composition respectively. He measured the optical constants of these films in the infrared (7 microns < λ < 33 microns) and used these constants to calculate the extinction of Rayleigh spheres of the same nominal composition. Both compounds exhibit broad extinction peaks centered near 10 and 19 microns which compare favorably with those found in astronomical sources.

A similar study was done on the properties of amorphous iron silicates produced by the reactive sputtering of $FeSi$ and Fe_2Si cathodes in Ar/O_2 atmospheres (Day, 1981). Although the peak positions for the $FeSiO_3$ and Fe_2SiO_4 films are essentially the same as in their magnesium counterparts, the calculated extinction efficiencies are 30% to 75% lower. Measurements of the far infrared

79

transmission of both amorphous magnesium and iron silicates indicates that the extinction falls off as $\lambda^{-1.8}$.

d. Smokes

Kamijo et al. (1975) produced fine particles of carbon, iron, iron oxide and silica, the mean diameter of which ranged between 4-100nm. Iron and iron oxide condensates exhibited some crystal structure while carbon and silica smokes were amorphous. In all cases however, the small particles were observed to form chainlike 'necklace' structures similar to those found in the laser condensed smokes of Stephens and Kothari (1978).

Day (1975) produced ∽50-60nm diameter forsterite spheres by striking an arc between hollow graphite electrodes containing natural fosterite. This method was later used in the study of Krätchmer and Huffman (1979) mentioned previously. Although the initial condensates were glassy, annealing at 800C converted the particles to crystalline olivine. The optical constants of this material were then measured in the range (9 microns < λ < 25 microns). These spheres were probably not true smokes - vapor phase condensates - but rather were more likely small molten fragments thrown from the electrodes and rapidly quenched by the surrounding gas (Day, 1976).

A similar technique - evaporation in an electric arc - has been used by Lefevre (1970) to produce smokes of iron, carbon, silicon

carbide and silica. Grain sizes in this study were in the range (10nm < r < 200nm). Optical absorption measurements of these particles were made and compared with Mie calculations for infinite cylinders in the range 360nm < λ < 700nm. Good agreement was obtained only for silica - possibly indicative of the need for better optical constants for the other materials. In all cases the particles again formed chainlike 'necklace' structures similar to those mentioned previously.

Day and Donn (1978a,b) describe the production of Si_2O_3 (and amorphous magnesium silicate) smoke by the evaporation of SiO (plus magnesium) into Ar, H_2 or Ar/H_2O atmospheres at low pressures (P < 10 torr). In this study the condensate was shown to condense directly from the gas phase and was extremely sensitive to the temperature of the ambient gas; i.e. no condensate formed at T ≈ 500C at SiO-Mg evaporation rates sufficient to produce copious quantities of smoke at room temperature. The infrared spectrum of the amorphous magnesium silicate showed some similarity to the observed 10 and 20 micron feature of astronomical sources and annealed (at 1250C) to form crystalline forsterite.

Although the experimental conditions under which particle formation occurred in this system were not well defined, these results were significant since they demonstrated the non-equilibrium nature of the condensation process in such refractory systems. This was evident both from the amorphous nature of the condensates and from the drastic inhibition of particle formation at 500C in a system predicted thermodynamically to condense at ~1400C (Larimer and Grossman, 1974)

81

from a vapor lower in concentration than that studied. The
condensation of $SiO-H_2$ and $Mg-SiO-H_2$ systems were investigated more
thoroughly for this dissertation (see Chapters 5 & 6). All of the
qualitative findings of Day and Donn (1978a,b) were confirmed and put
on a much more quantitative basis. In addition, the infrared spectra
of these condensates were shown to bear a significant resemblance to
the 8-25 micron spectrum of OH 26.5 + 0.6 as the samples were annealed
in vacuum at 1000K for times ranging up to 167 hours.

II. Nucleation Theory

The partial pressure of a chemical species, in equilibrium with a
liquid or solid of similar composition, is determined uniquely by the
temperature of the system. If, however, no solid or liquid phase
exists, then it is possible for the vapor to become supersaturated as
the temperature of the system decreases (assume that interactions with
the walls are insignificant). Nucleation theory attempts to predict
the rate of condensation as a function of the degree of
supersaturation, ambient temperature and chemical composition of the
cooling system. One of the earliest solutions to this problem is
based upon thermodynamic principles and assumes that the condensing
clusters can be approximated by liquid drops (Becker and Döring, 1935;
Volmer and Weber, 1926). This approach is known as the Becker-Döring
or Classical theory of homogeneous nucleation (see Reiss, 1977,
Abraham, 1974).

This section will be divided into three subsections. In the first, I will briefly sketch the basic derivation of classical nucleation theory. In the second, I will outline some of the modifications and alternatives to classical theory which have been suggested over the years. In the third, I will review an application of classical theory (based upon a steady state approximation) in which the time dependent nucleation rate for a cooling gas is calculated as a function of the cooling trajectory and the inherent properties of the condensate.

a. The Classical Theory of Homogeneous Nucleation

If we assume that the bulk of the cooling, supersaturated gas is in the form of monomers and that these react to form a quasi steady state distribution of n-mers, then the equilibrium number density of such clusters will be given by

$$N_n = N_1 \exp(-\Delta G_\bullet / kT) \tag{1}$$

where N_1 is the number density of monomers, N_n is the number density of n-mers, $\Delta G_\bullet$ is the free energy of formation of an n-mer from monomers and T is the temperature of the system.

If one assumes that the clusters are liquid drops, then the free energy of formation of these drops from monomeric vapor will be the

sum of two terms, one dependent on the volume and the other on the surface area of the cluster. The free energy of this system is given

$$\Delta G_e = -nkT\ln S + s_n \sigma \tag{2}$$

by Equation (2), where S is the supersaturation ratio, s_n is the surface area of a cluster and σ is the surface tension of the liquid. Since the cluster is assumed to be spherical, its radius, r, and surface area are given by $r = [(3nm)/(4\pi\rho)]^{1/3}$ and $s_n = 4\pi r^2$ respectively. These can be calculated if one knows the density of the cluster, ρ, and the mass of a monomer, m. Equation (2) can therefore be written as

$$\Delta G_e = -(4\pi r^3)/(3v)kT\ln S + 4\pi r^2 \sigma \tag{3}$$

where v is the volume per monomer in the cluster.

The maximum in ΔG_e, the activation energy barrier, ΔG_e^*, in the formation of clusters from monomers and r_c, the radius of the 'critical' cluster at which ΔG_e is observed, are easily calculated by taking the derivative of Equation (3) with respect to r. These quantities are given by Equations (4) and (5) respectively. The

$$\Delta G_e^* = (16\pi\sigma^3 v^2)/(3[kT\ln S]^2) \tag{4}$$

$$r_c = (2\sigma v)/(kT\ln S) \tag{5}$$

C-2

equilibrium number of critical sized clusters is found by substituting Equation (4) into Equation (1).

The steady state rate of formation of critical sized clusters, J, is the product of a number of factors. These include the monomer impingement rate per unit surface area of the cluster, β, the surface area of the critical sized cluster, s^*, the number density of critical clusters, N_n^*, and the rate at which these critical clusters re-evaporate. For simplicity, the sticking coefficient of a monomer onto a cluster is usually assumed to be unity. The nucleation rate is therefore given by

$$J = (2\sigma/\pi m)^{1/2} v N_1^2 \exp[-(16\pi\sigma^3 v^2)/(3(kT)^3(\ln S)^2)] \qquad (6)$$

where it has been assumed that Z, the rate at which re-evaporation occurs, is given by Equation (7) (Reiss, 1977).

$$Z = (\Delta G_e^* /[3\pi k T n_c^2])^{1/2} \qquad (7)$$

It can be seen from inspection of Equation (6) that the nucleation rate is extremely sensitive to the ambient temperature, the concentration of monomers (both N_1 and S) and to the surface energy of the cluster, σ. Nucleation theory assumes that the surface energy of a cluster is equal to the surface energy of the bulk liquid (or solid) and that v, the volume of a monomer in the cluster, is also equal to its bulk value. Criticism of these assumptions, as well as objections

concerning the proper form of ΔG_e^*, have been the basis of virtually all of the controversy in this field.

These objections, as well as some of the suggested modifications, will be discussed in the next subsections. However, it must be noted that experimental evidence obtained on systems which require relatively low supersaturations in order to nucleate, and which condense as liquids, are found to agree quite well with the predictions of classical nucleation theory (Adamson, 1976).

b. Modifications and Alternatives to Classical Nucleation Theory

A long standing debate in the literature concerns the 'proper' form of ΔG_e^*. Lothe and Pound (1962) feel that Equation (4) does not adequately account for the ststistical mechanical contributions from the translational and rotational degrees of freedom of the monomers as they combine to form n-mers. Their alternative formulation, when applied to the nucleation of water vapor, indicates that the nucleation rate should be 10^{12} to 10^{17} times faster than the rate predicted by classical theory (Lothe and Pound, 1962).

Several authors (Reiss, 1977; Blander and Katz, 1972) have argued that such factors are already accounted for by the liquid drop approximation. More important, Blander and Katz (1972) have shown that there is a mistake in the original derivation of ΔG_e^* and that Equation (3) should contain an additional term on the right hand side

($+ kT \ln S$). This results in an additional factor of S^{-1} in the pre-exponential factor of Equation (6). This factor is not important for the nucleation of most systems studied to date since the required supersaturations have usually been relatively small. However, for the nucleation of more refractory materials such as SiO, FeO, etc., S can be on the order of 10^5 and this additional factor can therefore become significant.

Another major problem in the classical formulation of nucleation theory is the assumption that quantities such as surface tension, density and ΔG, for bulk materials, can be applied to small clusters (Nishioka and Pound, 1977; Tolman, 1948, 1949; Abraham, 1974). Such assumptions could lead to errors as large as 10^{17} (Oriani and Sundquist, 1963) for the nucleation rate of water vapor and might actually cancel the predicted increase of $\sim 10^{17}$ mentioned earlier (Lothe and Pound, 1962). Because of such uncertainties, Bauer and Frurip (1977) have proposed a model for the nucleation of highly supersaturated systems based upon a kinetic approach. They find that the rate determining 'step' occurs at a size greater than that of the critical cluster and that the overall nucleation rate is determined by the rate at which $\Delta G_s(r)$ decreases beyond the critical cluster. Their model predicts that refractory compounds tend to nucleate slower than the rate predicted by classical theory.

An alternative, kinetic approach to nucleation, which utilizes quantities which can in principle be measured in an equilibrium system, has been formulated by Katz and Donohue (1979). It is

interesting to note that their predicted nucleation rate (assuming an
ideal gas) is identical to that predicted by classical theory. Of
course nucleation, by definition, can never occur in an ideal gas.
Nevertheless, their formalism does offer the possibility of using
measured cluster concentrations, obtained under equilibrium
conditions, to predict the nucleation rate in a supersaturated system.
When one remembers that theoretical rates can vary by as much as 10^{34}
depending upon which terms are deemed important, such a reliance upon
an experimentally based prediction is indeed an asset. This formalism
has recently been extended to treat the case of nucleation for systems
in which the condensible monomer is produced by the chemical reaction
of originally noncondensible gas (or liquid) phase components (Katz
and Donohue, 1982).

Finally, Gillespie (1981) has shown that homogeneous nucleation
can be viewed in terms of a stochastic process. In this model, the
equilibrium, pre-nucleation cluster distribution is determined by the
probability that an (n-1)-mer will gain a monomer to become an n-mer,
verses the combined probabilities that an n-mer will either lose or
gain a monomer. It is shown that, with numerous reasonable
assumptions, this model reduces to an expression for the nucleation
rate identical to that predicted by classical theory. In addition,
the model allows one to calculate the 'time lag' before the onset of
nucleation due to the time required to establish a population of
critical nuclei. Again, it is in principle possible to measure the
various quantities necessary to predict the nucleation rate of a

particular system of interest. This is especially true of a system in which the size of the critical nucleus is expected to be small.

c. Time Dependent Nucleation Theory

Draine and Salpeter (1977) have devised a model, based upon classical nucleation theory, which can be used to predict the nucleation rate, the average size of the final clusters and the dispersion about this mean for a cooling, supersaturated vapor. These quantities are calculated in terms of two dimensionless parameters, θ and η, as well as other rather strangely dimensioned quantities. These additional quantities are used to describe the cooling trajectory of the gas and the thermal properties of the condensing clusters. θ is defined in such a way that $k\theta_N$ is essentially equal to the surface free energy per surface site for a cluster of N monomers. η is defined as the number of times an average monomer can be expected to collide with (and stick to) an average surface site during one supersaturation ratio e-folding time on the cooling trajectory of the gas.

The derivation of this model is extremely complex – and is further obscured by the use of a host of parameters specifically defined in terms of sums and ratios of more familiar quantities. This model also relies heavily upon classical nucleation theory and is therefore subject to most of the same problems mentioned in subsection b above.

Draine ans Salpeter (1977) find that the 'critical'
supersaturation at which nucleation occurs from the vapor is given by

$$\ln S_c = \beta_* ^{-1}[1+(\beta_*/\beta_*')(\ln\Lambda/8\ln\eta)-(8\ln\eta)^{-1}] \qquad (8)$$

where $\beta_* \equiv (2T/\theta)^{3/2}(\ln\eta)^{1/2}$, $\beta_*' \equiv \beta_*-3\epsilon/2$, $\epsilon \equiv$
$[(\gamma-1)^{-1}-B/\kappa T]^{-1}[d\ln(\theta/T)/d\ln T]$, $B \equiv \kappa T(d\ln(n_{sat})/d\ln T)$, $\gamma \equiv$
$1+(d\ln T/d\ln[n])$, n is the total density of condensible material,
$a = (2^{13}/3)(\pi/3)^{1/2}(\beta_*'/\beta_*)^4(T_*/\theta_*)^5(\ln\eta)^{9/2}/(\lambda\langle f^3\rangle)$, $\lambda \equiv$
$c_1(1-X)^{-1}n^{-1}$, X is the mass fraction of condensible material, c_1 is
the concentration of monomers and $\langle f^3\rangle = 1-\exp(\beta_*)$.

Of these quantities, B can be determined experimentally; γ is
determined by the assumed cooling trajectory and 'ideality' of the
gas. The dependence of θ on T is virtually anyone's guess as is the
dependence of θ on N. The concentration of monomers is time dependent
and n and X are arbitrary input parameters. Many of these terms are,
of course, redundant - not to mention confusing. Nevertheless, the
average size of the final cluster distribution is given by

$$\langle N_{final}\rangle = (2/\pi)^{1/2}(3e/2^9)(\beta_*/\beta_*')^3\langle f_3\rangle(\theta/T_*)^3(n/\ln\eta)^3 \qquad (9)$$

and is thus quite sensitive to both θ and η since β_*, β_*', and $\langle f^3\rangle$
also each depend on these quantities.

The relative dispersion in the mean cluster size distribution -
in terms of the number of monomers incorporated into the cluster - is
given by

$$\langle (N^{1/3} - \langle N^{1/3} \rangle)^2 \rangle^{1/2} \langle N \rangle^{-1/3} \approx 0.28 (\theta/T)^{1/2} (\ln \eta)^{-1/2} \quad (10)$$

where the factor 0.28 was empirically chosen to make the equation
agree with the results of numerical calculations. The application of
this theory to the condensation of grains in the atmospheres of stars
will be discussed in section III below.

III. Astrophysical Applications of Nucleation Theory

Nucleation theory has been used to calculate the conditions under
which graphite grains might condense in the atmospheres of cool,
carbon rich stars (Donn et al., 1968; Fix, 1969). Salpeter (1974a)
used a form of nucleation theory, modified to account for the
temperature increase of the clusters because of the high latent heat
of condensation of crystalline species, to treat the condensation
process in both oxygen and carbon rich stars. He then predicted the
conditions under which either dust alone, or a mixture of both gas and
dust might be ejected from the atmospheres of such stars (Salpeter,
1974b).

An excellent summary of the problems encountered in the application of nucleation theory to condensation processes in stellar atmospheres is given by Tabak et al.(1975). These authors specifically discuss the effects caused by the assumption of bulk parameters (ΔG, γ, crystal structure) in such calculations. These authors also discuss the result of using the Lothe-Pound formula rather than the classical model. They show that the nucleation of carbon grains is extremely sensitive to the value adopted for γ. They also note that the value for the surface free energy, γ, which might be appropriate for graphite clusters, is a matter of considerable uncertainty.

Yamamoto and Hasegawa (1977) -hereafter YH- independently formulated a time dependent model of nucleation to calculate the size distribution of the grains formed in astrophysical systems. In general, their formalism is quite similar to that of Draine and Salpeter (1977) - hereafter DS - in that nucleation is found to depend sensitively on two parameters, μ and Λ, which are analogous to θ and η of DS. The application of YH theory is made much easier due to the inclusion of some extremely useful tables; one of which tabulates r_* - the radius of the final clusters - as a function of μ and $\log\Lambda$ is particularly valuable.

YH apply their model to calculate the condensation sequence of a gas of solar composition. They obtain qualitative verification of the conclusions derived by Blander and Katz (1967), i.e. that nucleation barriers can effectively disrupt the thermodynamic condensation

92

sequence proposed by Larimer (1967) or Grossman (1972). Of special interest, YH are careful to note most of the possible problems which could alter their conclusions. Such problems include uncertainties in γ, effects of the condensation of species formed by chemical reactions in the gas phase and possible effects of heterogeneous nucleation on the surfaces of 'pre-existing' grains. In the case of nucleation in stellar atmospheres, these would be the grains which condense first and could therefore lower the condensation barrier for less refractory materials.

Deguchi (1980) has used the combined YH-DS nucleation model to study the effect of grain formation on the gas phase chemical composition of cool circumstellar envelopes. He shows that although the YH-DS model is based upon classical nucleation theory, inclusion of the correction factor proposed by Lothe and Pound (1962) only changes the total number of predicted grain nuclei by a factor between 8 and 64. Due to the other uncertainties inherent in the analysis, this disagreement is unimportant.

Deguchi (1980) finds that ~90-99% of the metals in the ejected gas condense into grains when the mass loss rate is equal to 10^{-5} solar masses per year. More than 99% of the refractories condense at mass loss rates less than 3×10^{-6} solar masses per year. He also calculates that nucleation occurs at ~4-6 times the stellar radius. Given the uncertainties in the model, these conclusions are in reasonable agreement with the calculations of Hagen (1978). However, this may be fortuitous since Hagen (1978) concludes that grain

93

formation occurs as a consequence of stellar mass loss while Deguchi (1980) finds that nucleation drives it in stars heavier than 1.5 solar masses.

Draine (1979) has applied the time dependent nucleation model of DS to the condensation of graphite in carbon rich protoplanetary nebulae and novae. Although the theory successfully predicts the formation of graphite in such sources, it cannot form silicate grains in the outflow from normal giants and supergiants without the invocation of density enhancements on the order of factors of 100 over the densities derived using the assumption of a steady flow.

In a later paper (Draine, 1981), condensation in such outflows is shown to be possible due to the fact that both the SiO monomer and small (10 atom) 'olivine' grains can be characterized by temperatures considerably less than that characteristic of the translational velocity of the gas. Even with these approximations however, the size of the critical clusters thought to nucleate in such environments is barely larger than that for which the DS model begins to fail. In addition, one can only speculate about the properties of a 10 atom 'olivine' cluster since olivine 'monomers' already require at least 7 atoms. Condensation processes in such systems must surely be influenced by the reaction rate of MgO (or FeO) + SiO molecules to form critical clusters in the gas phase. This problem is discussed in somewhat more detail in Chapter 6.

Lefevre (1979) has shown that the growth of grains which nucleate in stellar sources is very sensitive to the temperature of the clusters and that this temperature is, in turn, likely to be different than that of the ambient gas. This result is not dependent upon the formation rate of critical clusters but rather considers only the subsequent growth of these clusters into macroscopic grains. He concludes that the supersaturation ratio used in theories applied to astrophysical regions should be defined in terms of the equilibrium temperature of the critical cluster rather than that of the ambient gas. This, of course, requires that one be able to calculate the temperatures of monomers, dimers,...n-mers,...small grains. This problem is discussed in more detail in Chapter 3.

IV. Nucleation Experiments at High Supersaturations

Very little experimental work has been done on the condensation of refractory materials, although the nucleation of more volatile species – i.e. water – has been studied for decades. Such work formed the experimental basis upon which classical nucleation theory was built. It is only more recently that the vapor phase nucleation of refractory species became interesting. This is due in large measure to the importance of such processes in the formation of particulates in the combustion of coal and other fuels, and the desire to control pollution from such sources. Refractory aerosols are also produced by the recondensation of meteoric materials in the upper atmosphere and

in numerous industrial processes. It should be obvious from the previous sections that these processes are also important in astrophysics.

Dorfeld and Hudson (1973) attempted to experimentally determine the degree of graphite condensation which might be expected in the expanding envelopes of cool, carbon rich stars. This was done by allowing hot ($\sim$2000K) mixtures of methane and hydrogen to expand through a small orifice into a vacuum. The final CH_4/H_2 ratio was determined by mass spectroscopy and compared with the initial ratio. A decrease was taken to be indicative of the formation of graphite in the expansion. It should be noted that the formation of graphite could not be directly observed in this system. The expansion was scaled so that the number of termolecular collisions in the experiment was equal to the number expected over the timescale of the stellar outflow. They concluded that little or no graphite condensation could be expected in such sources and obtained an upper limit of 10% of the available carbon condensed into grains.

These results might be due to the short timescales over which the reactions were followed in the laboratory as opposed to those available in stellar sources. They might also be explained by the fact that, in this experiment, carbon atoms were not readily available but had to be produced by the dissociation of CH_4. However, the dissociation of methane should become increasingly difficult as the gas expands due to the decrease in the average energy available to break the C-H bonds as the gas cools. An equilibrium carbon atom

96

concentration was probably never approached in this system and their conclusions are therefore at least suspect.

Bauer and coworkers have studied the nucleation of supersaturated metal vapors as a function of ambient temperature in a series of shock tube experiments. Freund and Bauer (1977) experimentally determined the binding energy per atom for the reaction $nFe \rightarrow Fe_n$. They found that the expression $\Delta E_n / n = \Delta E_{\bullet}(1-n^{-0.25})$ adequately represented their data. $\Delta E_{\bullet}$ is the sublimation energy of the bulk metal. This result is interesting in that it demonstrates that monomers are bound much less strongly to small clusters than to the bulk metal.

Frurip and Bauer (1977a) determined the temperature dependence of the critical supersaturation ratio for iron, lead and bismuth. They showed that, even allowing for a substantial degree of experimental error, neither the classical nor the Lothe-Pound theory could be used to predict their results. In addition, due to the probable dependence of the surface tension on temperature, they questioned if such measurements could reasonably be used to distinguish between these theories.

Frurip and Bauer (1977b) developed a technique by which an independent determination of the nucleation flux could be made. They then used this technique and their previous results on the temperature dependence of the condensation of lead, bismuth and iron to develope a kinetic theory of nucleation (Bauer and Frurip, 1977). This theory completely abandoned the liquid drop approximation and the concept of

97

a 'constrained equilibrium distribution'. Unfortunately, this theory
is extremely difficult (if not impossible) to apply to most systems of
astrophysical interest since it requires the input of detailed
reaction rate constants for all species of importance. Such detailed
information is obviously not available at the present since even the
chemical composition of some grain forming regions is still a matter
of debate (Zuckerman, 1980).

Recently, Stephens and Bauer (1981) have reported measurements of
the critical pressure for the onset of avalanche nucleation as a
function of ambient temperature for the condensation of Fe, Si, Fe/Si,
FeO_x and SiO_x. In all cases there was substantial disagreement
between the measurements and predictions based on either the classical
or the Lothe-Pound formulations of nucleation theory.
Supersaturations observed in these shock tube experiments ranged from
~10 for iron to several orders of magnitude for the SiO_x system.

A comparison of the shock tube data of Stephens and Bauer (1981),
obtained at temperatures between 1250K and 4200K, and that obtained in
a quasi steady state system at temperatures between 750K and 1000K is
presented in Chapter 5. This chapter reports measurements of the
temperature dependence of the onset of avalanche nucleation in an
$SiO-H_2$ system as a function of temperature in a system similar to that
used in the work of Day and Donn (1978a,b). When the magnitude of the
possible error in both experiments is combined with the fact that the
temperature ranges of the measurements do not overlap, a detailed

comparison of these two sets of results meaningless. However, the overall agreement between these different methods appears to be quite good.

V. Summary

It has been demonstrated (Krätchmer and Huffman, 1977; Day, 1979, 1981) that an amorphous iron or magnesium silicate can produce infrared extinction (8 microns < λ < 25 microns) which is quite similar to that observed in obscured, oxygen rich, stellar sources. The spectra of more crystalline materials does not reproduce such observations. Most theories of nucleation rely upon the attainment of equilibrium conditions (at least before the onset of nucleation) and predict the formation of a thermodynamically stable (in most cases a crystalline) solid.

The results of nucleation experiments on refractory materials, similar to those which might condense in astronomical environments, deviate considerably from the predictions of both the classical and Lothe-Pound formulations of nucleation theory. It must be emphasized that these experiments were performed in terrestrial laboratories where the kinetic temperature of the gas, the vibrational temperature of the clusters and the surface temperatures of the grains were virtually identical. This is not likely to be the case in most of the regions currently believed to be sources of fresh interstellar grains.

99

This point is discussed in more detail in Chapter 3.
Experimental results for the avalanche condensation of $SiO-H_2$ and
$Mg-SiO-H_2$ systems as a function of the ambient gas temperature are
reported in Chapters 5 and 6 respectively.

References

Abraham, F.F., 1974, Homogeneous Nucleation Theory (Academic Press, New York)

Adamson, A.W., 1976, Physical Chemistry of Surfaces (Wiley, New York) Chapter VIII

Allamandola, L.J., Greenberg, J.M. and Norman, C.A., 1979, Astron. Astrophys., 77, 66

Bauer, S.H. and Frurip, D.J., 1977, J. Phys. Chem., 81, 1015

Becker, R. and Doring, W., 1935, Ann. Physik, 24, 719

Blander, M., et al., 1969, Abstract 32nd Annual Meeting of the Meteoritical Society

Blander, M. and Katz, J., 1967, Geochim. et Cosmochim. Acta, 31, 1025

Blander, M. and Katz, J., 1972, J. Stat. Phys., 4, 55

Cameron, A.G.W., 1973, in Interstellar Dust and Related Topics, Greenberg and van de Hulst eds. (D.Reidel, Boston) p. 545

Day, K.L., 1974, Ap.J., 192, L15

Day, K.L., 1975, Ap.J., 199, 060

Day, K.L., 1976a, Icarus, 27, 561

Day, K.L., 1976b, Ap.J., 210, 614

Day, K.L., 1977, MNRAS, 178, 49P

Day, K.L., 1979, Ap.J., 234, 158

Day, K.L., 1981, Ap.J., 246, 110

Day, K.L. and Donn, B., 1978a, Ap.J., 222, L45

Day, K.L. and Donn, B., 1978b, Science, 202, 307

Deguchi, S., 1980, Ap.J., 236, 567

Donn, B., Wickramasinghe, N.C., Hudson, J. and Stecher, T.P., 1968, Ap.J., 153, 451

Dorfield, W.G. and Hudson, J.B., 1973, Ap.J., <u>186</u>, 715

Draine, B.T., 1979, Astrophys. Space Sci., <u>65</u>, 313

Draine, B.T., 1981, in <u>Physical Processes in Red Giants</u>, Iben and
      Renzini eds. (D.Reidel, Boston) p. 317

Draine, B.T. and Salpeter, E.E., 1977, J.Chem.Phys., <u>67</u>, 2230

Duley, W.W. and Williams, D.A., 1979, Nature, <u>277</u>, 40

Duley, W.W. and Williams, D.A., 1981, MNRAS, <u>196</u>, 269

Dybwad, J.P., 1971, J.Geophys.Res., <u>76</u>, 4023

Fix, J.D., 1969, MNRAS, <u>146</u>, 51

Freund, H.J. and Bauer, S.H., 1977, J.Phys.Chem., <u>81</u>, 994

Frurip, D.J. and Bauer, S.H., 1977a, J.Phys.Chem., <u>81</u>, 1001

Frurip, D.J. and Bauer, S.H., 1977b, J.Phys.Chem., <u>81</u>, 1007

Gilman, R.C., 1969, Ap.J., <u>155</u>, L185

Gillespie, D.T., 1981, J.Chem.Phys., <u>74</u>, 661

Grossman, L., 1972, Geochem. et Cosmochim. Acta, <u>36</u>, 597

Hagen, W., 1978, Ap.J.Suppl., <u>38</u>, 1

Hagen, W., Allamandola, L.J. and Greenberg, J.M., 1979, Astrophys.
      Space Sci., <u>65</u>, 215

Hayatsu, R., Scott, R.G., Studier, M.H., Lewis, R.S. and Anders, E.,
      1980, Science, <u>209</u>, 1515

Hecht, J.H., 1981, Ap.J., <u>246</u>, 794

Hoyle, F., 1981, preprint # 71

Hoyle, F. and Wickramasinghe, N.C., 1977, Nature, <u>268</u>, 610

Hoyle, F. and Wickramasinghe, N.C., 1979, Astrophys. Space Sci., <u>65</u>,
      241

Hoyle, F. and Wickramasinghe, N.C., 1981, preprint # 65

Kamijo, F., Nakadu, Y., Iguchi, T., Fujimoto, M.K. and Takada, M.,
975, Icarus, 26, 102

Katz, J.L. and Donohue, M.D., 1979, Adv.Chem.Phys., 40, 137

Katz, J.L. and Donohue, M.D., 1982, J.Coll>Interfac.Sci., galley proof

Khare, B.N. and Sagan, C., 1971, Nature, 232, 577

Khare, B.N. and Sagan, C., 1973, Icarus, 20, 311

Khare, B.N. and Sagan, C., 1979, Astrophys. Space Sci., 65, 309

Knacke, R.F. and Kratchmer, W., 1980, Astron.Astrophys., 92, 281

Larimer, J.W., 1967, Geochim. et Cosmochim. Acta, 31, 215

Larimer, J.W. and Grossman, L., 1974, Rev.Geophys.Space Phys., 12, 71

Lefevre, J., 1970, Astron.Astrophys., 5, 37

Lefevre, J., 1979, Astron.Astrophys., 72, 61

Legere, A., Klein, J., de Cheveigne, S., Guinet, C., Defourneau, D.
and Belin, M., 1979, Astron.Astrophys., 79, 256

Lord, H.C., 1968, Ph.D. Thesis, Univ. Cal. (San Diego)

Lothe, J. and Pound, G.M., 1962, J.Chem.Phys., 36, 2080

Meyer, C., 1971, Geochem. et Cosmochim. Acta, 35, 551

Nishioka, K. and Pound, G.M., 1977, Adv.Coll.Interfac.Sci., 7, 205

Oriani, R.A. and Sundquist, B.E., 1963, J.Chem.Phys., 38, 2082

Reiss, H., 1977, Adv.Coll.Interfac.Sci., 7, 1

Salpeter, E.E., 1974a, Ap.J., 193, 579

Salpeter, E.E., 1974b, Ap.J., 193, 585

Stephens, J.R., 1980, Ap.J., 237, 450

Stephens, J.R. and Bauer, S.H., 1981, preprint

Stephens, J.R. and Kothari, B.K., 1978, Moon and Planets, 19, 139

Stephens, J.R. and Russell, R.W., 1979, Ap.J., 228, 780

Tabak, R.G., Hirth, J.P., Meyrick, G. and Roark, T.P., 1975, Ap.J.,
   196, 457

Tolman, R.C., 1948, J.Chem.Phys., 16, 758

Tolman, R.C., 1949a, J.Chem.Phys., 17, 118

Tolman, R.C., 1949b, J.Chem.Phys., 17, 333

Volmer, M. and Weber, A., 1926, Z.Physik.Chem., 125, 236

Webster, A., 1980, MNRAS, 192, 7P

Whittaker, A.G., 1978, Science, 200, 763

Whittaker, A.G., 1979, Carbon, 17, 21

Whittaker, A.G., Watts, E.J., Lewis, R.S. and Anders, E., 1980,
   Science, 209, 1512

Whittaker, A.G. and Wolten, G.M., 1972, Science, 178, 54

Wickramasinghe, D.T. and Allen, D.A., 1980, Nature, 287, 518

Wickramasinghe, N.C., 1971, Nature(Phys.Sci.), 234, 7

Yamamoto, T. and Hasegawa, H., 1977, Prog.Theor.Phys., 58, 816

Zaikowski, A., Knacke, R.F. and Porco, C.C., 1975, Astrophys. Space
   Sci., 35, 97

Zuckerman, B., 1980, in Infrared Astronomy, Wynn-Williams and
   Cruikshank eds. (D.Reidel, boston) p.275

Chapter 3. Vibrational Disequilibrium in Regions of Grain Formation

It is well known that in diffuse interstellar clouds the internal

energy of atoms and molecules shows extreme deviations from thermal

equilibrium. Donn (1975, 1979) pointed out that significant

deviations for molecular vibrational energy levels would occur in the

much denser regions where grain formation has been postulated. These

regions include novae and supernovae ejecta, the shells surrounding

cool stars, planetary nebulae and several models of the primordial

solar nebula. An approximate calculation by Thompson (1973) indicated

that nonequilibrium vibrational distributions are possible in the

atmospheres of cool supergiants. Unfortunately, the criterion adopted

by Thompson (1973) for the onset of non-LTE in astrophysical systems

lacks precision. Further, it does not permit the quantitative

analysis necessary to facilitate improved calculations of molecular

abundances or to gain a true understanding of the nucleation process

in such systems. In addition, his analysis suffers from the adoption

of incorrect H_{atom}-CO relaxation efficiencies. Geballe and Wollman

(1972) have observed an apparent non-equilibrium temperature

distribution in the CO spectra of cool stars. More thorough model

calculations by Carbon et al. (1976) have shown that such effects

might indeed be expected.

In this chapter we first calculate the vibrational distribution

and corresponding vibrational temperatures for the diatomic molecules

carbon monoxide and silicon monoxide over a wide range of gas kinetic temperatures and pressures for several values of a diluted black body radiation field. We then estimate the vibrational temperature of an idealized polyatomic molecule under similar conditions. Carbon monoxide was chosen because of its abundance in most regions of interest and silicon monoxide because it plays a major role in the condensation of numerous predicted grain materials. Most of the necessary molecular data are available for both.

The factors reponsible for the disequilibrium at low pressures are (1) low collision frequency, (2) general inefficiency of translational-vibrational energy exchange during collision (Kondrat'ev, 1964; Cottrell and McCoubrey, 1961) and (3) radiative lifetimes for vibrational transitions, which are generally in the range $10^{-1} - 10^{-3}$ s (Penner, 1959). The net effect is to make radiative decay comparable to or faster than collisional excitation. Consequently, at low pressures the vibrational energy distribution will be seriously perturbed from an equilibrium Boltzmann distribution by the radiative depletion of higher levels.

This effect can have a significant influence on a number of physico-chemical processes in low density cosmic clouds as is shown by the quantitive calculations of Dalgarno and Roberge (1979). This effect is of particular significance for molecular abundance distributions and condensation processes. It raises serious questions about analyses of these phenomena using the assumption of thermal equilibrium.

II. Method of Analysis

a. Model

As noted by Thompson (1973), at temperatures below 4000K electronic transitions are rare and do not significantly contribute to the vibrational population of CO. Furthermore, condensation of grains is expected to occur at temperatures below 2000K in regions where the radiative energy density has been considerably diluted. At such temperatures, the bulk of both CO and SiO occupy low vibrational states even at equilibrium. We treat both systems as multilevel molecules and solve for the populations of the lowest twelve levels at which point more than 99.99999% of the population has usually been accounted for.

A "vibrational temperature" can be defined by the ratio of the populations of two states such that

$$\frac{N_u}{N_\ell} = \exp \frac{-hc\,\omega}{kT_v} \qquad (1)$$

where N_u and N_ℓ are the populations of the upper and lower states, ω is the transition energy in cm^{-1}, h, c, and k have their usual meanings and T_v is the vibrational temperature. In equation (1) the statistical weights have been set equal to one as for the case of a harmonic oscillator. This is a good approximation for the low vibrational levels which are important here.

An exact calculation of the population of vibrational levels requires knowledge of the radiation field, collisional cross sections for the excitation of individual levels by all colliding species, as well as the radiative transition probabilities from occupied levels. In addition, the chemical composition, temperature and pressure of the region must be known. Because of these restrictions an exact calculation for any particular region cannot be carried out. However, a solution utilizing a few reasonable assumptions and somewhat idealized conditions can be expected to yield results sufficiently accurate for the treatment of problems in which the vibrational populations become important.

Vibrational equilibrium for harmonic oscillators has received a very general treatment by Rubin and Schuler (1956a,b; 1957). Their analysis is a good approximation for the low vibrational levels of molecules such as CO and SiO. We adopt their n level system and introduce diluted black body radiation through a dilution constant, W. We then determine the steady state vibrational distribution rather than the relaxation rate which was of interest in the much higher pressure systems of Rubin and Schuler and in which equilibrium is ultimately attained.

For n level systems we obtain the following set of differential equations for the steady state population of a given level, with the approximation that collisional and radiative transitions occur only between adjacent levels and all energy level spacings are the same:

$$\frac{dN_o}{dt} = N_1 (C_{10} + A_{10} + I_{10}) - N_o (C_{01} + I_{01}) = 0 \qquad (2)$$

$$\frac{dN_x}{dt} = N_{x-1}(C_{x-1,x} + I_{x-1,x}) + N_{x+1} (C_{x+1,x} + I_{x+1,x} + A_{x+1,x})$$

$$- N_x(C_{x,x+1} + I_{x,x+1} + C_{x,x-1} + I_{x,x-1} + A_{x,x-1}) = 0 \qquad (3)$$

where N_x is the population of level x and C_{xy}, A_{xy} and I_{xy} represent the probability of collisional, spontaneous radiative and induced radiative transitions from level x to level y, respectively.

We use the following relationships (Rubin and Schuler, 1957).

$$C_{j,j+1} = C_{j+1,j} \exp (- \frac{\Delta E}{kT}) \qquad C_{j+1,j} = (j + 1) C_{1,0}$$

$$A_{j+1,j} = \alpha B_{j+1,j} \qquad B_{j+1,j} = B_{j,j+1}$$

$$\rho_\nu = \alpha [\exp(\frac{\Delta E}{kT} -1)]^{-1} = \alpha Q \qquad \alpha = 8\pi h\omega^3_{j,j+1}$$

$$A_{j+1,j} = (j+1) A_{1,0}$$

where A and B are the Einstein coefficients, and ρ_ν is the black body radiation density at the energy of the transition of interest. Equations (2) and (3) are solved for population ratios and yield:

$$\frac{N_1}{N_0} = \frac{C_{10} \exp(-\hbar\omega/kT) + WQ A_{10}}{C_{10} + (1 + WQ) A_{10}} \tag{4}$$

$$\frac{N_x}{N_0} = \frac{\frac{N_{x-1}}{N_0}(x)(C_{10}\exp(-\hbar\omega/kT) + WQA_{10}) + \frac{N_{x+1}}{N_0}(x+1)(C_{10}+(1+WQ)A_{10})}{(x+1)(C_{10}\exp(-\hbar\omega/kT) + WQA_{1,0}) + (x)(C_{10}+(1+WQ)A_{10})} \tag{5}$$

where T is both the kinetic and color temperature of the system. This approximation for T will be considered further in section V.

b. Molecular Constants

The Einstein A's for SiO were taken from the work of Hedelund and Lambert (1972). For CO, $A_{j+1,j}$ was estimated using the approximation

$A_{j,j+1} = (j + 1) A_{10}$ where A_{10} was calculated from Chakarian (1970):

$$A_{10} = (64\pi^4/3h) Z\omega^3 (TM^2) \tag{6}$$

where TM is the transition moment (for CO, TM $= 1.04 \times 10^{-19}$) and Z is a constant which depends on the particular vibration - rotation transition of interest. For the P branch $Z = (J_u + 1)/(2J_u + 1)$ whereas for the R branch $Z = J_u/(2J_u + 1)$ where J_u is the rotational quantum number. Since we are concerned only with the total number of transitions per vibrational level we sum the R and P branch transition rates and Z therefore equals 1. Equation (6) was also used to

110

calculate values of A_{10} for our model polyatomic molecule using reasonable values for ω and TM.

C_{10} for CO, SiO and the model polyatomic molecule was initially calculated from the work of Millikan and White (1963) as adopted by Thompson (1973) for a harmonic oscillator (see Herzfield and Litovitz, 1959).

$$c_{10} = \frac{P}{\exp(1.16 \times 10^{-3} \mu^{1/2} \theta^{4/3}(T^{-1/3}-.015\mu^{1/4})-18.42)(1-\exp \theta/T)} \tag{7}$$

where P is the total pressure in atmospheres, μ is the reduced mass of the colliding system in units of molecular weight, θ is the energy of the transition in units of $^{\circ}$K and T is the kinetic temperature. The expression from which this formula is derived, an empirical relation fitted to a large number of experimental relaxation measurements under a very wide range of parameters (i.e., T, P, μ, θ) is good to better than a factor of 2 in most cases (Millikan and White, 1963).

The formalism of Millikan and White (1963) does not apply to the relaxation of diatomic species by atoms with open electronic shells. These atom-molecule collisions have been shown to be much more effective than previously predicted in transferring energy from the translational to vibrational degrees of freedom (von Rosenberg, Taylor and Teare, 1971; West, Weston and Flynn, 1977; MacDonald and Moore, 1978). Nikitin (1974) has proposed that Stark splitting of degenerate

electronic spin-orbit components can lead to resonant collisions and thus to more efficient translational to vibrational energy exchange.

Non-adiabadic electronic energy transfer will also be important in colliding systems where a stable reactive complex can be formed (see the review by Smith, 1976). In this case, Δv can be greater than ± 1. Carbon et al. (1976) have demonstrated that these energy exchange mechanisms can have a significant effect on the calculated deviation of CO from local thermodynamic equilibrium in the atmospheres of cool stars. These effects will be discussed in section V.

Because C_{10} for H atom-CO collisions is at most a factor of 10^3 higher than predicted by Millikan and White (1963) (see Figure 1 of Carbon et al. (1976)) we have for simplicity used a collisional rate (C_{10}) which is a factor of 10^3 higher than that calculated from their equations for this system. Similarly, because Fe atoms also very efficiently excite CO vibrational levels (von Rosenberg and Wray, 1971) and because this discrepancy is also of order 10^3, for iron we have again used a collisional rate which is 10^3 times that calculated from the work of Millikan and White (1963). These approximations should underestimate the disequilibrium of the system. C_{10} for O atom-CO collisions was derived from the work of Center (1973). C_{10} for H atom-SiO and CO-CO collisions were used as calculated from the equations of Millikan and White (1963). Although the use of these C_{10} values probably overestimates the degree of disequilibrium for H atom-SiO collisions, they should be correct for the CO-CO system.

The collisional relaxation rate, C_{10}, is proportional to the product of the pressure and the collisional efficiency. An increased efficiency combined with a proportionate decrease in pressure will leave the system unchanged. Therefore in the Figures the effect of a different choice of collisional efficiency is to multiply the pressure scale by a factor equal to the ratio of the original efficiency to the new efficiency.

Using equations (1), (4), and (5), the vibrational temperature of a particular excited state with respect to the ground state can be calculated.

III. Disequilibrium of Diatomic Molecules

Figure 1 is a plot of the vibrational temperature of CO as a function of H-atom pressure at a kinetic temperature of 2000K for various values of the radiative dilution coefficient W, (W = 1 for a black body radiation field, W = 0 in the absence of radiation). It is obvious from the figure that although the radiation field provides a lower limit to the vibrational temperature it has little efffect on the pressure at which the system begins to depart from equilibrium. It should be noted that there is little difference between the degree of disequilibrium for W equal to zero and W equal to a few tenths until the vibrational temperature is well below the kinetic temperature.

Figure 1.   Vibrational temperataure of CO as a function of total
pressure in an H-atom gas at a kinetic temperature of 2000 K for
various values of the radiative dilution coefficient, W.   (W = 0 in
the absence of a radiation field.)
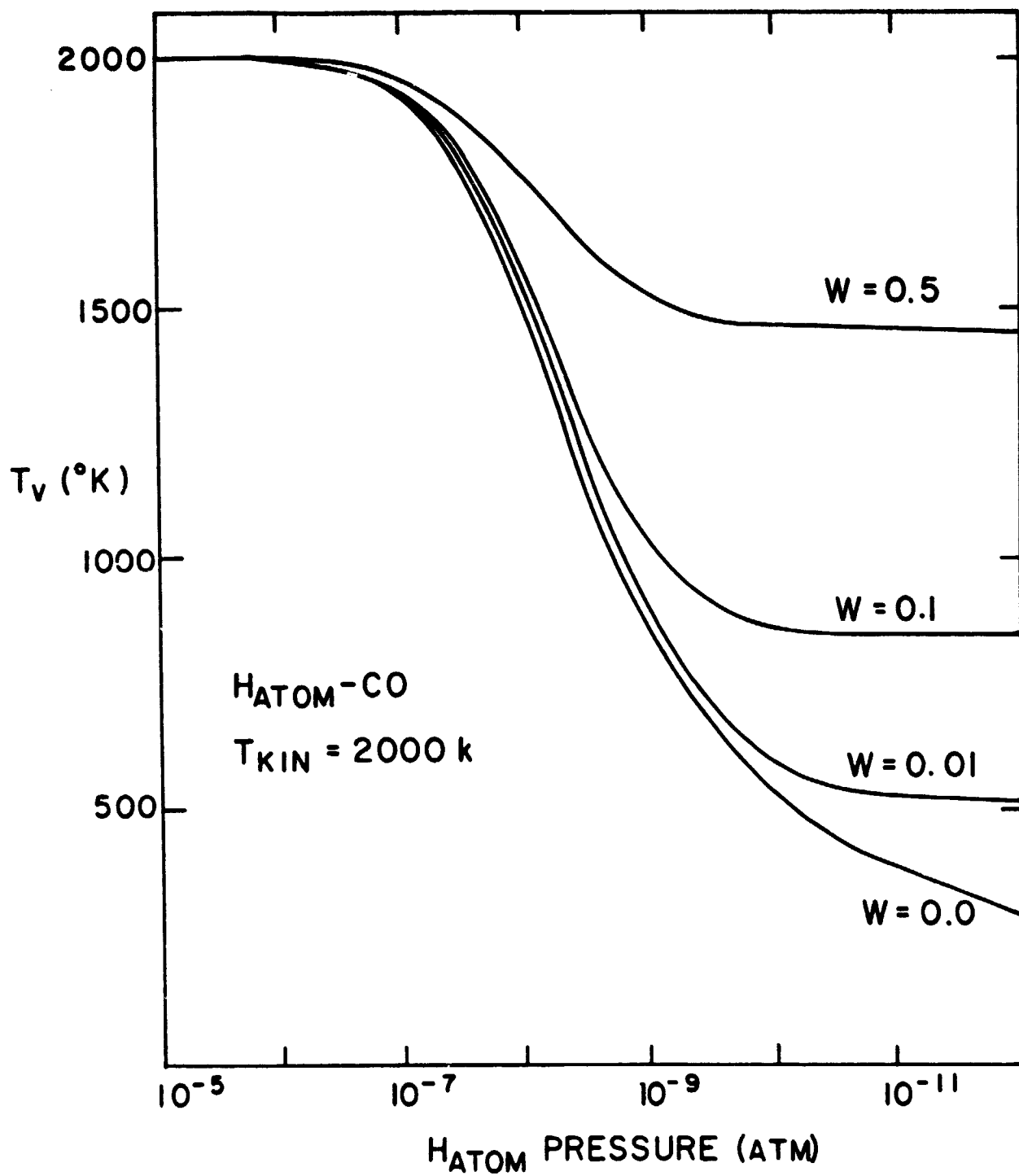
It should be noted that for abundant molecular species such as CO the optical depth at the wavelength of the fundamental frequency could be considerably higher than average due to the trapping of resonance radiation by the CO molecules. In most cases of interest however, the density of molecular species should be low enough that this effect does not become important.

Another interesting feature is that under any particular set of conditions, all vibrational level populations can be represented by a Boltzman distribution at a characteristic vibrational temperature. This results from the fact that our model for diatomic molecules has an analytical solution which is independent of the vibrational level;

$$
T_v = \frac{T}{1 + \frac{kT}{hc\omega} \ln \frac{1 + C_{1,0}/A_{1,0} + WQ}{C_{1,0}/A_{1,0} + WQ \exp(hc\omega/kT)}}
\tag{8}
$$

Unfortunately, this equation requires that both the Einstein A coefficients and the collisional efficiencies for the higher vibrational levels be given by the idealized formulae of Rubin and Schuler (1957). This precludes the use of more accurate results, suc as the calculation of the Einstein A coefficients for SiO by Hedelund and Lambert (1972). Although equation (4) assumes the same idealized dependence of the C and A coefficients for higher vibrational levels as does (8), it is a trivial task to seperate the variables in such a

116

way that equation (4) could accomodate better data as it becomes available. This is not true of equation (8).

Thompson (1973) stated that non-LTE effects become important when the rate of downward collisional transitions equals that of spontaneous radiative transitions. We find from equations (1), (4) and (5) that when these rates are equal at a kinetic temperature of 2000 K and a dilution coefficient, W, of 0.5, the vibrational temperature of CO is 1705 K. In the absence of a radiation field (W = 0) the above conditions yield CO vibration temperatures of 1380 K. When Thompson's criterion is satisfied the system is already far removed from equilibrium. Further, his criterion provides only a qualitative measure of disequilibrium and cannot be used to determine the consequences of the disequilibrium upon other phenomena, for example, molecular equilibrium or particle condensation.

Figure 2 is a plot of the average vibrational temperature of CO as a function of H-atom pressure for various values of the gas kinetic temperature in the absence of radiation. Figure 3 is the analogous plot for SiO. Because of the use of classical collisional efficiencies for H-SiO, the SiO pressure scales will be too high. If this system behaves as does H-CO, the correction factor may be as high as 1000. As there are no experimental measurements for H_{atom}-SiO collisions, the classical results were retained.

Figure 2. CO vibrational temperature as a function of total pressure in an H atom gas. Each line represents a calculation at the gas kinetic temperature of the T_v intercept, $W = 0$.

$H_{ATOM}-CO$

T_V (°K)

3000

2500

2000

1500

1000

500

H_{ATOM} PRESSURE (ATM)

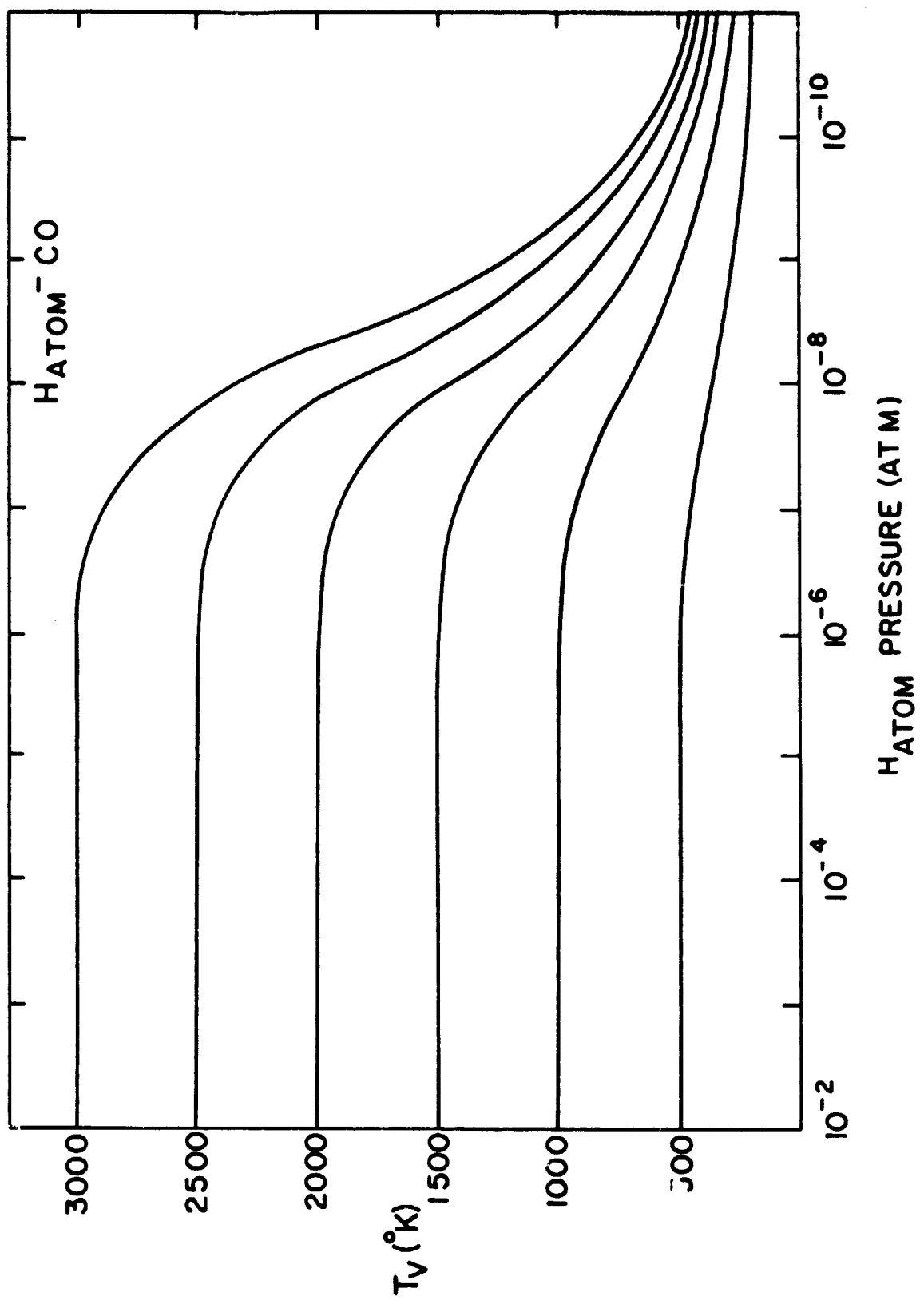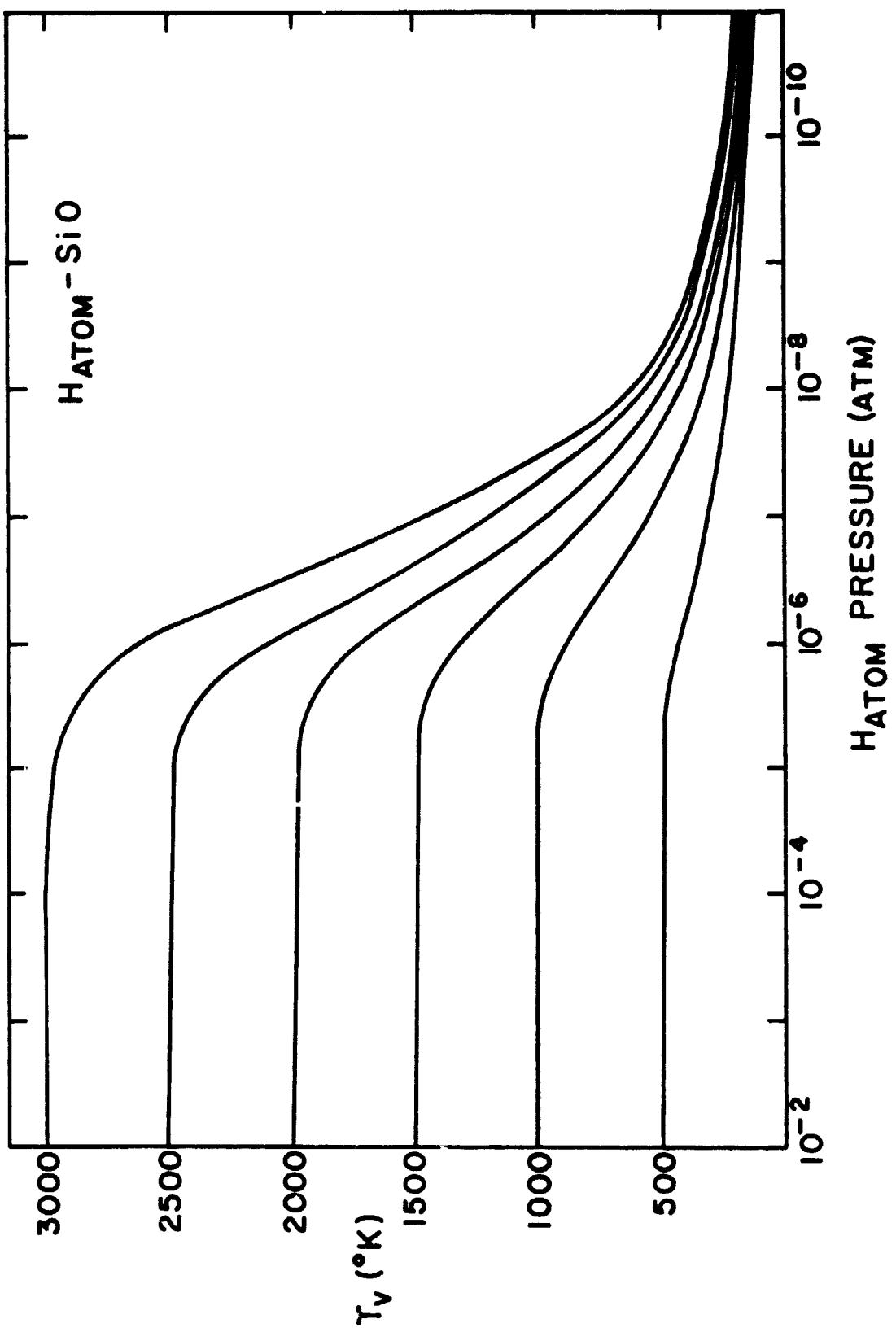10^{-2} 10^{-4} 10^{-6} 10^{-8} 10^{-10}

Figure 3. SiO vibrational temperature as a function of total pressure in an H-atom gas. Each line represents a calculation at the gas kinetic temperature of the T_v intercept, W = 0.
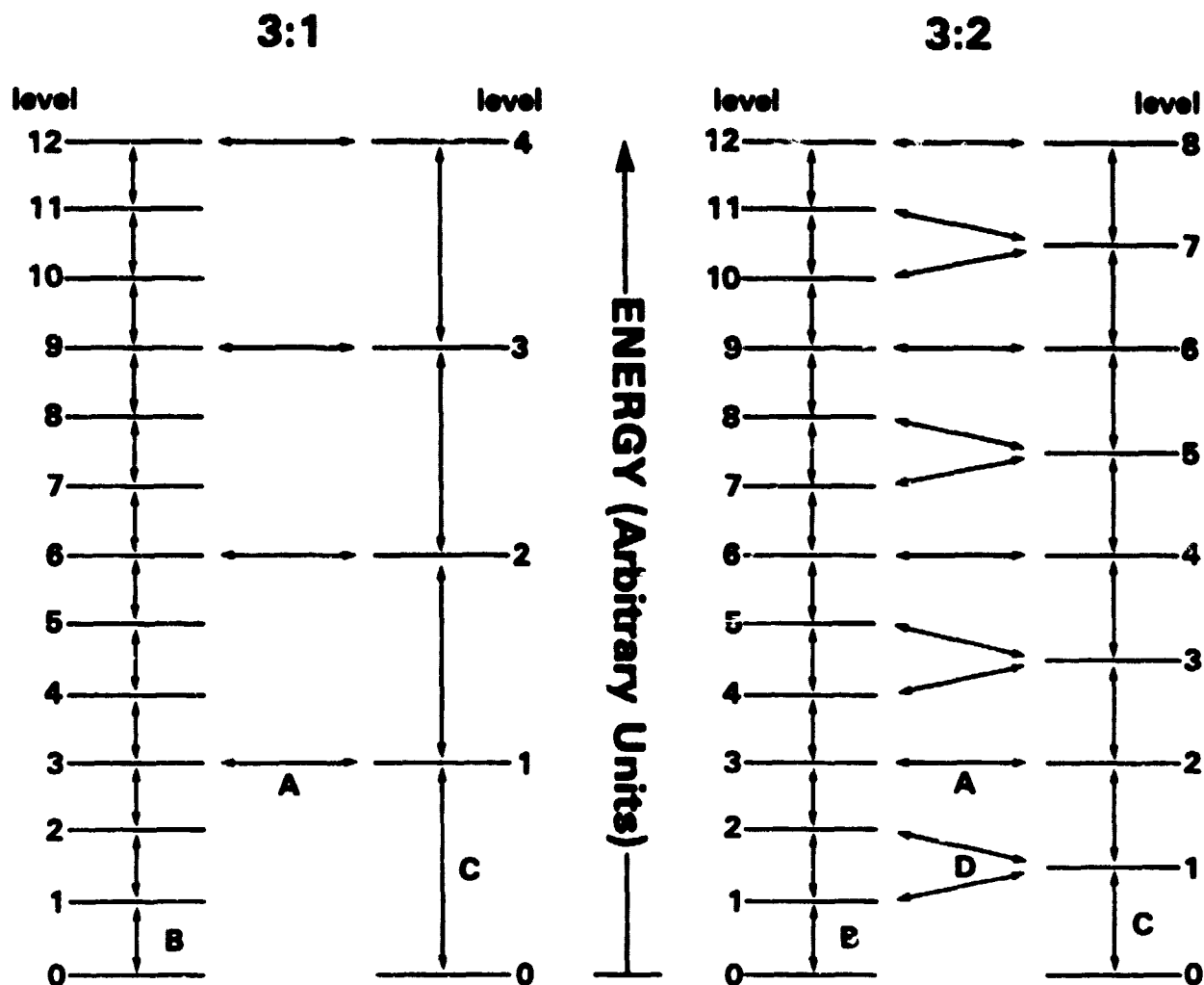
$H_{ATOM}-SiO$

IV. Disequilibrium of Polyatomic Molecules

The extreme vibrational disequilibrium found for diatomic molecules in clouds and its consequences for dissociation (Dalgarno and Roberge, 1979) calls for an investigation of the vibrational behavior of polyatomic molecules. These more complex species with many vibrational modes cannot be analysed as accurately as can diatomic molecules (McDonald, 1979). Lambert (1962, 1977) reviewed intramolecular vibrational energy conversion. Generally, the relaxation process can be characterized by a single rate, indicating rapid collisional internal energy transfer, if the energy of the more energetic fundamental is less than twice that of the lesser. Otherwise each mode has a separate relaxation rate.

In order to carry out an analysis for polyatomic molecules similar to that for diatomics we used a hypothetical molecule with two fundamental modes. In our initial calculations the energy of mode 2 was assumed to equal three times the energy of mode 1. We then assume that collisionally induced energy exchange between modes is relatively rapid compared to other relaxation processes (Figure 4). This is based in part on Lambert's discussion cited earlier and in part on the effectiveness of internal energy transfer when long lived complexes are formed (McDonald, 1979). The latter appears possible in atom-molecule collisions. We also assume that our hypothetical molecules are not excited in both vibrational modes simultaneously. We therefore ignore all transitions which would either originate or end in such a state. This greatly simplifies the kinetic equations

Figure 4. Schematic representation of transfer processes in hypothetical dual mode polyatomic models with a 3:1 and 3:2 ratio of vibrational fundamental energies.

MODEL POLYATOMIC MOLECULES

3:1

3:2

ENERGY (Arbitrary Units)

level ... 12 11 10 9 8 7 6 5 4 3 2 1 0

level ... 4 3 2 1 0

level ... 12 11 10 9 8 7 6 5 4 3 2 1 0

level ... 8 7 6 5 4 3 2 1 0

A   B   C

A   D   B   C

Rate of A >> B > C
No off resonance
transfer allowed

Rate of A >> D > B > C
Off resonance transfer
allowed (D)

B and C contain both collisional and radiative terms
A and D contain only collisional terms

which describe the steady state population distribution and allows us to treat seperately the high and low energy modes in a manner which is analogous to our treatment of diatomic molecules in equation (3) by the addition of terms of the form $N_x(G_{x,y}\delta_{3x,y})$ where $G_{x,y}$ is the rate of transfer between resonant levels of modes 1 and 2 and the Kronecker delta allows transfer between modes only at resonance. The validity of this assumption will be discussed at the end of this section after the model and its results have been presented.

Because of rapid intermode relaxation and the occurrence of several high energy modes in polyatomic molecules (Herzberg, 1945) our two mode molecules can be taken as an approximate representation of real, more complex polyatomics. To calculate the vibrational distribution we allow the following set of relaxation processes: (1) radiative excitation and de-excitation involving adjacent levels within a mode; (2) similar collisional processes and (3) rapid internal energy transfer between modes near resonance. Our initial treatment assumes that (3) is much more rapid than either (1) or (2). We therefore obtain the steady state populations in mode 1 from equation (9)

$$\frac{dN_x}{dt} = N_{x+1}(A_{x+1,x}+C_{x+1,x}+I_{x+1,x}) + N_{x-1}(C_{x-1,x}+I_{x-1,x}) + N_y(G_{y,x}\delta_{3x,y})$$
$$- N_x(A_{x,x-1}+C_{x,x-1}+I_{x,x-1}+A_{x,x+1}+C_{x,x+1}+G_{x,y}\delta_{3x,y}) = 0 \qquad (9)$$

where the subscript x indicates vibrational levels of the low energy mode, and the subscript y indicates levels of the high energy mode. Similarly equation (10) was used to obtain the steady state populations in mode 2.
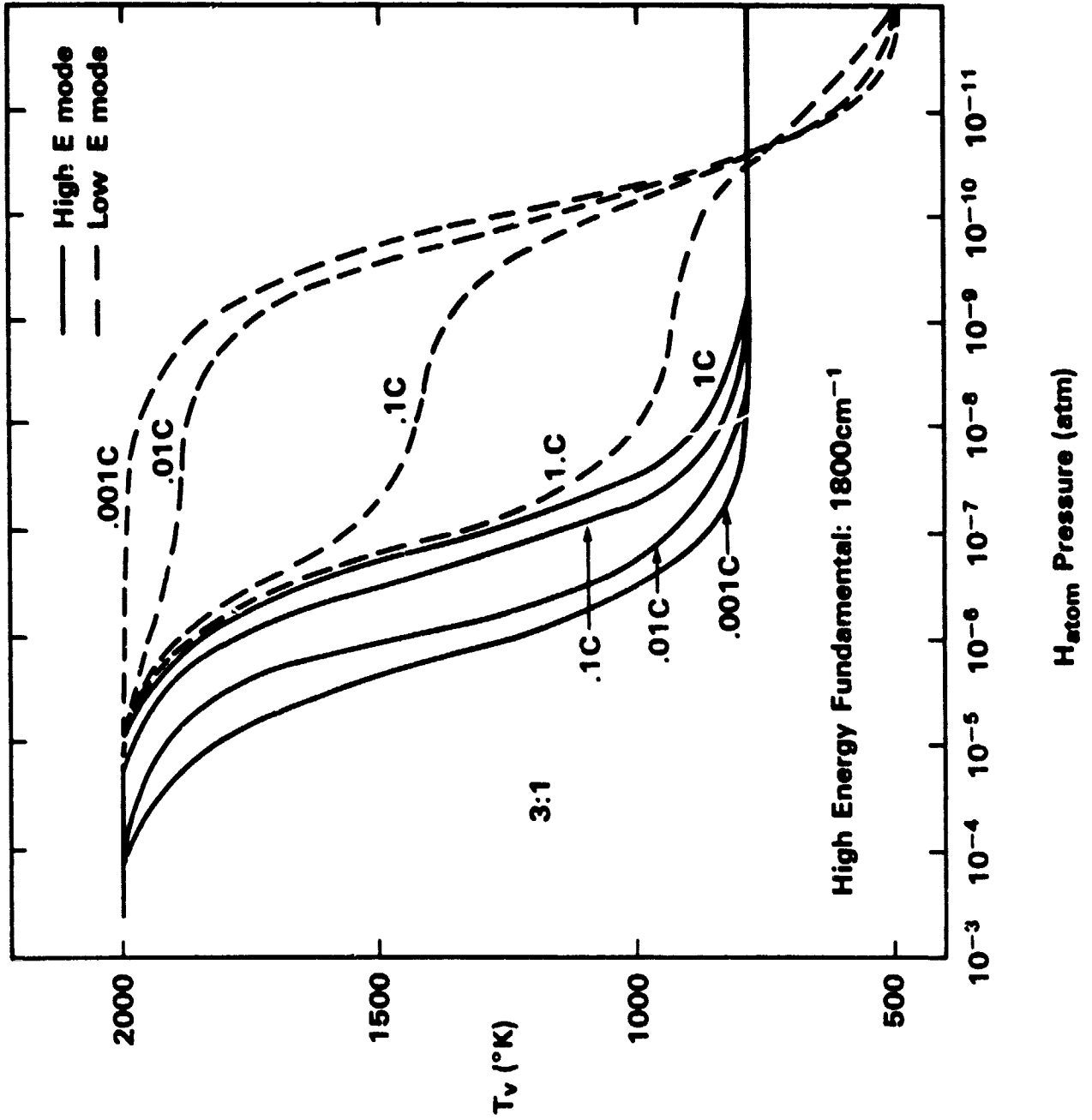
$$\frac{dN_y}{dt} = N_{y+1}(A_{y+1,y} + C_{y+1,y} + I_{y+1,y}) + N_{y-1}(C_{y-1,y} + I_{y-1,y}) + N_x(G_{x,y}\delta_{3x,y})$$
$$- N_y(A_{y,y-1} + C_{y,y-1} + I_{y,y-1} + C_{y,y+1} + I_{y,y+1} + G_{y,x}\delta_{3x,y}) = 0 \qquad (10)$$

In this case, every level in the high energy mode will be in resonance with a low energy mode.

Figure 5 is a typical plot of the vibrational temperature of our hypothetical dual mode polyatomic molecule as a function of H atom pressure. The plot was generated in the same way as were those for the diatomic molecules using the following parameters; $T_{kinetic}$ = 2000 K, W = 0.1; mode 1, ω = 1800 cm^{-1}, TM = 10^{-19}; mode 2, ω = 600 cm^{-1}, TM = 10^{-20} cm^{-1}; molecular weight of polyatomic molecule = 60. Each of the upper four curves represents the vibrational temperature of the low energy fundamental when the rate of intermode transfer (Process A in Figure 4) is set at 10^{-3}, 10^{-2}, 10^{-1} and 1 times the collision rate (C). Similarly each of the lower curves represents the temperature of the higher energy mode at these same intermode transfer rates.

In contrast to our diatomic calculations, temperatures of various levels in a single mode normally differ by up to about 30% from the average. As coupling between the modes is increased this discrepancy increases until in the highly coupled systems the lowest levels of the low energy mode are at considerably higher temperature than are the upper levels. These upper levels have temperatures comparable to those of the high energy mode and are therefore far from equilibrium. It should be noted that variation of the molecular parameters used to

Figure 5. Vibrational temperature of 3:1 polyatomic model as a function of total pressure and intermode coupling efficiency. Upper curves are the temperatures of the low-energy fundamental, lower curves are the temperatures of the high energy fundamental.

High Energy Fundamental: 1800cm^{-1}

High E mode
Low E mode

.001C
.01C
.1C
1.C
1C
.1C
.01C
.001C

3:1

T_v (°K)

2000

1500

1000

500

H_{atom} Pressure (atm)

10^{-3} 10^{-4} 10^{-5} 10^{-6} 10^{-7} 10^{-8} 10^{-9} 10^{-10} 10^{-11}

128

generate Figure 5 does not change the general trends. For instance, decreasing the energy or transition moment for either mode still shifts the curves to lower pressures. Similarly, increasing W would set a lower limit to the vibrational temperature as in the case of CO or SiO, without effecting the pressure at which non-LTE effects begin. However, variation of the collisional efficiency can no longer be compensated for by a simple shift of the pressure scale since this change now effects the relative importance of processes (2) and (3).

It might be argued that our model allows too few intramolecular transitions to give an accurate representation of the upper levels of the molecule. However, the addition of more intramolecular transitions should tend to increase the rate of depopulation of the upper levels by allowing quicker access to the higher energy transitions which first depart from thermal equilibrium. In this respect our model appears biased towards thermal equilibrium, yet significant non-LTE effects are observed.

In order to test the above hypothesis and so that we might have data on the behavior of systems where the ratio of the fundamentals is less than two to one, we constructed a model in which every third level of the lower energy mode was in resonance with every second level of the higher energy fundamental (Figure 4). We then calculated the vibrational temperatures for two cases.

In the first case we allowed only resonant intermode transfer. In the second we allowed both resonant tranfer and non-resonant

intermode transfer. The rate of non-resonant tranfer was calculated using the formula of Millikan and White (1963) and the appropriate energy difference between levels. In both cases we observe significant departure from LTE as the pressure and radiative dilution coefficient decrease. However, when off resonant transfer was allowed we find that vibrational temperatures in the transition region were significantly (>15%) lower than when these transitions were forbidden. As the pressure continues to decrease however, the vibrational temperatures of these two cases converge. It should also be noted that the onset of non-LTE effects occurs at virtually the same pressure in both calculations, only the degree of disequilibrium in the transition region is effected.

We now discuss our assumption that no molecule is simultaneously excited in both vibrational modes. Only about twenty percent of an equilibrium distribution of our 3:1 model polyatomic molecules $(\omega_1=1800\text{cm}^{-1},\omega_2=600\text{cm}^{-1})$ at a temperature of 2000K will be excited in both vibrational modes. As the vibrational temperature of the molecule decreases with decreasing pressure and radiation density this fraction rapidly approaches zero. Furthermore, inclusion of all of the transitions which were excluded by this assumption would simply increase the coupling between vibrational modes. We have shown in Figure 5 that as the coupling between modes increases, the vibrational temperatures of the modes approach one another. Inclusion of these transitions would therefore not tend to keep any mode in thermal equilibrium. Since we are not attempting to calculate exact vibrational temperatures for any specific molecule, but instead are

interested in discovering the general trend of polyatomic molecules in regions of low pressure and radiation density, we feel that this assumption has little effect on our conclusions. We emphasize again that these model polyatomic molecules are used only as an aid to understand the effects of interaction between coupled modes in a large molecule.

We are concerned primarily with the effects of vibrational disequilibrium on chemical equilibrium and grain nucleation. Thermal dissociation is a major process in such phenomena and occurs mainly from vibrationally excited molecules in states near the dissociation limit (Kondrat'ev, 1964). Unimolecular dissociation experiments (Rabinovich and Tardy, 1977) show that extremely rapid intramolecular energy transfer ($^{\sim}10^{-12}$s) occurs above the dissociation limit. In addition, high vibrational levels are more closely spaced than are lower ones. This tends to increase the importance of near resonant transitions in intermode energy transfer. A third effect is that at high vibrational energies the molecule becomes appreciably distorted and a normal mode description is no longer applicable. Recent discussions of molecules in such highly excited states are given by McDonald (1979) and Rice (1975).

Our treatment of the lowest vibrational levels of polyatomic molecules indicates that a considerable degree of disequilibrium can be expected in regions of low pressure and radiation density. Because such disequilibrium increases as the coupling between vibrational modes is increased and because such coupling increases as the modes

become increasingly excited, one should expect that the vibrational modes most likely to be out of equilibrium are those near the dissociation limit. Since these modes play a major part in the dissociation of polyatomic molecules and since our analysis tends to underestimate the importance of vibrational disequilibrium in polyatomic systems, polyatomic molecules are expected to be more abundant in regions of low pressure and radiation density than would be expected on the basis of equilibrium kinetic or thermodynamic calculations.

V. Discussion of Results by Region

a) Atmospheres of Cool Stars, Circumstellar Shells and Planetary Nebulae. In these regions, H atom collisions will be the dominant contributor to translation-vibration relaxation. Figures 2 and 3 are applicable in such regions.

It can easily be seen from Figure 2 that CO is significantly out of equilibrium at pressures less than 10^{-8} atm. Because we have deliberately overestimated the efficiency of collisional relaxation, this should be an underestimate of the disequilibrium in the system. From Figure 3 we see that SiO begins to depart from equilibrium at pressures less than 10^{-6} atm. If SiO-H atom collisions are more efficient than predicted by Millikan and White (1963) then these curves will overestimate the disequilibrium in the system. By using the proceedure previously discussed, if H atom-SiO collisions were

found by experiment to actually be 10^3 more efficient than predicted by Millikan and White (1963) then the pressures in Figure 3 would be multiplied by 10^{-3}. SiO vibrational populations would then depart from equilibrium at pressures less than about 10^{-9} atm.

As can be seen from Figures 2 and 3 it is likely that CO and SiO will only be significantly in disequilibrium in the uppermost regions of cool stars. This is consistent with the conclusions of Carbon et al. (1976). According to Figure 5 and the previous discussion, this behavior will also apply to most polyatomic species. However, in the lower pressure environment more characteristic of circumstellar shells where pressures are expected to be in the range 10^{-11}–10^{-12} atm. (Hagen, 1978) both CO and SiO will significantly depart from thermal equilibrium. Similar departures should occur in the low pressure grain forming stage of an evolving planetary nebula where pressures are of order 10^{-10} atm. (Draine, 1979). For these regions the color temperature of the stellar radiation field and the kinetic temperature of the gas should be comparable during the epoch of grain formation.

b) <u>Novae and Supernovae</u>. Vibrational relaxation in expanding novae envelopes, and to a lesser degree in the outer envelopes of supernovae, will be dominated by H atom collisions. Therefore, Figures 2 and 3 also apply to these regions. In regions where H atoms are effectively absent, such as the innermost zones of supernovae, metallic atom collisions dominate. In an intermediate zone, O atom or CO molecule collisions could be the dominant interaction. Figures 6, 7 and 8 are applicable for Fe, O or CO rich environments respectively.

Figure 6. CO vibrational temperatures as a function of total pressure in an Fe-atom gas. Each line represents a calculation at the gas kinetic temperature of the T_v intercept, $W = 0$.

Fe$_{ATOM}$-CO

T_V(°K)

3000

2500

2000

1500

1000

500

Fe$_{ATOM}$ PRESSURE (ATM)

10^2 10^0 10^{-2} 10^{-4} 10^{-6}
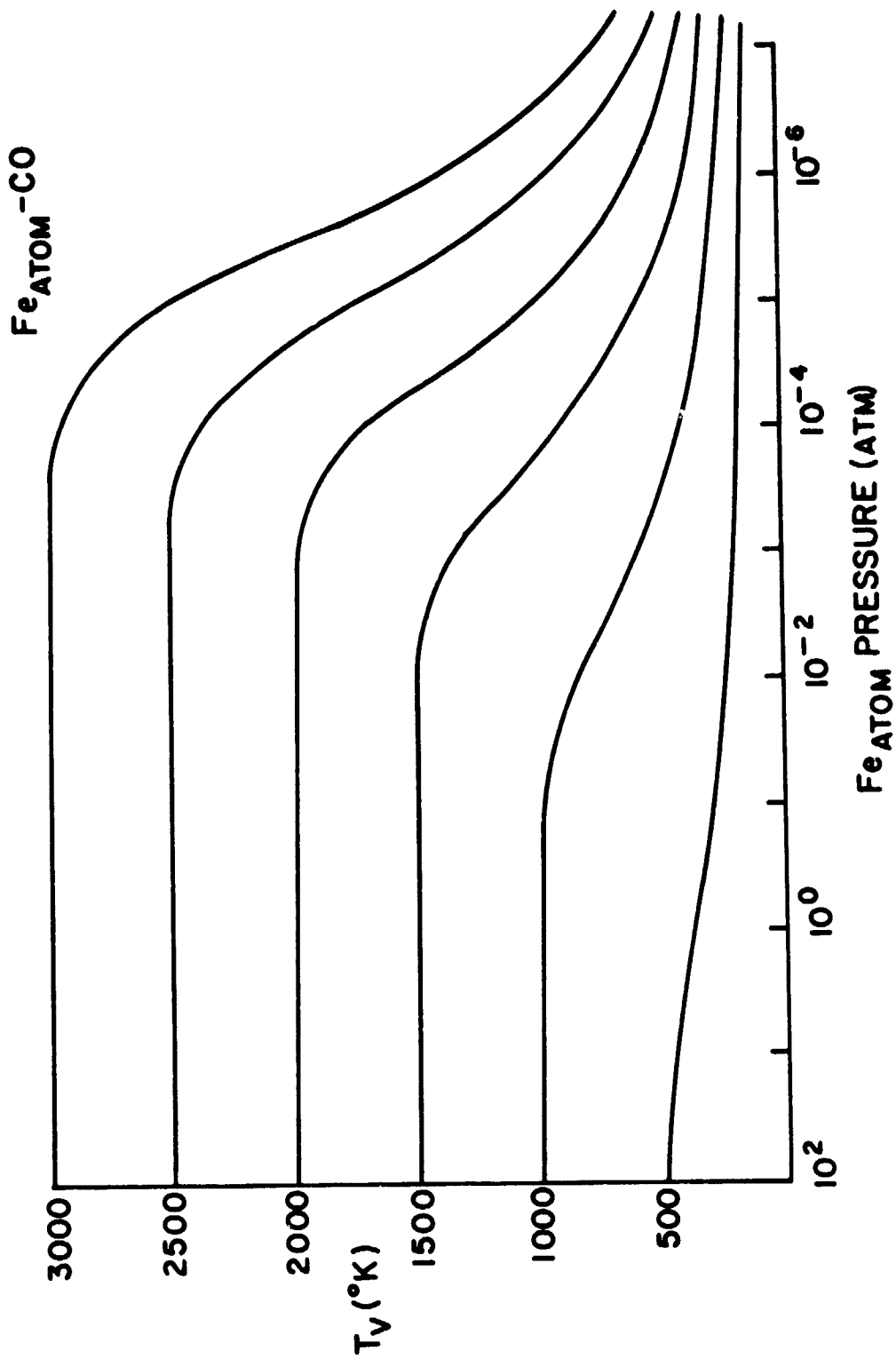
135

Figure 7. CO vibrational temperature as a function of total pressure in an O-atom gas. Each line represents a calculation at the gas kinetic temperataure of the T_v intercept, $W = 0$.
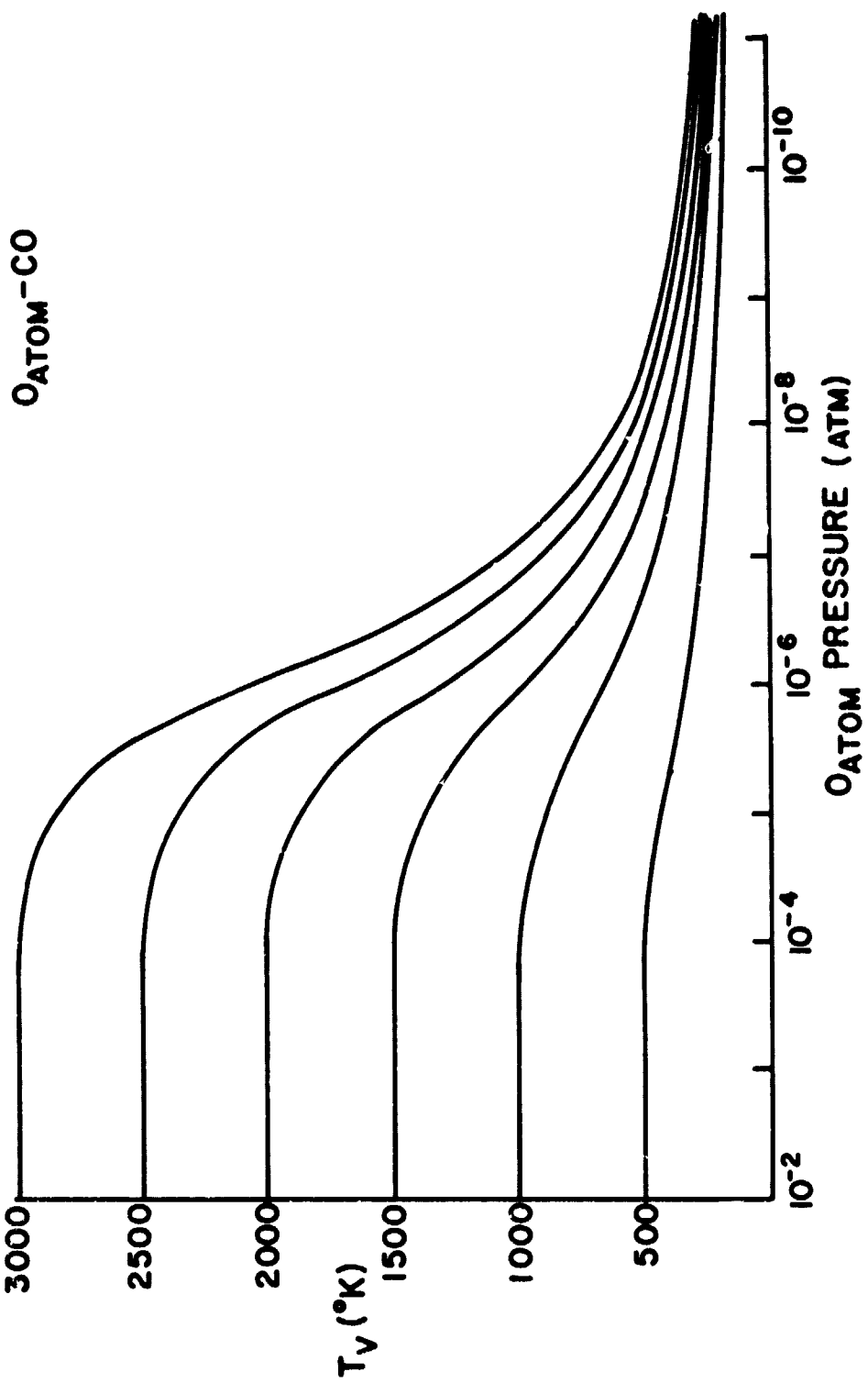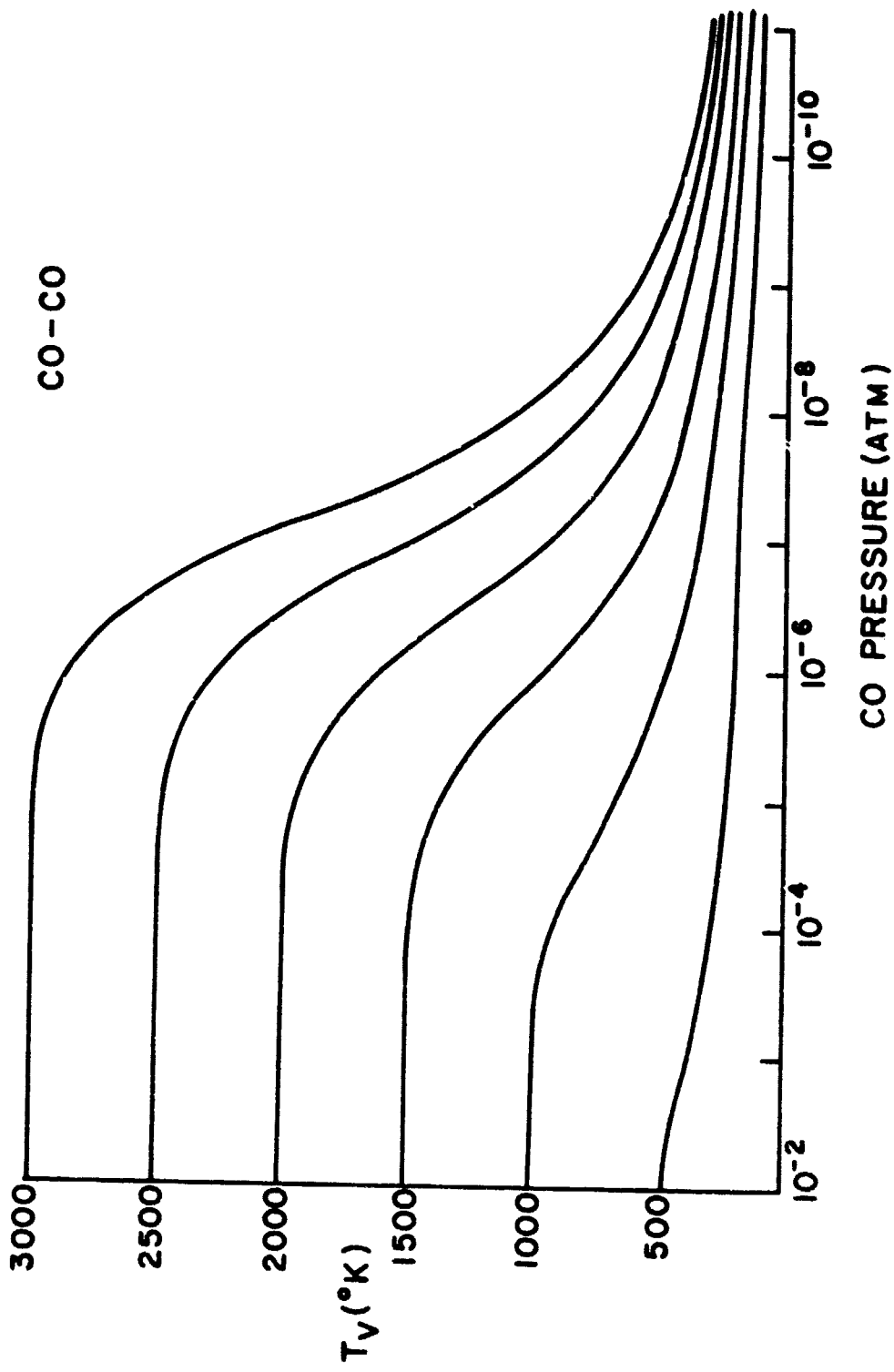
Figure 8. CO vibrational temperature as a function of total pressure in a CO-molecule gas. Each line represents a calculation at the gas kinetic temperature of the T_v intercept, W = 0.

CO – CO

$T_V (°K)$

CO PRESSURE (ATM)

Photospheric temperatures for novae are of order 10^4K at the time of observed grain condensation (Sparks, Starrfield and Truran, 1978). The dust condenses at $r \sim 5\times10^{14}$ cm (Ney and Hatfield, 1978) whereas the photosphere occurs at $r \sim 2\times10^{12}$ cm (Sparks, Starrfield and Truran, 1978). The ultraviolet flux ($\lambda < 2000$ Å) is comparable to that at the surface of a 4000K star and electronic transitions can be ignored. The energy density in the infrared ($\lambda > 1$ micron) on the other hand is only a few percent of the 4000K black body flux. Condensation of grains is generally postulated at pressures near 10^{-10} atm. Under these conditions the system should significantly depart from equilibrium.

Supernovae photospheric temperatures at the time of condensation ($t \sim 10^7$ sec) are approximately $5-7\times10^3$K (Kirshner et al., 1973). At this time the outermost zone of ejecta will be at a radius 15-100 times larger than the photosphere (Arnett and Falk, 1976). The innermost material (at $r \sim 15$ $r_{phot.}$) will experience a UV flux which is comparable to that on the surface of a 4000K star so that electronic transitions can again be ignored. As in the case of novae, the infrared flux will be only a few percent f that of a 4000K black body. Pressures will be below 10^{-10} atm. Condensation would therefore occur in a system which is again out of thermal equilibrium.

c) Primitive Solar Nebula. Figures 2 and 3 apply to models of the primitive solar nebula. Because of the enhanced efficiency of non-adiabadic H atom collisions it appears probable that many, if not

all, molecular species will be in thermal equilibrium under the conditions predicted in most models of the nebula (see for instance Cameron and Pine, 1973; Cameron, 1978). Only the lowest pressure regions ($p \lesssim 10^{-7}$ atm) will show non-equilibrium population distributions.

VI. Discussion of Results: Molecular Distributions

a) Molecular Parameters. In systems containing numerous molecular species, many combinations of molecular parameters are possible. A molecule with low Einstein A and relatively high C_{10}, which would be the characteristics of a species with small dipole moment and a low fundamental vibration frequency, would remain close to equilibrium even at relatively low pressures. Conversely, one with high A and relatively low C_{10} - a species with a high dipole moment and more energetic vibration fundamental - would depart from an equilibrium vibrational distribution at higher pressures. Therefore, different molecular species in a particular region might be expected to be out of equilibrium to different degrees.

For diatomic molecules it is possible to estimate the vibrational temperature of a particular molecular species if one knows both the transition moment (TM) and vibrational fundamental (ω) by the use of Figures 9 and 10. Figure 9 is a plot of the vibrational temperature of a diatomic molecule as a function of H atom pressure in the absence of radiation at a gas kinetic temperature of 2000K for lines of constant transition moment. The molecular weight and vibrational

Figure 9. Vibrational temperature as a function of H atom pressure at a gas kinetic temperature of 2000K in the absence of radiation for lines of constant transition moment. All other molecular parameters are those of CO.
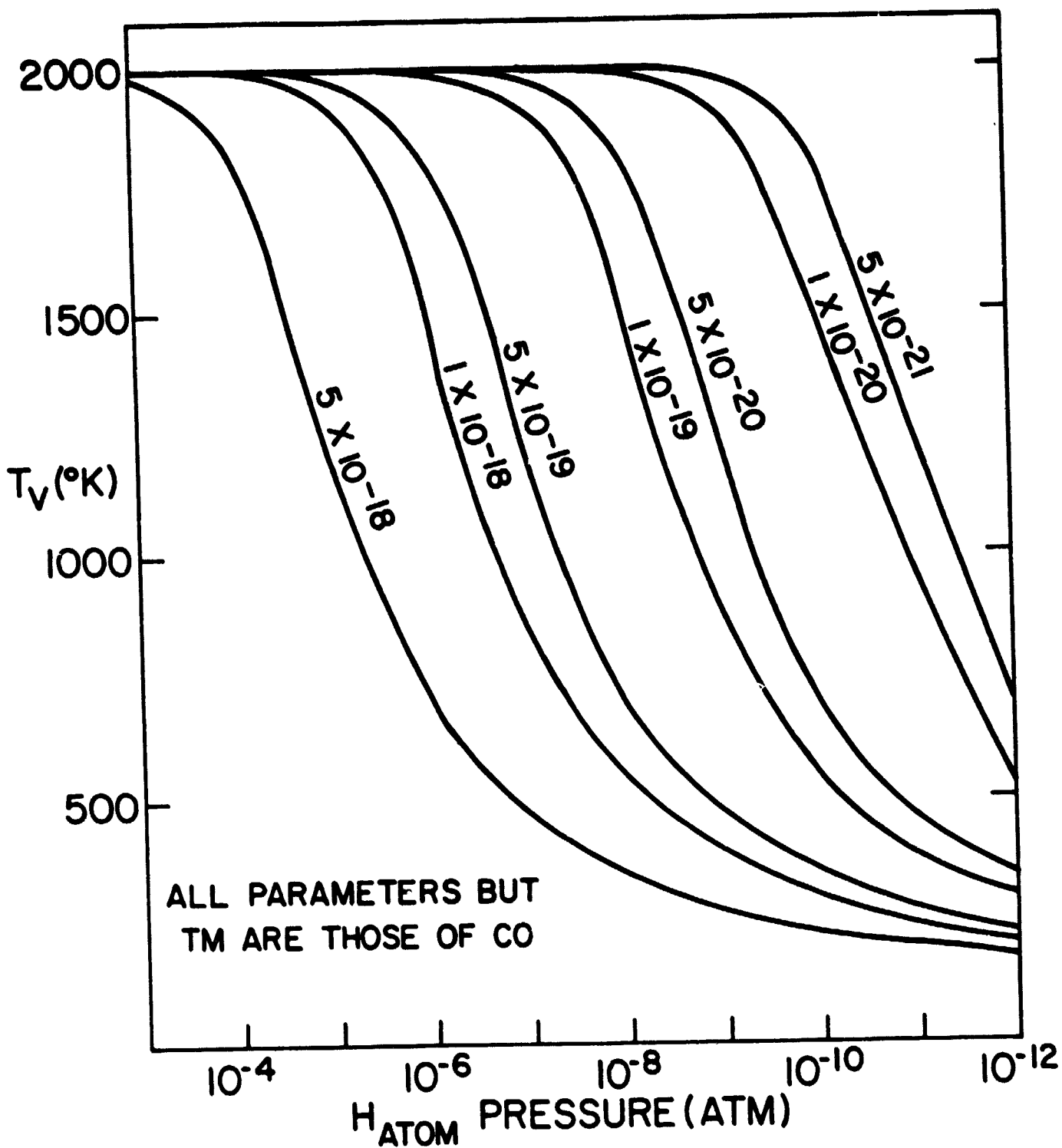
fundamental are those of CO. Figure 10 is a similar plot for lines of constant ω. Again the molecular weight and transition moment are those of CO. For both figures the $C_{1,0}$ calculated from the work of Millikan and White (1963) has been multiplied by 10^3 and should therefore underestimate the vibrational disequilibrium of the system. The use of the molecular weight of CO in the calculation introduces no error into our estimate since only the reduced mass of the colliding system is of importance. Since we already assume that all collisions are with atomic hydrogen this term is very nearly unity for most molecules of interest.

The following procedure will yield an approximate vibrational temperature for a diatomic molecule of known ω and TM. First find the line of constant transition moment corresponding to the molecule of interest on Figure 9 and note the difference (in units of pressure) between this line and that of CO (1×10^{-19}). Next, add or subtract this difference from the pressure scale of Figure 10. Now find the line of constant ω which corresponds to the vibrational fundamental of the molecule of interest and read the vibrational temperature as a function of H atom pressure directly from the previously modified pressure scale.

b) Non-Adiabadic Collisions. Relaxation of molecules via non-adiabadic electronic or "complex forming" reactive interactions (Smith, 1976) is again expected to depend specifically on the dominant colliding species. These species can vary in efficiency by factors of 10^4 (Glanzer and Troe, 1975) for the relaxation of the same molecule.

Figure 10. Vibrational temperature as a function of H atom pressure at a gas kinetic temperature of 2000K in the absence of radiation for lines of constant energy of the fundamental vibrational mode. All other molecular parameters are those of CO.
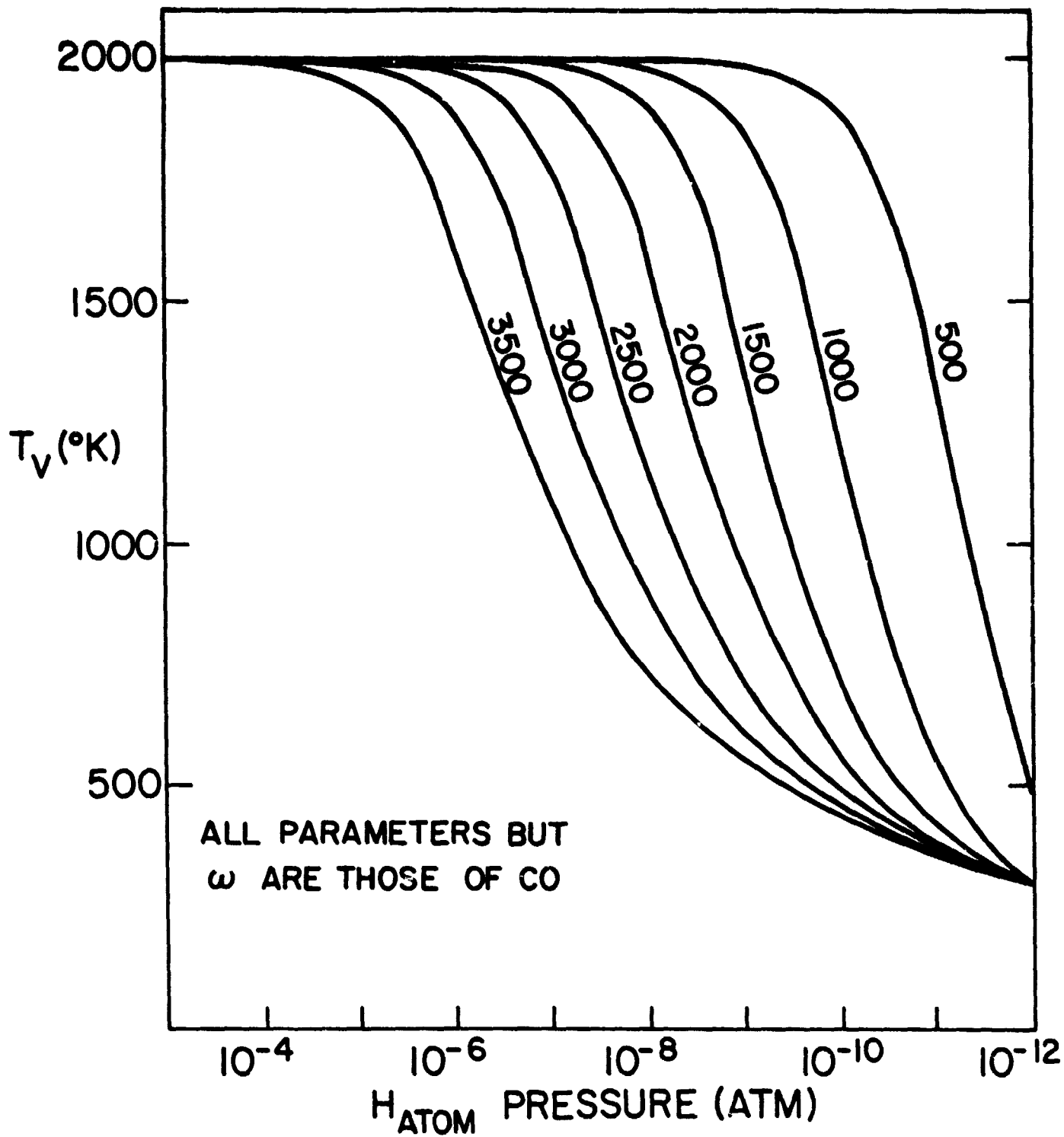
Although it seems likely that atomic hydrogen will be the dominant colliding species in most systems of astrophysical interest, few measurements have been made of its relaxation efficiency for molecules expected to occur in these regions. Such measurements are necessary before more exact calculations of the vibrational populations of these molecules is possible.

c) Assumption of Thermal Equilibrium. Molecular dissociation preferably occurs from the upper vibrational levels (Smith, 1976, Yau and Pritchard, 1979). If these levels are depleted for any reason, then the molecule is more stable with respect to its atomic constituents. This is amply demonstrated by the calculations of Dalgarno and Roberge (1979), cited earlier, which found that the molecular dissociation rate for CO and, to a lesser degree, for H_2, decreased by orders of magnitude as the total density decreased. Molecular equilibrium calculations, such as those by Tsuji (1964, 1973), can therefore not be applied to regions of lower pressure. It seems clear that new calculations which account for the varying degrees of vibrational disequilibrium in regions such as circumstellar shells, novae and planetary nebulae are called for. Before such molecular distribution calculations can be attempted however, one needs Einstein A values for ground electronic state vibration-rotation transitions and H atom-molecule relaxation efficiencies for each molecule of importance in the region under consideration. In addition, a suitable model of the rate of internal energy transfer for polyatomic molecules is required. Ideally, state selected reaction rates for individual vibrational levels should be used in such regions

147

although, due to the complexity of the systems, some suitable approximations might need to be made. Unfortunately, almost none of these data are currently available in the literature.

The implications of these results for grain condensation are considerable. The non-equilibrium character of nucleation for cosmic systems has been discussed in several papers (Donn, 1975, 1979a) and experimental evidence applicable to astronomical systems has been obtained (Day and Donn, 1978a, b). The analysis of the present chapter shows that the gas can deviate significantly from equilibrium before condensation begins. Thus, it is unlikely that classical nucleation theory is applicable. A procedure for treating condensation on a purely kinetic basis has been proposed by Donn (1979b) and is being developed further (Donn et al, 1980).

It is interesting to note that Arrhenius and De (1973) and De (1978) have determined that small grains embedded in a low density gas may be much cooler than their surroundings. The present work has indicated that many molecular species are similarly out of equilibrium at low pressures. The evidence is now compelling that thermal equilibrium in low density clouds is no longer an acceptable approximation. The extent to which such an assumption may be a useful approximation must be examined for the specific problem under discussion.

VII. Conclusions

Vibrational disequilibrium becomes increasingly significant in CO and SiO as the total density of particles and radiation decreases. Some degree of disequilibrium, which will depend on specific molecular properties will occur for most heteronuclear molecules—including polyatomic species—in low density clouds such as the expanding shells of cool stars, novae and supernovae. Previous work which assumed that thermodynamic equilibrium had been attained in such regions must be reexamined in light of the present calculations. Einstein A values and H atom relaxation efficiencies for di and tri-atomic metal hydrides, carbides, nitrides, oxides and sulfides are necessary before more accurate calculations of molecular abundances under these conditions can be made. Vibrational disequilibrium has significant implications for the calculation of many chemical processes and characteristics of low pressure, low optical depth regions.

References

Arnett, W. D. and Falk, S. W., 1976, Ap. J., <u>210</u>, 733.

Arrhenius, G. and De, B., 1973, Meteoritics, <u>8</u>, 297.

Cameron, A.G.W., 1978, Moon and Planets, <u>18</u>, 5.

Cameron, A.G.W., and Pine, M. R., 1973, Icarus, <u>18</u>, 377.

Carbon, D. F., Milkey, R. W. and Heasley, J. N., 1976, Ap. J., <u>207</u>, 253.

Center, R. E., 1973, J. Chem. Phys., <u>58</u>, 5230.

Chakarian, C., 1970, J. Quant. Spec. and Rad. Trans., <u>10</u>, 271.

Cottrell, T. L. and McCoubrey, 1961, <u>Molecular Energy Transfer</u>, butterworth's Inc., Washington, D. C.

Dalgarno, A. and Roberge, W. G., 1979, Ap. J., <u>233</u>, L25.

Day, K. L. and Donn, B., 1978a, Ap. J., <u>222</u>, L45.

Day, K. L. and Donn, B., 1978b, Science, <u>202</u>, 307.

De, B., 1978, in <u>Proc. 8th Lun. Sci. Conf.</u>, Pergammon Press, N.Y., p. 79.

Donn, B., 1976, Mem. Soc. Roy. Sci. Liege, Ser. 6, Tome IX, p. 499.

Donn, B., 1979a, in <u>Protostars and Planets</u>, ed. T. Gehrels, U. Ariz. Press, Tucson, p. 100.

Donn, B., 1979b, EOS, Trans. Am. Geophys. Union <u>60</u>, 300.

Donn, B., Hecht, J., Khanna, R., Nuth, J., Stranz, D. and Anderson, A., Surface Science, <u>106</u>,546

Draine, B. T., 1979, Astrophys. Space Sci., in press.

Geballe, T. R. and Wollman, E. R., 1972, Ap. J., <u>177</u>, L27.

Glanzer, K. and Troe, J., 1975, J. Chem. Phys., <u>63</u>, 4352.

Hagen, W., 1978, Ap. J. Supp., 38, 1.

Hedelund, J. and Lambert, D. L., 1972, Astrophys. Lett., 11, 75.

Herzberg, G., 1975, Molecular Spectra and Molecular Structure: II.
Infrared and Raman Spectra of Polyatomic Molecules (Van Nostrand
Reinhold Company, New York, 1945).

Herzfield, K. E. and Litovitz, T. A., 1959, Absorbtion and Dispersion
of Ultrasonic Waves, Academic Press, N.Y.

Kirshner, R. P., Oke, J. B., Penston, M. V. and Searle, L., 1973, Ap.
J., 185, 303.

Kondrat'ev, V. N., 1964, Chemical Kinetics of Gas Reactions, Pergammon
Press, N. Y., page 271

Lambert, J. D., 1962, in Atomic and Molecular Processes, ed. D. R.
Bates (Academic Press, New York, 1962) Chap. 20.

Lambert, J. D., 1979, Vibrational and Rotational Relaxation in Gases,
(Clarendon Press, Oxford, 1977).

Lattimer, J. M., Schramm, D. N. and Grossman, L., 1978, Ap. J., 219,
230.

MacDonald, R. G. and Moore, C. B., 1978, J. Chem. Phys., 68, 513.

Millikan, R. C. and White, D. R., 1963, J. Chem. Phys., 39, 3209.

Ney, E. P. and Hatfield, B. F., Ap. J., 219, L111.

Nikitin, E. E., 1974, in Physical Chemistry, An Advanced Treatise,
eds. H. Eyring, D. Henderson and W. Yost, Vol. 6A, Academic Press,
N.Y.

Penner, S. S., 1959, Quantitative Molecular Spectroscopy and Gas
Emissivities, Addison-Wesley, Reading, Mass.

Rabinovitch, B. S. and Tardy, D. C., 1977, Chem.Rev.,77, 369

Rice, S. A., 1975, in Excited States Vol. 2 ed. E. C. Lim, Academic Press, N.Y. page 111

Rubin, R. J. and Schuler, K. E., 1956a, J. Chem. Phys., 25, 59.

kubin, R. J. and Schuler, K. E., 1956b, J. Chem. Phys., 25, 68.

Rubin, R. J. and Schuler, K. E., 1957, J. Chem. Phys., 26, 137.

Salpeter, E. E., 1977, Ann. Rev. Astron. Astrophys., 15, 267.

Smith, I.W.M., 1976, Acc. Chem. Res., 9, 161.

Sparks, W. M., Starrfield, S. and Truran, J. W., 1978, Ap. J., 220, 1063.

Thompson, R. I., 1973, Ap. J., 181, 1039.

Tsuji, T., 1964, Ann. Tokyo Ast. Obs., 9, 1.

Tsuji, T., 1973, Astron. and Astrophys., 23, 411.

von Rosenberg, C. W., Taylor, R. L. and Teare, J. D., 1971, J. Chem. Phys., 54, 1974.

von Rosenberg, C. W. and Wray, K. L., 1971, J. Chem. Phys., 54, 1406.

West, G. A., Weston, R. E. and Flynn, G. W., 1977, J. Chem. Phys., 67, 4873.

Yau, A. W. and Pritchard, H. O., 1979, J. Phys. Chem., 83, 134.

Chapter 4.

Extinction Measurements of Small Iron and Magnetite Grains

Both Iron (Fe) and Magnetite (Fe_3O_4) have previously been proposed as constituents of interstellar grains (Huffman, 1977). Fe grains have been proposed on the basis of cosmic abundance (Schalen,1936), as a universal condensate (Lewis and Ney, 1979), and as a possible cause of the 4.6 μ^{-1} (220 nm) feature in the Interstellar Extinction curve (Huffman, 1977). Fe_3O_4 has been considered because it has been found in meteorites and because it is a possible cause of the Very Broad Structure in the Interstellar Extinction curve (Huffman, 1977; Whittet, 1981). If either type of magnetic grain exists it would help to explain the polarization of starlight which is thought to be caused by grains aligned by the interstellar magnetic field (Huffman, 1977).

This chapter reports laboratory measurements of the optical properties of Fe and Fe_3O_4 grains. These results are discussed in terms of the effect of such particles on the extinction observed in the interstellar medium or in circumstellar shells. Special regard is given to the recent reports of anomalous extinction curves which lack the 4.6 μ^{-1} feature. This chapter represents a collaborative effort between Dr. James Hecht (NASA/NRC Resident Research Associate at Goddard Space Flight Center) and myself. Dr. Hecht performed

theoretical Mie calculations on small iron and magnetite particles. My primary responsibility was to obtain the experimental extinction and size distribution measurements.

II. Experimental Procedure

The thermal dissociation of iron pentacarbonyl, via the reaction $Fe(CO)_5 \rightarrow Fe + 5CO$, occurs at temperatures in excess of $200^{\circ}C$ (Mellor, 1962). The reaction produces an extremely supersaturated iron vapor which quickly nucleates (Frurip and Bauer, 1977) yielding solid iron particles. In our experiments very small iron grains ($\sim 25nm$ in radius) were produced by the thermal decomposition of dilute mixtures of $Fe(CO)_5$ in either an argon or hydrogen carrier gas. Dilution was such that $1:10 > Fe(CO)_5$: Carrier Gas $> 1:1000$. Total pressures were from 10-50 torr. Dissociation occured at temperatures in excess of $275^{\circ}C$ and was accomplished as follows.

Carrier gas, the flow rate of which was regulated by a needle valve, was allowed to flow into a flask containing $Fe(CO)_5$. The flask was immersed in a slush bath to regulate the partial pressure of $Fe(CO)_5$. The use of various slush baths yielded a range of $Fe(CO)_5$ pressures between 0.05 torr (chloroform slush) and 2.6 torr (benzyl Alcohol slush) in discrete steps. The gas mixture was then allowed to flow into the bottom of a furnace which was enclosed within a 150 l stainless steel bell jar. Constant pressure was maintained within the

system by pumping at the top of the furnace using an auxiliary mechanical pump. Before each run the bell jar was pumped for at least two hours, and in most cases overnight, to pressures less than 5 X 10^{-5} torr at temperatures in excess of $300^{\circ}C$.

The furnace is a resistively heated mullite cylinder 6 inches in diameter and 18 inches high through which four equidistant, equatorial, one inch diameter, holes had been drilled. Six inch long, one inch ID alumina tubes had been inserted into each hole and aligned with the four window ports of the bell jar so that the interior of the furnace could be viewed. These tubes eliminated significant perturbation of the temperature profile of the system. A 300W Xe arc lamp was placed in front of one of the MgF_2 windows and qualitative observations of the smoke color and intensity could be obtained by looking through the window port which was 90° to the lamp port. By using a polarizing filter an estimate could also be made of the polarization of the light scattered by the smoke through an angle of 90° to the incident beam. Extinction measurements were made by placing a monochromator by the port opposite to the lamp port.

Measurements were made with a 0.3m scanning monochromator in the range from λ^{-1} between 1.4-5.1μ^{-1}(λ between 190-650nm). A steady rate of particle production was established within the system and an extinction spectrum I_{ext} (λ) was recorded. The system was then mechanically pumped to remove all particles from the gas phase and an unobscured lamp spectrum, I_0 (λ) was taken. The quantity in (I_0/I_{ext}) is proportional to the extinction of the smoke. Because of the

155

large range in the intensity of the Xe lamp, measurements were made in eight spectral ranges and scaled to one another in regions of mutual overlap. The results, shown in Fig. 1, will be discussed in a later section. A broadband filter (FWHM=40nm) centered at $4.6\mu^{-1}$(216nm) was used to obtain the data for $\lambda^{-1} > 4.3\mu^{-1}$($\lambda < 235$nm). This filter, placed before the entrance slit, eliminated background caused by scattering of visible light within the monochromator.

Particles collected during our runs and analyzed by x-ray diffraction within several hours of their production were found to consist of α-Fe, Fe_3O_4, and γ-Fe. We believe that the Fe_3O_4 either formed in transfer to the diffraction apparatus or from low level O_2 contamination which reacted with Fe particles on the walls of the system. This could have occurred during the two hour period while the system was cooling to room temperature. Granqvist and Buhrman (1976) also reported finding Fe_3O_4 in their Fe particles even under extremely clean conditions. We do not feel that such contamination could have affected our measurements of Fe particle extinction for the following reason.

Our measurements involved only those grains suspended in the gas phase. Observations indicated that the residence time of individual particles, in the gas phase, was on the order of minutes even at the highest system pressure used. As the particles settled or were pumped away they were replenished by freshly nucleated grains. The leak rate necessary to oxidize a measurable fraction of these grains on this short time scale would be comparable to the rate at which $Fe(CO)_5$ was

Figure 1. Experimental data points represent measurement of extinction vs λ^{-1} from 1.5 to 6.0 μ^{-1} in eight overlapping spectral regions (see text). The light scattered at 90° was 100% polarized in all spectra. Overlapping points are scaled to one another. The absolute scaling of the extinction is arbitrary. The solid (dashed) line represents calculations using JC(MO) data, as described in the text, of E, the extinction per unit length. For the JC calculation the point at 2.5μ^{-1} is arbitrarily fit to the data. For MO the point at 5.0 μ^{-1} is arbitrarily fit.
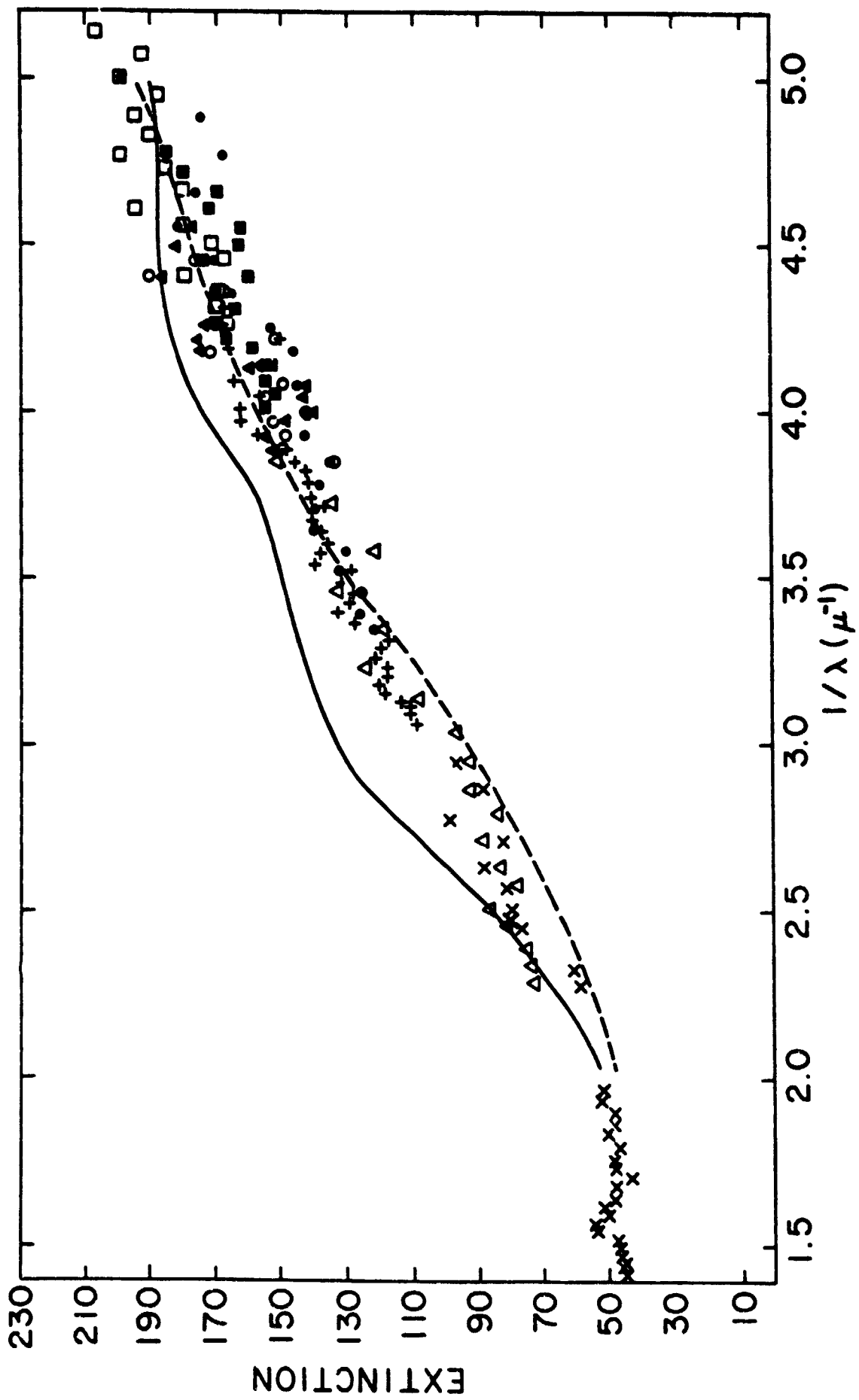
introduced into the furnace. Such a leak rate would have made it impossible to pump the system below 10 microns much less below 10^{-5} torr.

Particles allowed to accumulate on the walls of the furnace for two weeks at temperatures greater than $300^{\circ}C$ were found to be pure Fe_3O_4. Analysis by a scanning electron microscope (SEM) indicated that a typical particle had a radius of 25nm although 5-10% of the total had radii as large as 50nm. A considerable amount of clumping could be seen in the SEM photographs although we feel, because of polarization measurements discussed later, that most, if not all, of this occurred on the walls rather than in the gas phase.

The extinction spectra of the Fe_3O_4 grains collected from our system was obtained by first dispersing them in ethanol and then despositing this on a clean sapphire window. The ethanol evaporated and I_{ext} was recorded. The window was then cleaned and I_o was taken. Ln (I_o/I_{ext}) is shown in Fig. 2 and discussed later.

Finally, measurements of ln (I_o/I_{ext}) were made for large (> 50 nm radius) Fe particles using a low dispersion (14nm/mm) monochromator equipped with an optical multichannel analyzer. This allowed the acquisition of spectra, in the range of $1.2\mu^{-1}$ (830nm) to $2.65\mu^{-1}$ (375nm), to be completed in seconds. It thus became possible to obtain I_{ext} over the entire spectral range in a time small compared to the rate at which the size distribution of the cloud was changing. An example of this is shown in Fig. 3. Fig 3A was taken just after a

Figure 2. Solid line is a plot of E VS λ^{-1} arbitrarily scaled to 100, for a "distribution" of Fe_3O_4 particles where $N(25nm)$ is 13 times $N(50nm)$. Points represent experimental measurements of the extinction of Fe_3O_4 particles, collected from our system. The experimental point at $5.0\mu^{-1}$ is arbitrarily scaled to the theoretical curve.
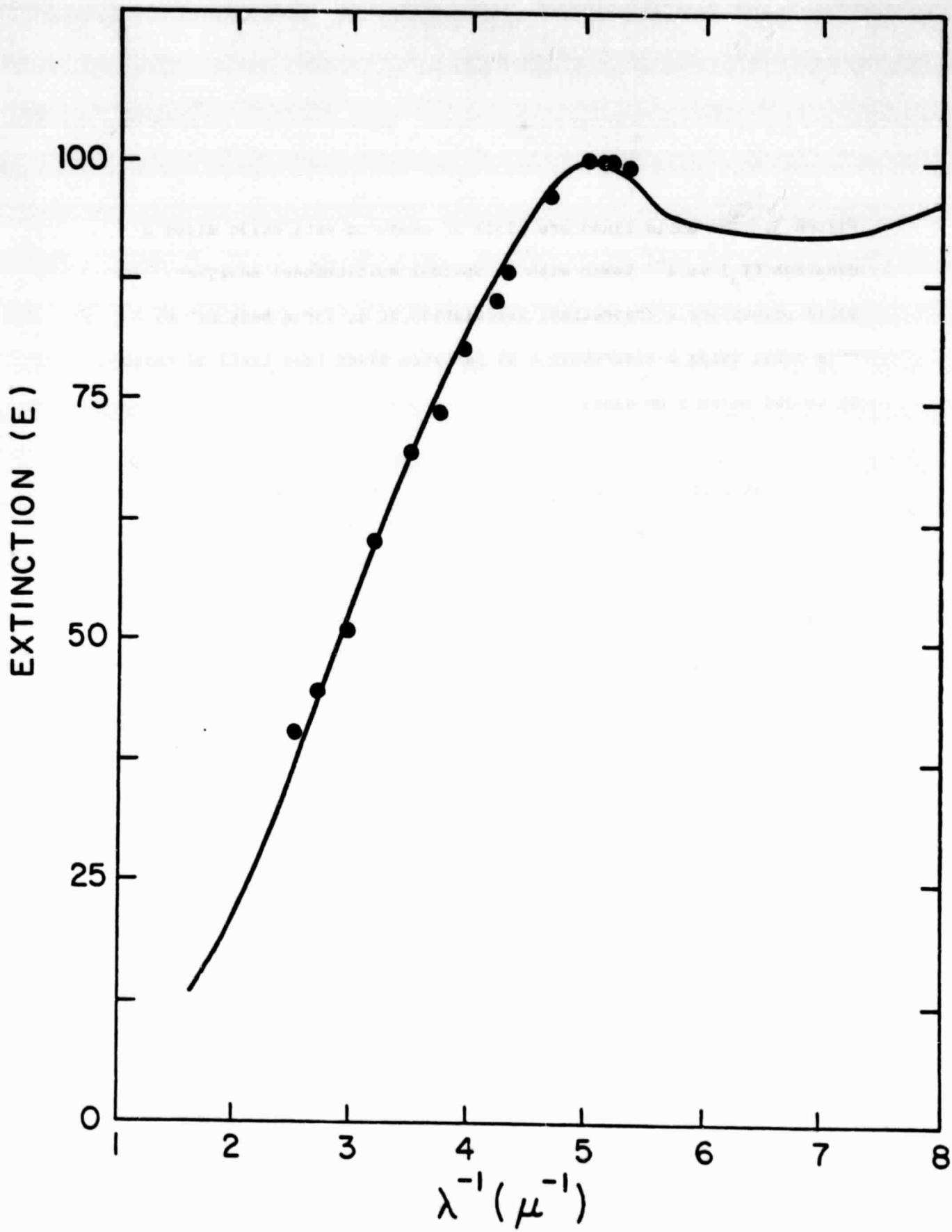
Figure 3. The solid lines are plots of measured extinction minus a constant (Y_0) vs λ^{-1} taken with an optical multichannel analyzer. The solid points are a theoretical calculation of E, for a best fit to this data, using a distribution of particle sizes (see text) of radius 65 to 100 nm in 5 nm bins.

A. Taken after a steady state cloud was formed. NC for a < 75 nm is four times NC for a > 75 nm.

B. Taken after cloud has settled for 100 seconds. Nc for a < 75nm is ten times NC for a > 75 nm.

162
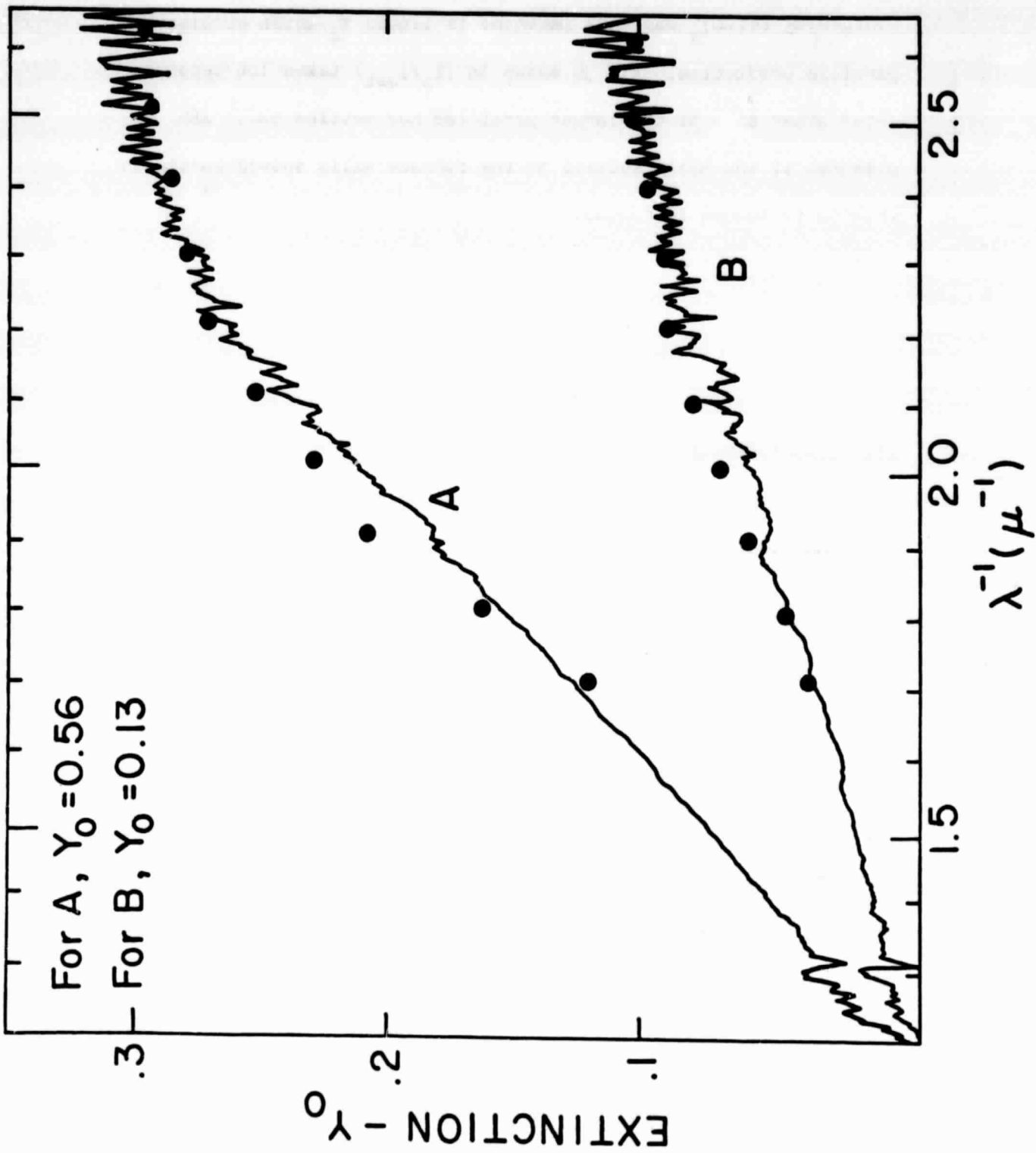
steady state particle distribution had been established. The flask containing Fe(CO)$_5$ was then immersed in liquid N$_2$ which eliminated particle production. Fig 3B shows ln (I_o/I_{ext}) taken 100 seconds later after some of the larger particles had settled out. SEM pictures of the smoke settled on the furnace walls showed particles from 50 to 1000nm in radius.

III. Computational Procedure

THE FOLLOWING IS A SUMMARY OF THE COMPUTATIONAL PROCEDURE USED IN THIS STUDY AND WAS WRITTEN BY DR. HECHT, WHO ALSO PERFORMED THE CALCULATIONS.

The use of Mie theory to calculate the extinction, ln (I_o/I), has been discussed by many authors (see for example Hecht, 1979 or Huffman, 1977). Briefly an efficiency factor, Q, can be calculated for a given particle radius, a, and incident photon wavelength, λ. E(a) the extinction per unit length, is then equal to Q times the particle number density, N, and the geometric cross-section, C. The total extinction per unit length, E, for a given wavelength is equal to the sum of E(a) taken over all particle sizes. This can be compared with experiment by normalizing the peak of each curve (theory and experiment) to a common value and comparing the shape of the resultant curve as a function of wavelength. To make these

calculations, the complex dielectric constant, $\tilde{\epsilon} = \epsilon_1 + i\, \epsilon_2$, is needed. For Fe these were taken from Johnson and Christy (1974, hereafter JC) and from Moravec, Rife, and Dexter (1976; hereafter MO);for Fe_3O_4 these were taken from Schlegel, Alvarado and Wachter (1979)).

Calculations of E(a) were made from 124 to 602nm(8.1 to $1.7\mu^{-1}$) in 6 nm steps, for particle sizes from 5 nm to 100nm, in radius, in 5nm intervals. Mie theory also allows the polarization of the light scattered at 90° to be calculated and this was done over the same ranges.

In some calculations it was found necessary to calculate E(a) for a coated grain such as Fe_3O_4 coated with H_2O ice. Calculations were made from 130 to 290 nm(7.69 to $3.45\, \mu^{-1}$) in 2nm steps. In these calculations a modified Mie theory is used (Kerker 1969; Hecht 1979). The $\tilde{\epsilon}(\lambda)$ for H_2O ice were taken from Greenberg (1968) and Dressler and Schnepp(1960). Linear interpolations were made between points.

Mathis, Rumpl, and Nordsieck (1977; hereafter MRN) have shown that the interstellar extinction curve can be fit when N(a) da, the number density of particles between a and a+da, is given by

$$N(a)\ da = Ka^{-3.5}\ da \qquad (1)$$

where K is a constant depending on the particle material. Since in this paper only relative extinction curves are calculated, K can be

set equal to 1. For Fe and Fe_3O_4 we have calculated E for a MRN type distribution of particle sizes from 2.5 to 102.5 nm. This was done by taking 20 bins 5nm wide starting at 5nm and ending at 100nm. The Q for each bin is constant (i.e., Q(5nm), Q(10nm)...Q(100nm) and E(a) for each bin is integrated using eq. 1. The 20 values of E(a) are then added to give a MRN type extinction curve for Fe and Fe_3O_4.

IV. Results

Iron

Calculations: Using values for $\tilde{\varepsilon}$ from either JC or MO it was found that E(a) could peak anywhere from $7.7\mu^{-1}$ (130nm) to $1.7\mu^{-1}$ (580nm) depending on particle size. Most of these peaks are extremely broad [half width at half maximum (HWHM) > 100nm]. Morever, the position of the calculated peak is extremely dependent on particle size. Using the constants of JC(MO) a 25 nm particle had a peak at $6.0\mu^{-1}(5.6\mu^{-1})$ and a HWHM of 144nm (108 nm). For comparison a 50nm radius particle had a peak at $5.0\mu^{-1}(5.1\mu^{-1})$ and a HWHM of 138 nm (126 nm). The MRN results, plotted in Fig. 4, show that using the data from JC, E increases with energy, while the data from MO predicts a peak near $6.0\mu^{-1}$.

Measurements: Particle sizes determined from SEM pictures indicated that individual particles were near 25 nm in radius with a few larger

Figure 4.   Calculations of E vs λ^{-1} for a MRN type distribution of Fe
            particles (See text).

   A.   Taken from Moravec et al.(MO) data for the dielectric
        constants.

   B.   Taken from Johnson and Christy(JC) data for the dielectric
        constants.

        The peak value of E is arbitrarily normalized to 100.
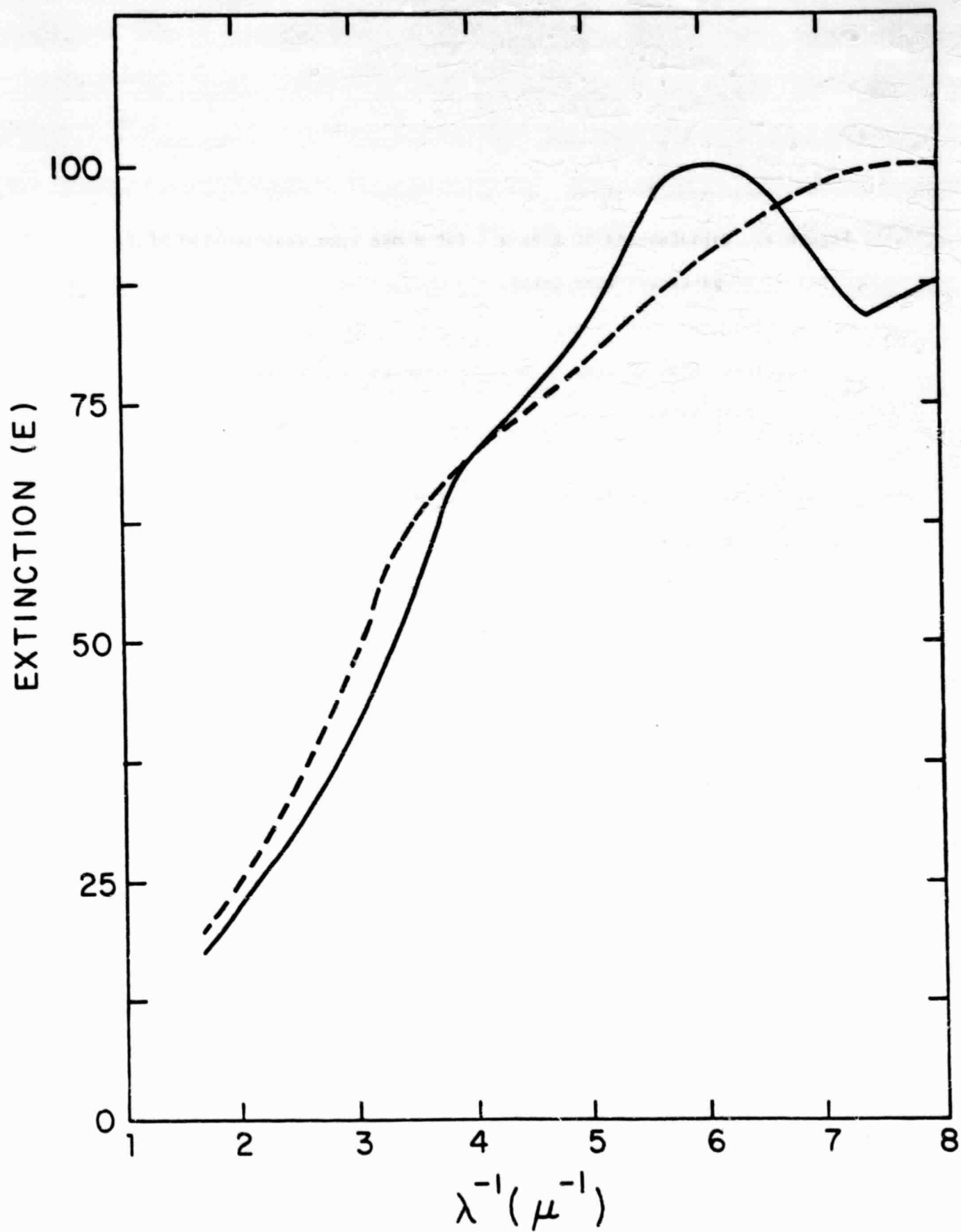
particles present (50nm). Formation of larger particles, via
clumping, probably did not occur in the gas phase.

Visual measurements of the optical polarization indicated that
the light scattered at 90° was 100% vertically polarized. From
previous work this indicates that the ratio of vertically to
horizontally polarized light was better than 100:1 (Hecht,1980). Mie
calculations indicate that this is consistant with a gas phase
particle size of less than 40 nm.

Fig. 1 shows the results of the measurements from 1.5 to 4.9 μ^{-1}.
Also shown are some theoretical calculations for a two bin
distribution where N(25nm) is 13 times N(50nm). As can be seen the MO
points lie within the experimental uncertainty while the JC points
give a slightly poorer fit.

Fig. 3 shows the results for the OMA eperiment where the dust
cloud was allowed to settle. Notice that the plateau which begins at
2.4 μ^{-1} has disappeared after 100 seconds. The model used to fit
these curves results in relatively fewer larger particles being
present after 100 seconds. This is consistent with larger particles
settling out faster. The plateau is not a small particle resonance
feature.

Magnetite

Calculations: The E(a) for Fe_3O_4 can peak over a wide range from .6μ^{-1}(178nm) to 2.0 μ^{-1}(500nm). The variability in E(a) with particle size is much less severe than with Fe. A 25nm particle has a peak at 196 nm and HWHM of 114nm, while a 30 nm particle peaks at 202 nm and has a HWHM of 120 nm. This suggests that a real absorption occurs and it should be noted that the measured absorption coefficient of magnetite does show a peak near 200 nm.

A MRN type curve was also calculated and is shown in Fig. 5a. Noteworthy is the shoulder starting near 5μ^{-1} (200nm). Also shown is a modified MRN curve, Fig 5b, where an additional number of 40 nm particles, equal to .007 the density of 5nm particles in our standard MRN distribution, are added to the distribution shown in Fig. 3a. Note that the shoulder shifts to longer wavelengths.

Measurements: Since the Fe_3O_4 particles were presumably Fe particles, which were oxidized after having initially settled on the furnace walls, the size distribution should be similar to that of the Fe experiments although clumping could add a significant number of larger particles. Shown in Fig. 2 is the Fe_3O_4 extinction data plotted on the same graph as a dual bin distribution of Fe_3O_4 particles where N(25 nm) is 13 times N(50 nm).

170

Figure 5. Calculation of E VS λ^{-1} for a MRN type distribution of

Fe$_3$O$_4$ particles (See text)

A. Standard MRN distribution

B. Same as A with some additional 40 nm radius particles (See

text).

E is arbitrarily normalized, at its peak value, to 100.
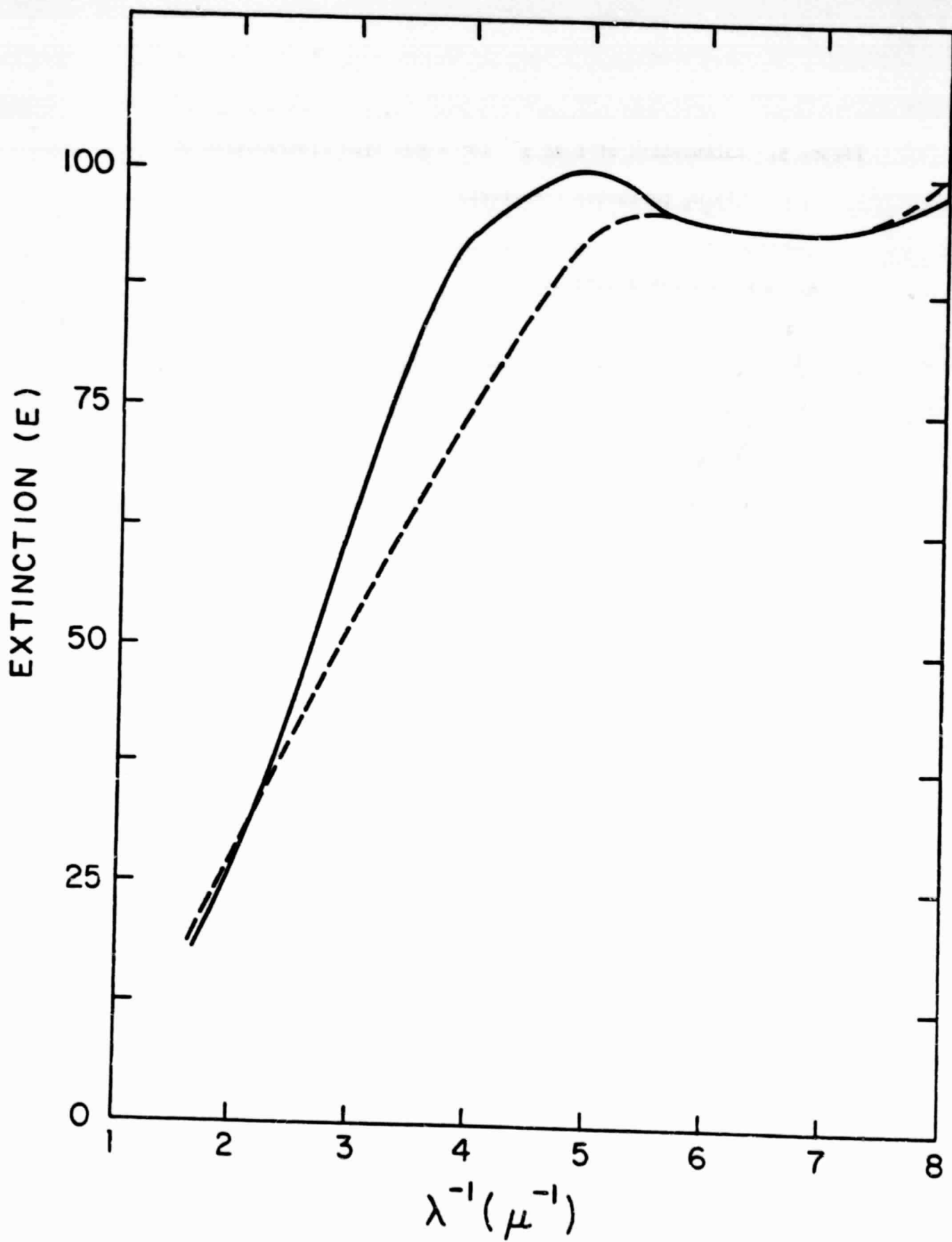
V. Discussion

The results and procedures of the previous sections will be
discussed in relation to (A) the 4.6 μ^{-1}(220 nm) peak in the
Interstellar Extinction curve, (B) the Very Broad Structure in the
Interstellar Extinction curve, and (C) the recently announced (Sitko,
Savage, and Meade, 1981, hereafter SSM; Snow and Seab, 1980) anomalous
extinction curves which show no prominent 4.6μ^{-1}(220 nm) feature.

(A)- Huffman (1977) in his review article on interstellar grains
suggests that Fe might be responsible for the 4.6μ^{-1}(220 nm) feature
in the Interstellar Extinction curve. It is known that, for small
spherical particles, when ϵ_1 is equal to -2 and ϵ_2 is near 0, a
resonance occurs in the small particle (less than 50 nm) extinction
curve. Because the MO and JC data for ϵ_1 are in disagreement Huffman
stated that if their measured values of ϵ_2, which were in agreement,
were too high by a factor of 2 then this resonance might be expected
to occur anywhere between 5.0μ^{-1}(200 nm) and 1.66μ^{-1}(600 nm) depending
on the true value of ϵ_1. The reason Huffman gave for the possible
error in the measurement of ϵ_2 was oxide contamination.

In our experiments we saw no evidence of any resonance peak
between 4.76μ^{-1}(210nm) and 1.66μ^{-1}(600nm) even when small (less than
50 nm) particles were present. In fact our data is consistant with
extinction curves derived from the MO data and possibly even from the
JC data. This is because, except where ϵ_2 is near 0, the extinction
is strongly dependent on ϵ_2 (the value of which both groups agree

upon). Therefore, .ile Fe could certainly contribute to the
Interstellar Extinction it does not seem to be responsible for the
$4.6\mu^{-1}$ (220 nm) feature.

(B) While our experimental data did not try to resolve the Very
Broad Structure, the theoretical calculations of E which we made
showed some interesting consequences of the hypothesis that the Very
Broad Structure is caused by magnetite, (Huffman, 1977; Van Breda and
Whittet, 1981). If the approximate 0.025 mag/kpc VBS is caused by
magnetite than the magnetite contribution to the Interstellar
Extinction curve at $5.0\mu^{-1}$ (200 nm) would be about one fifth the total
extinction. This would make magnetite an important component of the
mid UV portion of the Interstellar Extinction especially in regions
where graphite may not be present. However, magnetite is known to
have two strong IR absorption bands near 16 and $25\mu m$. These features
have been tentatively identified in C1 carbonaceous chondrites which
are known to contain magnetite (Huffman 1977). If magnetite is a
major component of interstellar dust grains then these features should
be seen as either IR absorption or emission features near IR sources.

(C) Recently SSM and Snow and Seab (1980) have reported
extinction measurements which do not show a $4.6\mu^{-1}$ (220nm) feature.
These spectra do seem to show a shoulder which begins at somewhere
between $4\mu^{-1}$ (250 nm) and $5\mu^{-1}$ (200nm). For discussion purposes we will
divide these spectra into three categories: (1) those which show a
change in the slope at about $5.8\mu^{-1}$ (170nm), (2) those which stay
nearly flat past $5.8\mu^{-1}$ (170nm), and (3) the spectrum of HD44179.

The extinction spectra of HD163296, HD31648, HD190073, AB AUR,
were discussed in SSM and all seem to show a moderate silicate IR
feature at 9.7μm. SSM note that recent work by Humpl indicates that a
rise in extinction at $\lambda^{-1} > 5.8\mu^{-1}(\lambda < 170$ nm) is typical of
silicates. We also note that recent calculations by Mathis and
Wallenhorst (1981) confirm this increase, especially when the size
distributions include small (10nm radius) silicate particles.
Therefore the increase in extinction past $5.8\mu^{-1}$(170nm) is probably
due to silicate particles. Although no IR spectra are available for
HD 29647(Snow and Seab, 1980) the silicate explanation probably also
accounts for the increase in its extinction curve.

These spectra also show a weak UV bump and/or shoulder beginning
near $4.2 \mu^{-1}$(240nm) in HD 31648, HD 163296, and HD 190073, and near
$5.0 \mu^{-1}$(200 nm) in AB AUR and HD 29647. Such features are
qualitatively similar to the magnetite features shown in Fig. 4. To
make a quantitative fit the exact particle size distribution is
needed. It would seem to be more profitable to attempt observation of
the IR features of magnetite. If such features were seen then there
would be strong evidence for the presence of Fe_3O_4.

The extinction spectra of HD 259431, HD 45677 and HD 50138 show
no increase in UV extinction and no silicate IR feature. Presumably
no silicates are present around these stars. The shoulder observed in
HD 259431 and HD 50138 are qualitatively similar to magnetite

extinction. As above, a search for magnetite IR features would provide more definitive proof of the presence of magnetite.

We do not believe the SSM suggestion that Fe grains have condensed around these stars according to the scheme of Lewis and Ney (1978). This scheme was based on the assumption of equilibrium condensation yet it is known from laboratory studies (Frurip and Bauer, 1977 and Bauer and Frurip, 1977) that Fe condensation is a strongly non-equilibrium reaction. Also, at low densities around stars, the vibrational disequilibrium problems discussed by Nuth and Donn (1981) can become important. Therefore while pure Fe condensation is not impossible, it is not as likely as Lewis and Ney proposed (Donn et al. 1981).

Finally, it should be noted that HD 45677 is probably not a good candidate for magnetite dust. That spectrum shows a sharp increase from 4 to $4.5\mu^{-1}$ (250 to 220 nm) with flat extinction before and after those energies. This resembles what would be expected from the small MgO particles proposed by Duley, Millar, and Williams (1979). There is even an IR feature near 20 μm which would be expected from such particles.

The extinction spectrum of HD44179, the illumination source for the Red Rectangle Nebula, is unique. It shows a shoulder beginning at $4.8\mu^{-1}$ (210nm) which might be due to magnetite. However, it also shows a large increase in extinction which begins near $6.3\mu^{-1}$ (153 nm) and

continues to about $6.8 \mu^{-1}$ (147nm). SSM suggest this could be due to the presence of either dust, molecular, or atomic species.

In Fig. 6 we show a calculation for the E(a) of a 15 nm Fe_3O_4 particle coated with a 7.5 nm H_2O ice shell. Also shown are selected points of the HD 44179 spectrum taken from SSM and scaled to this curve. This figure should be viewed with the knowledge that there are several variables, i.e. the exact values for ε of H_2O ice between 6 and 7 μ^{-1} (167 and 143 nm), the size distribution of magnetite particles, and the thickness of the ice shell. Nevertheless the feature is nearly reproduced. (Note that a separate distribution of uncoated magnetite particles and H_2O ice particles could also be found so that the feature is reproduced).

IR spectra of this object are available (Russell, Soifer, and Willner, 1978) and no 3.1 μm H_2O feature is seen. However the IR spectrum appears to arise from an optically thin shell and in order for the H_2O coatings to exist they must be in a cool region far away from the excitation source. From the strength of the UV extinction, the 3.1 μm extinction should be about 10% of the incident light. Furthermore, since the UV and IR radiation appear to come from different regions (Cohen et al., 1975) the ice coated dust may be a seperate grain population from that responsible for the infrared emission. The 3.1 μm feature would then not be present as a dip in the emission spectrum. Again the identification of magnetite would be confirmed if the IR magnetite bands could be detected.

Figure 6. Solid line is a plot of $E(a)$ vs λ^{-1} for a 15 nm Fe_3O_4 particle which has a 7.5 nm thick H_2O ice shell. The crosses are experimental points taken from Sitko et al.(SSM). The error bars represent our estimate of the uncertainty of selected points. The two points at 3.5 and 4.0 μ^{-1} are arbitrarily scaled to the plot.
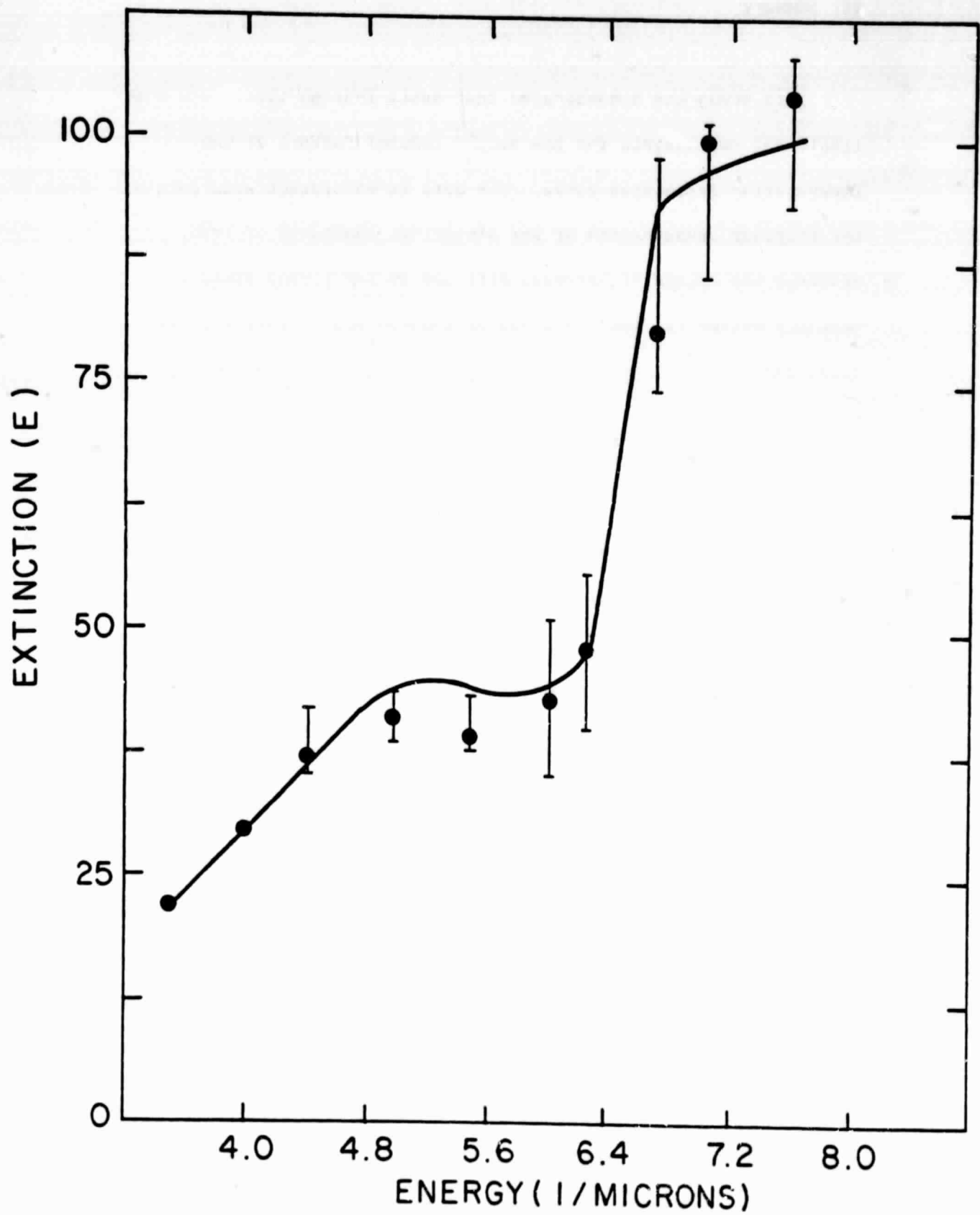
VI. Summary

This study has demonstrated that small iron particles are most likely not responsible for the $4.6\mu^{-1}$ (220nm) feature of the Interstellar Extinction curve. Our data is consistent with both of the previous measurements of the dielectric constants of iron, although the values of Moravec, Rife and Dexter (1976) yield a slightly better fit than do those of Johnson and Christy (1974). Measurements of the relative extinction efficiency of small magnetite grains are quite consistent with the recent determination of the optical constants of thin magnetite films by Schlegel, Alvarado and Wachter (1979). Calculations indicate that if magnetite is indeed responsible for the Very Broad Structure of the Interstellar Extinction Curve, then it should also account for about 20% of the total observed extinction at 200nm. If graphite were absent then the contribution of magnetite to the line of sight extinction could be much more significant. We have shown that this could actually be an explanation for the anomolous extinction curves recently reported toward several stars (Sitko, Savage and Meade, 1981 ; Snow and Seab, 1980).

We have demonstrated that the experimental apparatus described in the previous section is suitable for the production of very small iron particles. The size distribution and concentration of these particles can be controlled quite easily for relatively long periods of time so that measurements of the optical extinction of the smoke can be made. Incorporation of an OMA into the system allows data aquisition on a

much shorter timescale. If this were combined with a real time particle collection system it should be possible to obtain high resolution extinction spectra of very well characterized particle distributions. Such a system may become available at GSFC within a year.

It should also be noted that the flow system used to produce the iron particles can easily be adapted to produce other types of particles such as amorphous silica, silicon carbide, iron carbide and iron silicate by the use of suitable gaseous precursers. These include acetylene, iron carbonyl, silane and water vapor. Such a system should be able to establish a significant body of data for the optical properties of small amorphous grains of astrophysical interest.

C-3

References

Bauer D. J. and Frurip, 1977 J. Phys. Chem. **81**, 1015.

Cohen, M., et al., 1975, Ap. J., **196**, 179

Donn, B., Hecht, J., Khanna, R., Nuth, J., Stranz, D., and Anderson,
A.B., 1981 Surf. Sci., **166**, 576.

Dressler K. and Schnepp O., 1960 J. Chem. Phys. **33**, 270.

Duley, W. W., Millar, T. J., and Williams, D. A., 1979, Ap. Space
Sci., **65**, 69.

Frurip, D. J. and Bauer S. H., 1977 J. Phys. Chem. **81**, 1001.

Granqvist, C.G., and Buhrman, R. A., 1976, J. Appl. Phys. **47** 2200.

Greenberg, J. M., 1968, Nebulae and Interstellar Matter, edited by B.
G. Middelhurst and L. H. Adler (Chicago: University of Chicago
Press).

Hecht, J., 1979, J. Appl. Phys. **50** 7186.

Hecht, J., 1980, Personal Communication

Huffman, D.R., 1977, Adv. in Phys. **26** 129.

Johnson, P. B., and Christy, R. W., 1974, Phys. Rev. B, **9**, 5056.

Kerker, M., 1969, The Scattering of Light and Other Electromagnetic
Radiation (New York: Academic Press).

Lewis, J. S. and Ney, E. P., 1979, Ap. J. **234** 154.

Mathis, J. S., Rumpl, W. and Nordsieck, K. H., 1977, Ap. J. **217**, 425.

Mathis, J. S. and Wallenhorst, S. G., 1981, Ap. J., **244**, 483

Mellor, J. W., 1960, A Comprehensive Treatise on Inorganic and
Theoretical Chemistry, Vol _____ (Wiley, New York).

Moravec, T. J., Rife, J. C. and Dexter, R. R., 1976, Phys. Rev. B $\underline{13}$, 3297.

Nuth, J., and Donn, B., 1981, Ap. J., $\underline{246}$, 925

Russell, R. W., Soifer, B. T., and Willner, S. P. 1976, Ap. J., $\underline{220}$, 568.

Schlegel, A., Alvarado, S. F., and Wachter, P., 1979, J. Phys. C: Solid State Phys. $\underline{12}$, 1157.

Sitko, M. L., Savage, B. D., and Meade, M. R., 1981, Ap. J. $\underline{246}$, 161.

Snow, T. P. and Seab, C. G., 1980, Ap. J. $\underline{242}$, L83.

Van Breda, I. G., and Whittet, D. C. B., 1981, Mon Not R. Astr. Soc., $\underline{195}$, 79.

Whittet, D. C. B., 1981, Q. J. R. Astr. Soc., $\underline{22}$, 3.

Chapter 5 The Temperature Dependent Nucleation of SiO

The nucleation of refractory materials: metals, metal oxides, carbon and its compounds is a problem of considerable importance in astrophysics for which no suitable framework o experimental data is yet available. Most nucleation experiments involve either simple metals[1,2] or relatively low temperature organic compounds.[3,4] Few experimental studies have been performed involving more complex high temperature species.[5,6] Yet recondensation of such species from meteoritic materials could affect the earth's ozone balance[7] or be a source of particulate pollution from the utilization of low grade coal resources. We have therefore initiated a systematic study of the condensation of highly refractory species under carefully controlled laboratory conditions. These studies were initiated primarily to understand the formation and physical properties of the interstellar dust.[8]

Section II contains a complete description of the apparatus and procedure used in this work. Section III presents typical data obtained in the system as well as the methods by which such data can be analyzed in order to determine values of γ, the surface free energy of the condensate or J, the particle flux observed in the system. Section IV presents a comparison of the results obtained in our new system with those from the literature. In particular, we compare the value of γ obtained by our analysis with that which might be expected

of SiO_x ($X \approx 1.5$). We also discuss the applicability of an analysis based on the usual theories of homogeneous nucleation for a compound which does not condense to a solid which is thermodynamically stable under the conditions at which it forms. SiO condenses to SiO_x rather than to the predicted SiO_2 in agreement with the work of Day and Donn.[5] We also compare our results with the recent work of Stephens and Bauer[6] on the condensation of SiO at the much higher temperatures observed in their shock tube-laser scattering system. We find that our results, obtained at 700 K < T < 1000 K, extrapolate fairly well to those obtained in their system at 1250 K < T < 2200 K. Section V presents the conclusions which we believe can be drawn from this study.

II. EXPERIMENTAL PROCEDURE AND EQUIPMENT

A schematic representation of the apparatus used in this study is shown in Figure 1. SiO is evaporated from a resistively heated ceramic crucible 1/2" inside diameter, 1-1/2" deep. The temperature of the crucible is measured by a Pt/Pt 13% Rd thermocouple encased within a steel sheath and further shielded by a ceramic tube which is placed within the top of the crucible. Because it was found that the SiO tended to form a cap over the crucible which then served as the source of SiO vapor seen in the system, the thermocouple is situated so as to measure the temperature of the cap rather than the temperature of the interior of the crucible. It was found that this temperature could be kept within $\pm 5°$ K for extended periods even when the temperature of the ambient gas varied significantly.

Figure 1. Schematic Diagram of Experimental Apparatus (see text
for detailed description).

150ℓ STAINLESS STEEL BELL JAR

MULLITE FURNACE

COOLING WATER (OUT)

MgF₂ WINDOW

MONOCHROMATER

ALUMINA TUBE

SMOKE

FURNACE POWER

MgF₂ WINDOW

APERTURE

XENON ARC LAMP

CRUCIBLE

FURNACE POWER

CHROMEL-ALUMEL THERMOCOUPLE

OUTER HEATING COIL LEADS

INNER HEATING COIL LEADS

Pt /Pt 13 % Rh THERMOCOUPLE

TO MECHANICAL AND DIFFUSION PUMPS

COOLING WATER (IN)
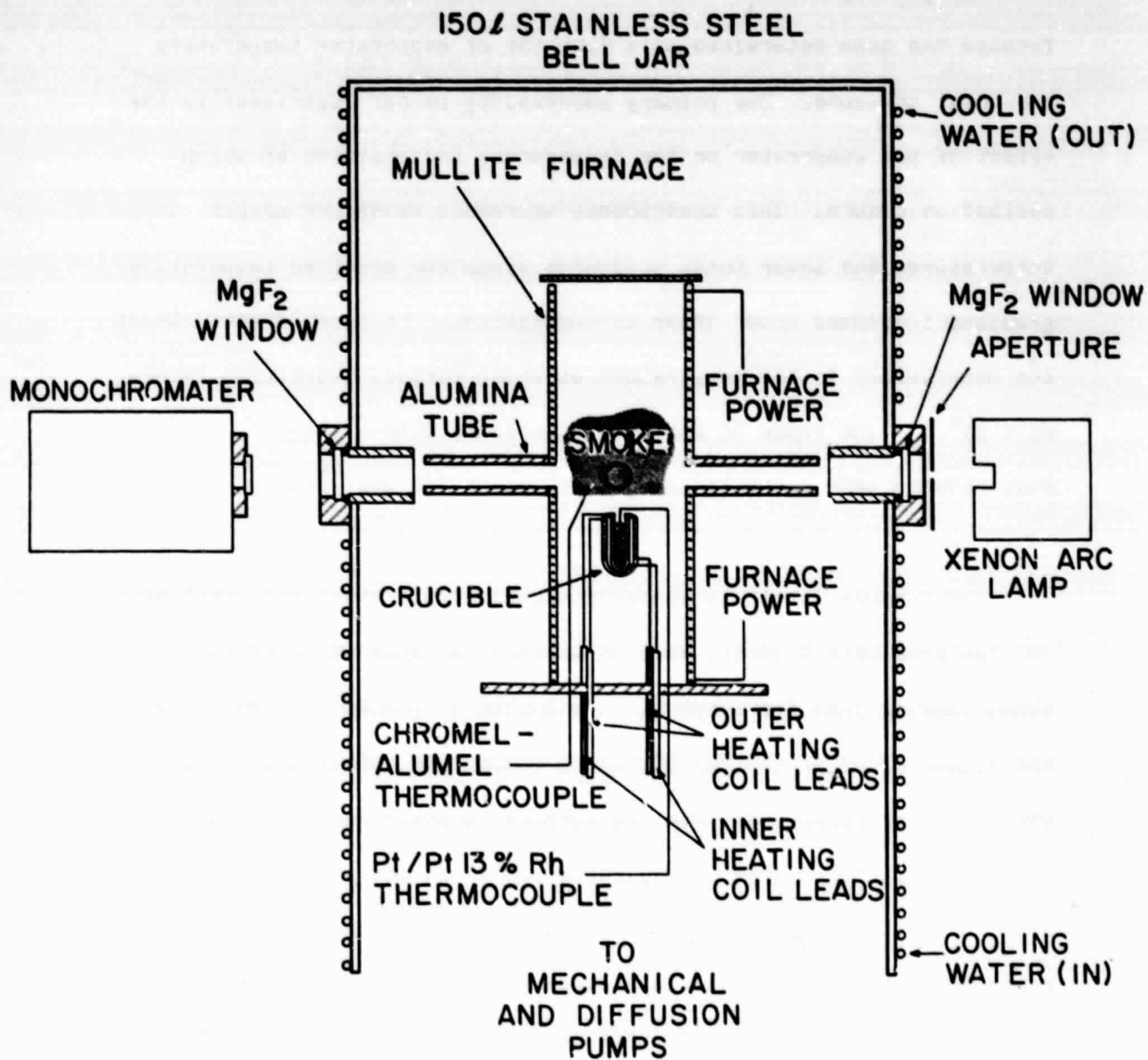
The SiO evaporator is enclosed within a 12" high, 4" inside diameter cylindrical, resistively heated mullite furnace. The furnace is used to control the ambient temperature at which condensation occurs. At right angles around the equator are four 1" inside diameter 5" long alumina tubes. The temperature profile of the furnace has been determined as a function of evaporator temperature and total pressure. The primary uncertainty in our experiment is the effect of the evaporator on the temperature and position at which nucleation occurs. This uncertainty increases at higher evaporator temperatures and lower total pressures since our observed temperature gradient increases under these circumstances. Our overall estimate of the uncertainty in the temperature at which particle formation occurs is $\pm$ 20° K. The range in ambient temperature within which measurements were possible lay between about 700 and 1000° K.

The furnace itself is enclosed within a 150ℓ stainless steel bell jar equipped with 4 ports, each of which is aligned with one of the tubes leading into the furnace. The system is pumped via mechanical and liquid nitrogen trapped diffusion pumps. We attain pressures in the 10^{-6} torr range even when the furnace is baked at temperatures near 750° K. The system is typically baked out for about 18 hours after it has been opened to the atmosphere before condensation experiments are begun. The total leak rate of the vacuum system is less than 25 μm/hour. Our experiments are typically carried out at total pressures in the range of 2 to 50 torr.

A high pressure Xenon arc lamp, mounted on the bell jar, is beamed through a MgF_2 window and through one of the alumina tubes. Observations at 90° to this beam give qualitative data on the condensate such as color and degree of polarization of the scattered light. We can also get some idea of the spatial extent of the particle formation in this way. A 0.3 meter monochrometer is mounted in line with the beam on the opposite side of the bell jar. Extinction measurements at 200 nm are used to determine the onset of condensation. In addition, the extinction spectrum of the condensates can be determined in situ from 195 nm to 800 nm.[9]

The vapor pressure of SiO as a function of temperature was determined thermodynamically. The experiments were done under reducing conditions (in H_2 gas) and P_{eq}(SiO) is therefore given by equation (1) over the evaporator.[10] A simple model of the

$$P_{eq}(SiO) = (760 \text{ torr}) \exp[12.81 (1 - \frac{2300.9}{T})] \qquad (1)$$

diffusion of the SiO vapor from the crucible to the region in which condensation is observed to occur, will reduce the partial pressure of SiO in this region by about a factor of 10. If convection is important this pressure could be further reduced.

Our measurements were obtained as follows. First, the system was cleaned and the evaporator filled with Union Carbide Select Grade silicon monoxide. The system was then evacuated and pumped overnight with a diffusion pump while the furnace remained at a temperature of approximately 300°C. Before a run, liquid N_2 was added to the trap

and the system was pumped for at least two more hours. The pump was then isolated from the system and H_2 gas introduced. After the temperature of the ambient gas reached equilibrium, the temperature of the SiO evaporator was increased until condensation was observed. This was indicated by a decrease in the intensity of light transmitted through the furnace and by the visual observation of scattered light at 90° to the beam of the Xe arc lamp.

We now increased the temperature of the ambient gas until the scattering (or extinction) disappeared. At this point we reinitiated condensation either by lowering the temperature of the ambient gas or by raising the temperature of the SiO evaporator. This cycle was repeated numerous times -- usually until the SiO evaporator was emptied.

We usually found that an increase (decrease) in the temperature of the ambient gas tended to increase (decrease) the temperature of the SiO crucible and vice versa. This change could be compensated for by a slight decrease (increase) in the voltage across the crucible. Although care was taken to hold the temperature of the crucible constant during a change in the furnace temperature, the temperature of the ambient gas was allowed to float freely as the temperature of the crucible was varied. Because of this, the temperature of the furnace generally increased during a run and yielded data at several condensation temperatures (see Figure 2).

Figure 2. Typical Data vs. Time. Shown are a) the current from the photomultiplier tube, b) the ambient temperature of the gas, (T > 450°C), and c) the temperatuare of the SiO evaporator (T > 925°C).
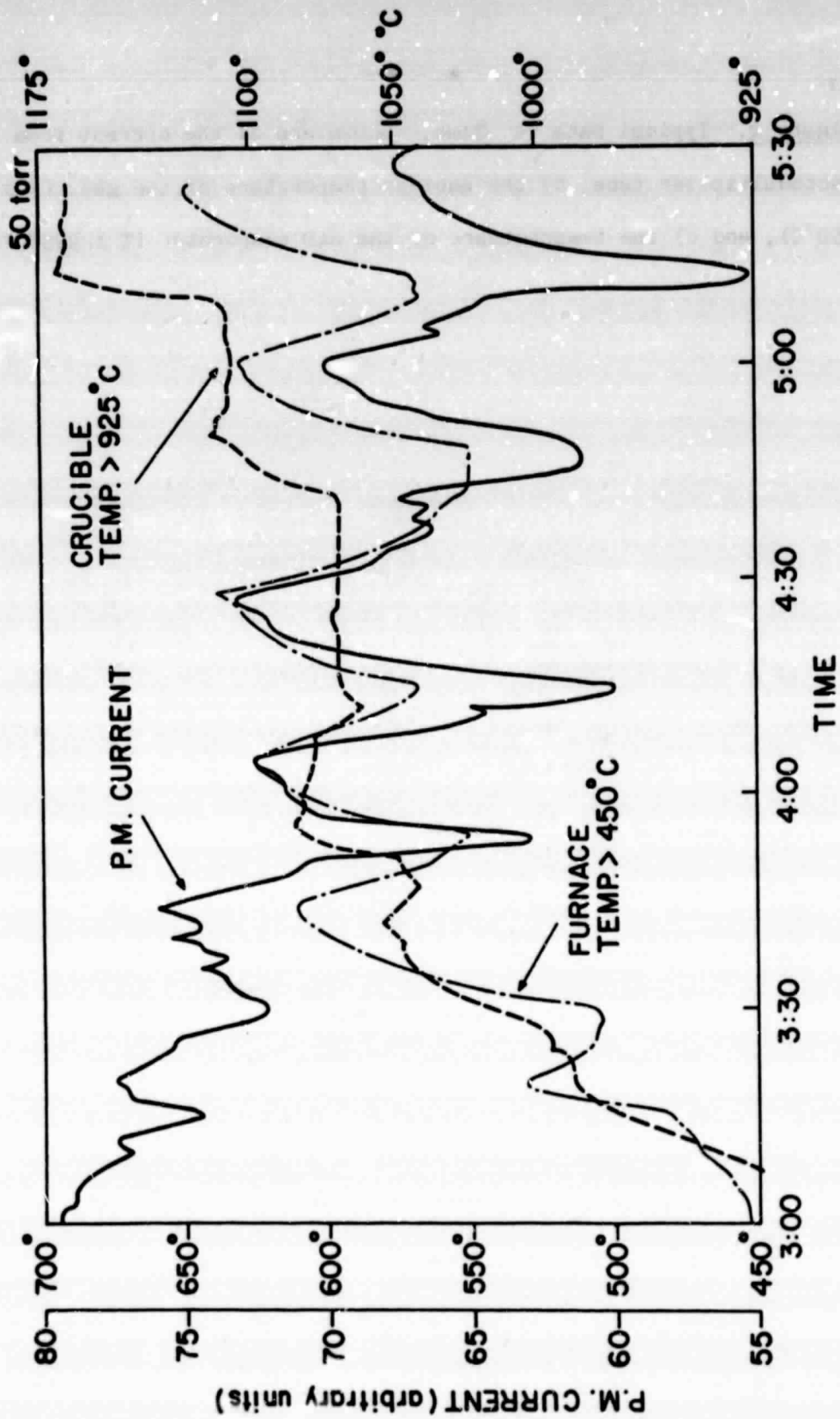
Thermocouple temperatures were monitored via strip chart recorder and the data read off at one minute intervals after completion of a run. The PM current was similarly treated using a separate, synchronized recorder. The conditions under which condensation began (ended) were usually determined visually by the onset (disappearance) of scattering during a run. the final data analysis was made more self-consistent by the use of the PM current which is a direct, quantitative measurement of the particle extinction in the system.

We arbitrarily defined the onset of particle formation to be the period at which ∿1% extinction was observed. It should be noted that the transition from 0% extinction to ∿5% extinction usually occurred on a time scale of only about 10-15 seconds. Because the temperatures of both the SiO evaporator and the ambient gas changed more slowly than did the measured extinction whenever avalanche nucleation occurred, these temperatures were quite well determined and changed only a total of 10-20 degrees between the time just prior to nucleation and the point at which significant extinction (∿10%) was observed.

III. RESULTS AND ANALYSIS

    a. First Order Analysis

        Figure 2 shows typical data collected during one experimental run at 50 torr. Shown are the furnace temperature, the evaporator

temperature and the current from the photomultiplier (PM) tube as a function of time. One can immediately notice that the PM current gradually decreases with time. We believe that this is due to a thin film of condensate which accumulates on the MgF_2 windows during the course of the experiment. One also notes that the PM current varies approximately inversely with evaporator temperature and directly with ambient furnace temperature. Since the current from the PM tube is proportional to the transmitted light at 200 nm, as the particle concentration increases, the PM current decreases. As expected, an increase in the evaporator temperature increases the partial pressure of SiO and therefore the rate of particle formation. This, in turn, increases the extinction. Conversely, a decrease in the furnace temperature causes an increase in the extinction, since such a decrease increases the supersaturation of the vapor and therefore also increases the rate of particle formation.

An estimate of the particle density can be obtained from extinction measurements using the relation[11]

$$I = I_o \exp(- N\pi a^2 \ell \, Q_{ext}) \qquad (2)$$

where I is the transmitted intensity, I_o is the incident intensity, N is the average particle density, a is the radius of the particles, ℓ is the path length and the extinction efficiency, Q_{ext}, is given by equation (3) for small particles.

$$Q_{ext} = \frac{24\pi a}{\lambda} \frac{\epsilon_2}{|\epsilon_1 + 2|^2 + \epsilon_2^2} \tag{3}$$

The light scattered from the particles at right angles to the incident beam was extremely blue and ~100% polarized. We estimate that the average particle radius (a) lies between 20-40 nm (see Kerker, 1969). The pathlength over which extinction occurred was seldom less than 2 cm and probably not more than 6 cm in length. Our extinction measurements were made at λ = 200 nm. If we use the optical constants for Si_2O_3 at 200 nm (ϵ_1 = 2.6; ϵ_2 = 0.1)[12] and choose 1% extinction as the point below which we define particle formation to cease, we find that log N = 9.7 ± 1.7.

The time scale over which nucleation occurs is not well defined. A lower limit to the nucleation rate can be obtained by observing the time needed for a stable cloud of particles to disperse after the SiO evaporator is turned off. In a typical experiment, a cloud causing 12% extinction disappears (< 1% extinction) about 5 seconds after power to the SiO evaporator is shut off. This yields a minimum formation rate of about 10^9 particles cm^{-3} s^{-1}.

A maximum rate can be estimated from kinetic arguments in the following manner. First, assume that SiO molecules stick on every collision and grow to ~20 nm radius particles. Each of these particles contains ~10^5 molecules if we assume $\rho \lesssim 1$ for a fluffy particle. For an $_{SiO}$ partial pressure on the order of 10^{-4} atm and an ambient gas temperature of approximately 900 K, the SiO-SiO collision

195

frequency is on the order of 10^6 s^{-1}. Therefore a typical particle forms in less than 10^{-1} s. Observations indicate particle formation (more than 1% extinction) can occur less than 1 second after a decrease in furnace temperature. This supports our estimate and implies a formation rate of at least 10^{10} particles cm^{-3} s^{-1}. This calculation ignores the fact that the collision cross section for a growing cluster increases as the 2/3 power of the number of molecules already incorporated within, as well as the fact that particles may only nucleate into clusters containing as few as 10^2-10^3 molecules before coagulation becomes an important growth process. If we include such factors our nucleation rate could easily be as high as 10^{15}-10^{16} particles cm^{-3} s^{-1} since each 20 nm particle could represent 10^2-10^3 clusters each containing 10^3-10^2 monomers.

The supersaturation was calculated in the following manner. First, we assume that the temperature of the SiO cap determines P(SiO) in the region just above the crucible and that this pressure can be determined using equation (1). Next, we assume that the SiO concentration gradient above the crucible can be modeled as a simple $1/r^2$ diffusion process. Finally, we assume that the equilibrium partial pressure of SiO at the point at which nucleation is observed to occur is determined by the temperature of the ambient gas through equation (1). Nucleation always occurred approximately 1/2 to 1 inch above the crucible. Therefore, as an example, if the crucible temperature was 1325K and nucleation occurred at an ambient temperature of 875K, the supersaturation would be $\sim 10^4$.

Figure 3 is a plot of the calculated supersaturation (S) of SiO vs ambient temperature (T) at times when extinction is just observable (between 0-1%). Data obtained when extinction is "turned off" due to an increase in ambient temperature is indistinguishable from that obtained when it is "turned on" due to a decrease in the ambient temperature. The experimental data from which the points in Figure 3 were calculated was obtained at total pressures of 50, 35 and 20 torr. Although the data obtained at 35 and 50 torr is quite similar, the points obtained at 20 torr seem uniformly high. This could be the result of a number of factors.

First, it is possible that diffusion at 20 torr could reduce the partial pressure of SiO in the region of nucleation by as much as a factor of ~0.75 as compared to data obtained at 35 or 50 torr. This small correction would suffice to lower all 20 torr data taken at temperatures less than 925 K into agreement with higher pressure results. Second, it should be noted that even the 50 torr data at 950 K is slightly higher than expected from a simple extrapolation of data taken at lower temperatures. This suggests the possiblity that as the crucible temperature increases, the region of nucleation moves away from the crucible. This would mean that the measured ambient temperatures in the region of nucleation could be too high by as much as 10-15 K while the estimated pressures for SiO could be high by as much as a factor of 6 due to the additional diffusion of the monomer away from the crucible before nucleation occurs. From previous temperature calibration measurements, we know that the temperature gradient away from the crucible increases as the temperature of the

197

Figure 3. Supersaturation vs. Ambient Temperature. Shown is data taken at 50 torr (filled circles), 35 torr (crosses) and 20 torr (open circles)) for SiO evaporator temperatures of 1525° K (region A), 1475° K (region B), 1445° K (region C) and less than 1370° K (all other data). These represent points at which condensation could just be noted ($J \sim 10^{11}$ cm^{-3} - s^{-1}).
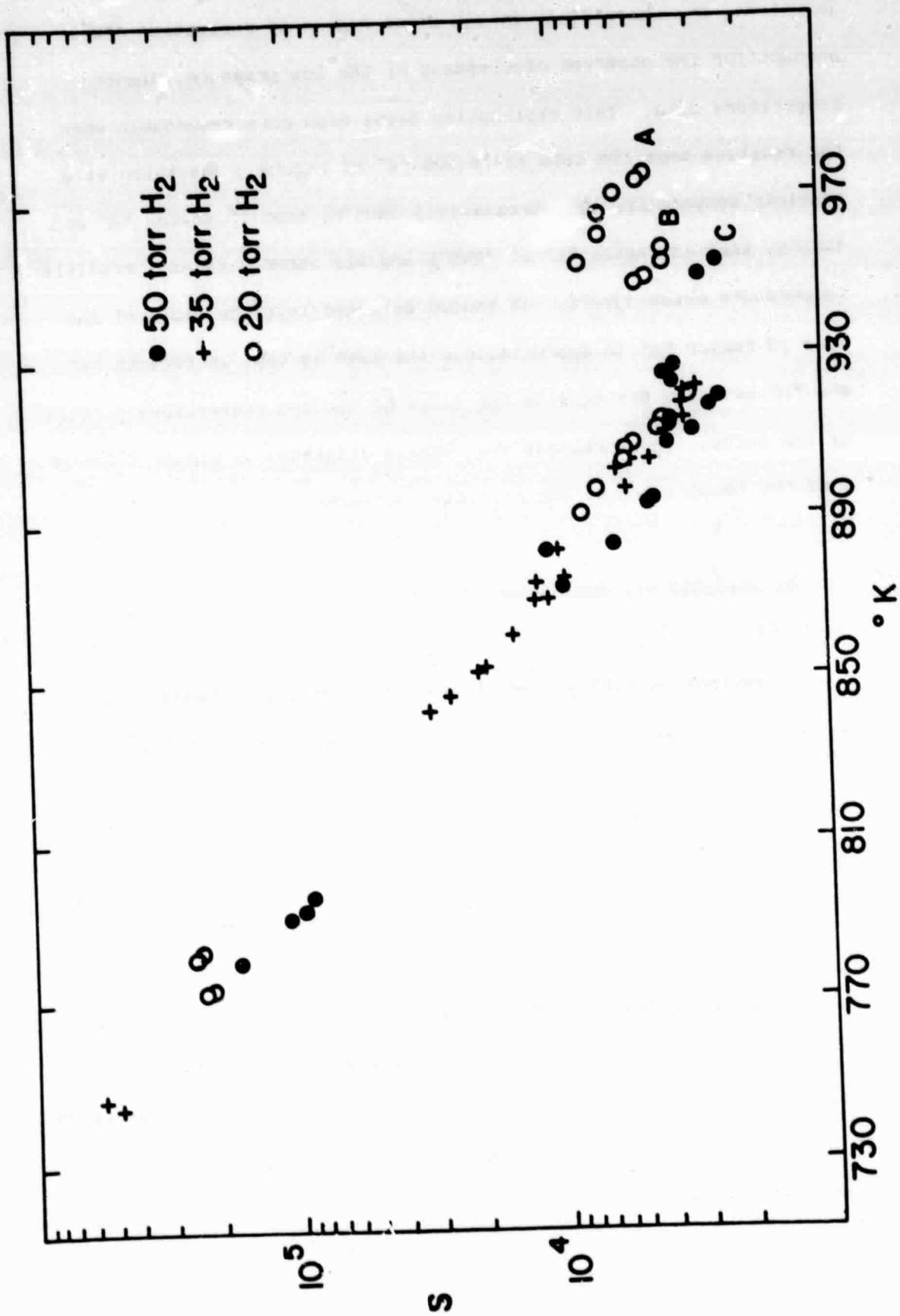
crucible itself increases and as the total pressure decreases. Therefore, the uncertainty in the exact region of nucleation could account for the observed discrepancy of the low pressure, higher temperature data. This explanation seems even more reasonable when one realizes that the data in region "A" of Figure 3 was taken at a crucible temperature of approximately $1525°K$, that in region "B" at $1475°K$, that in region "C" at $1445°K$ and all other data at a crucible temperature below $1370°K$. It should be noted that the slope of the data in region "A" is approximately the same as that in regions "B" and "C" and also the same as the slope of the low temperature portion of the curve. These regions are merely displaced to higher T and/or S as the temperature of the crucible increases.

b. Analysis via Nucleation Theory

Nucleation theory predicts that the particle formation rate (J) should be related to S and T by the following relationship[13]

$$ J = \left(\frac{2\gamma}{\pi m}\right)^{1/2} V N_1^2 \, \exp \frac{-16 \pi \gamma^3 V^2}{3k^3 T^3 (\ell nS)^2} \qquad (4) $$
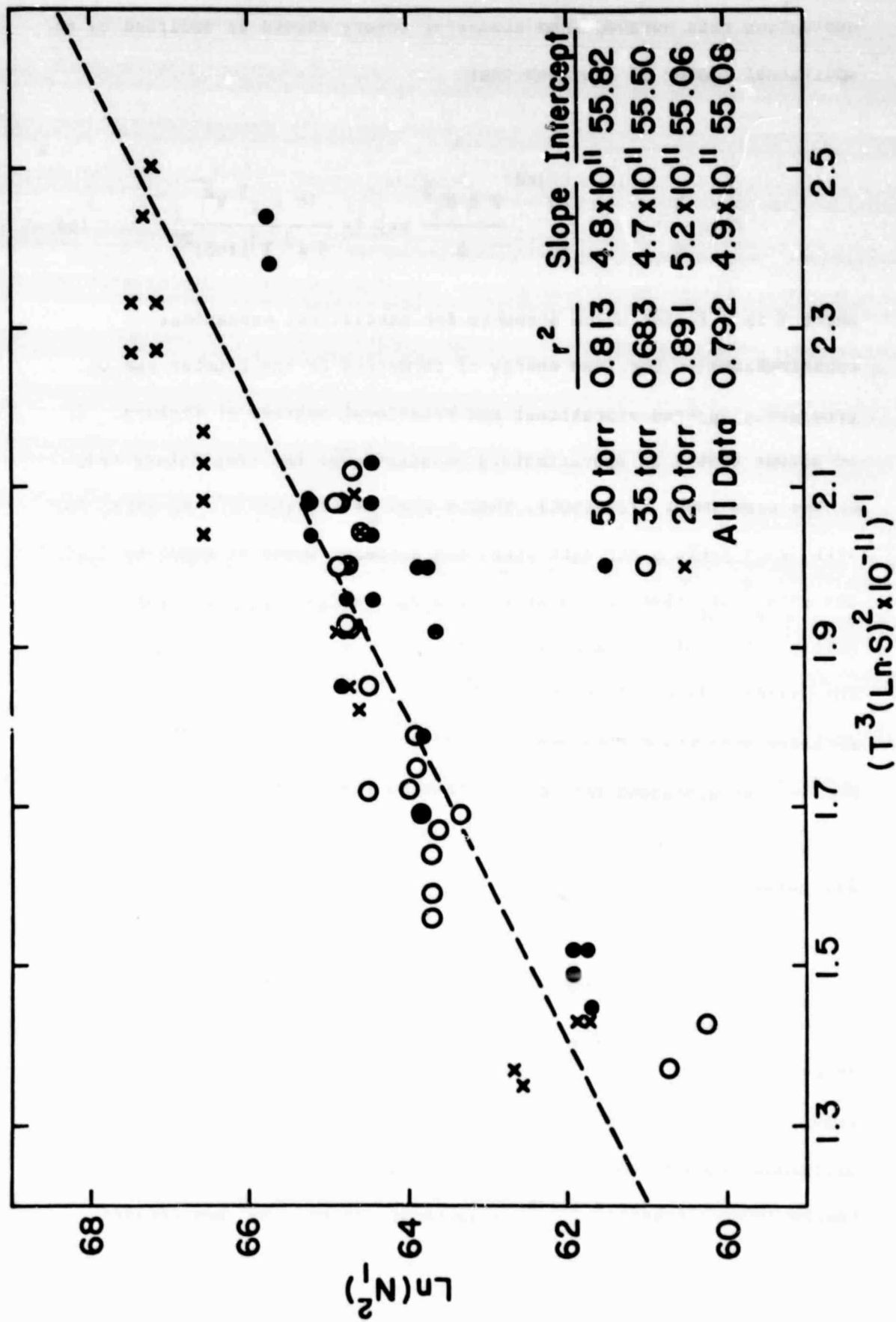
where γ is the surface free energy, m is the mass of the condensing molecule, V is the volume of the condensing molecule, N_1 is the number density of the monomer and k is Boltzman's constant. If the variation in N_1 is small, it is easy to see that for constant J, an increase in T necessitates a corresponding decrease in S.

Equation (4) can be rearranged to the following expression,

$$\frac{C_2 \gamma^3}{T^3 (\ell n S)^2} + \ell n \left(\frac{J}{C_1 \gamma^{1/2}}\right) = \ell n (N_1^2) \qquad (5)$$

where $C_1 = [(2V^2)/(\pi m)]^{1/2}$ and $C_2 = 16 \pi V^2/(3k^3)$. A plot of $(T^3 (\ell n S)^2)^{-1}$ vs $\ell n(N_1^2)$ should be a straight line if γ remains approximately constant over the temperature range of the experiment. An average value for γ can be obtained from the slope of this line if V can be estimated. This in turn allows one to calculate J independently from the value of the $\ell n(N_1^2)$ intercept. Figure 4 is a plot of $(T^3 (\ell n S)^2)^{-1}$ vs $\ell n(N_1^2)$ in which the calculated supersaturations have been corrected empirically for the temperature of the crucible. As can be seen, the slopes of the three sets of data obtained by a linear regression analysis lie between 4.7×10^{11} and 5.2×10^{11} with an average slope of 4.9×10^{11}. If we use a value of 2.4×10^{-23} cm^3 for V, this implies a value of ~ 500 ergs/cm^2 for the surface free energy of the condensate. If we then use this value for γ, assume a value of 7.3×10^{-23} g for m and use the value of the overall $\ell n(N_1^2)$ intercept given in Figure 4, we calculate J to be about 5×10^{13} particles/cm^3. This is in reasonable agreement with our previous estimate for J from the optical extinction measurements discussed above.

<u>Figure 4.</u> $\underline{(T^3 (\ell nS)^2)^{-1}}$ vs. $\underline{\ell n(N_1)^2}$. Shown are the slope, intercept and correlation coefficient for runs at 50 torr (filled circles), 35 torr (open circles), 20 torr (crosses) and the combined data as obtained from a linear regression analysis. Also shown is the resulting best fit through all of the data.

	Slope	Intercept
• 50 torr	4.8×10^{11}	55.82
○ 35 torr	4.7×10^{11}	55.50
× 20 torr	5.2×10^{11}	55.06
All Data	4.9×10^{11}	55.08

	r^2
• 50 torr	0.813
○ 35 torr	0.683
× 20 torr	0.891
All Data	0.792

x-axis: $(T^3 (\mathrm{Ln}\cdot S)^2) \times 10^{-11})^{-1}$

y-axis: $\mathrm{Ln}(N_1^2)$

A modification to Becker-Doring theory[14] predicts that the nucleation rate derived from classical theory should be modified by an additional factor of X/S such that

$$J' = \frac{X}{S} \cdot J = \left(\frac{2\gamma}{\pi m}\right)^{1/2} \frac{V\, X\, N_1^2}{S} \exp\left(-\frac{16\,\pi\,\gamma^3\, V^2}{3\, k^3\, T^3 (\ln S)^2}\right) \tag{6}$$

where X is a factor which accounts for statistical mechanical contributions to the free energy of formation of the cluster due to previously ignored vibrational and rotational degrees of freedom. If we assume that X is approximately constant over the temperature range of the experiment (725-950K), then a plot of $(T^3(\ln S)^2)^{-1}$ vs $\ln(N_1^2/S)$ will again yield a straight line, the slope of which is equal to $C_2\gamma^3$. The $\ln(N_1^2/S)$ intercept, however, now equals $[\ln(J/\gamma_1^{1/2}) - \ln X]$. Recalculation of the data plotted in Figure 4 according to equation (6) yields a value of 650 ergs/cm^2 for γ. If we assume that our particle production rate must lie between about 10^9 and 10^{16} particles cm^{-3} s^{-1} as discussed previously, then we find that $11.5 \lesssim \ln X \lesssim 25$.

IV. DISCUSSION

We have derived values for the surface free energy of our condensate—nominally Si_2O_3—from plots of $(T^3(\ln S)^2)^{-1}$ vs either $\ln(N_1^2)$ or $\ln(N_1^2/S))$ of 500 and 650 ergs/cm^2 respectively. Earlier calculations of γ based on extrapolation of measured values for silicious slags to concentrations of 100% SiO_2 yield values in the region 180-273 ergs/cm^2.[15,16] A value of 259 ergs/cm^2 was derived

from measurements of the heat of solution of amorphous silicic acid[17] while Elliot, Gleiser and Ramakrishna[18] give a value of 350 ergs/cm^2 for liquid silicates in general. Blander and Katz[19] estimate the surface free energy of solid silicates to be 850 ergs/cm^2. Bruce[20] gives the following formula for the average surface free energy of β-cristobalite as a function of temperature

$$\gamma = (925 - 0.193 \ T) \ \text{ergs/cm}^2. \tag{7}$$

It should be noted that γ for this allotrope of SiO_2 varies only slowly with temperature. Bruce[20] expects γ for tridymite, which has a lower density, to be lower and γ for quartz to be higher. Since it is probable that our amorphous condensate has a lower density than any crystalline form of SiO_2, its surface free energy should be still lower. It should be noted that Phillip[12] feels that the optical properties of compounds of the type SiO_x ($0 \leq x \leq 2$) vary continuously throughout the series. If this applies to other properties as well, then the value of γ for Si_2O_3 should be between that for silica ($\gtrsim 300$ ergs/cm^2) and that of silicon metal (~ 728 ergs/cm^2). Therefore, the values which we derive ($\sim 500 \leq \gamma \leq \sim 650$ ergs/cm^2) seem quite reasonable.

In spite of the fact that we derive reasonable values for both γ and J using techniques based on nucleation theory, one must still question whether such results could be fortuitous. The fundamental question in this system is, "What does S mean?" We evaporate SiO and nucleate Si_2O_3. This has previously been noted by Day and Donn[5] and

is confirmed in these samples by the presence of a characteristic feature in the infrared absorption spectrum at 11.5 μm[21]. Although the structure of Si_2O_3 has not been definitely determined[22], measurement of the Si concentration in our sample via x-ray fluorescence confirms this stoichiometry. One possible structure that has been suggested for this compound is that of a typical SiO_4 tetrahedral network in which every fourth O atom is missing[22].

If the sample is annealed under vacuum at 750 K for periods on the order of 10-20 hrs the 11.5 μm peak disappears and is replaced by a peak at 12.5 μm which is characteristic of amorphous silica. It is not unusual for samples collected in our system to show both 11.5 μm and 12.5 μm absorption bands. It is known that SiO is the primary silicon bearing species in the vapor when either SiO or SiO_2 is vaporized under reducing conditions.[10] Nevertheless, supersaturation is defined in terms of the partial pressure of a gas phase species in equilibrium with a solid phase. If the solid phase which actually nucleates is itself unstable at the temperatures at which nucleation occurs, then a thermodynamic formulation of the problem could be in serious error. Under such conditions, nucleation might easily be controlled by such kinetic considerations as which polymorph first forms a metastable phase even if this phase is not ultimately the most thermodynamically stable under the conditions of the experiment.[23,24] In fact, Ostwald[25] concluded that the most stable phase will generally not be the first to nucleate.
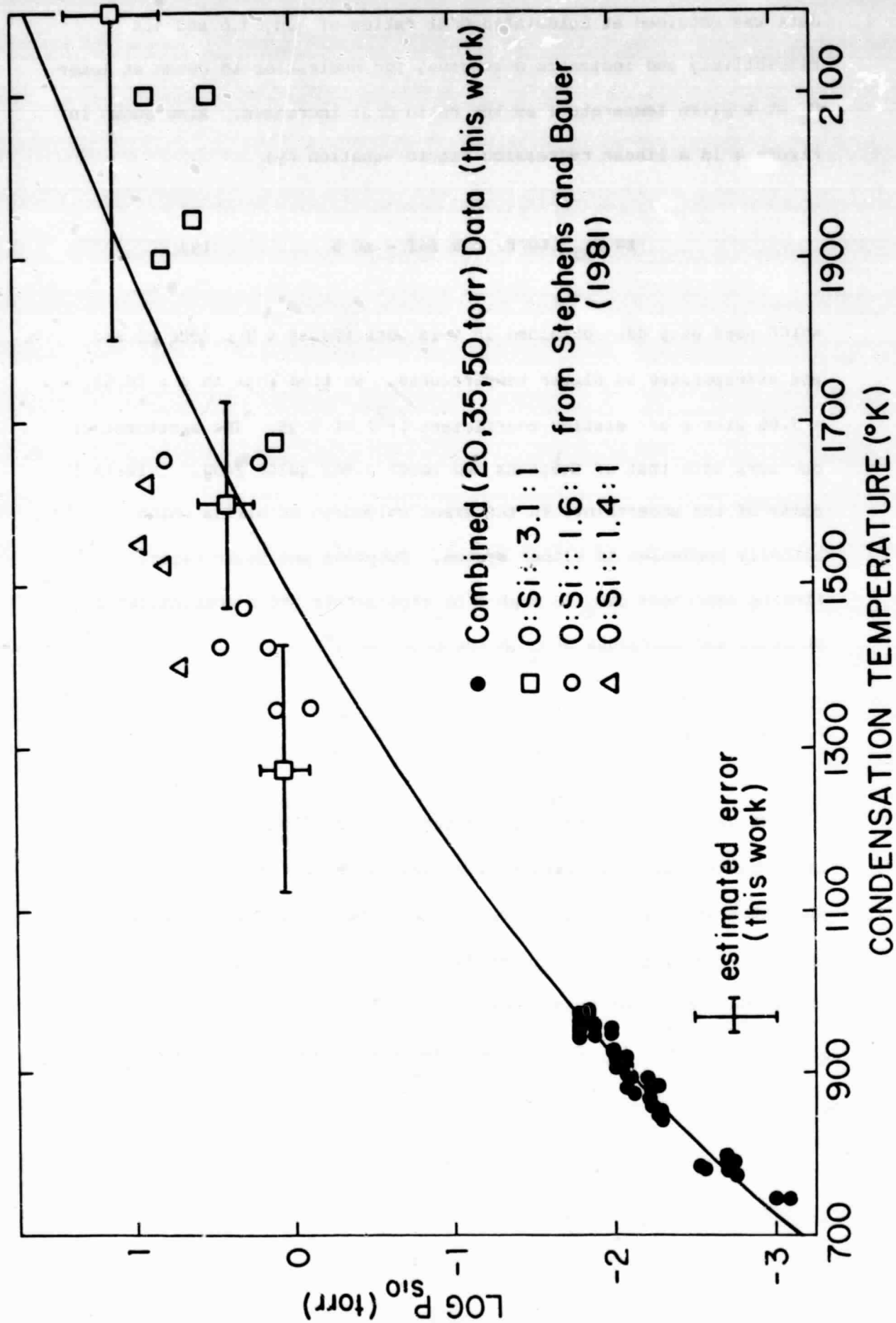
A further problem arises if one uses our values of γ, T and S in order to calculate n_c, the number of monomers in a "critical" sized cluster. This is given by standard Becker-Doring theory as

$$n_c = 32 \pi \gamma^3 V^2/3(KT \ln S)^3. \tag{8}$$

Typical values of n_c derived from our data indicate that the critical sized cluster at a temperature of 750K is the monomer. At 900K the critical nucleus becomes the dimer while at a temperature in excess of 950K n_c is the trimer. At such small values of n_c the applicibility of the liquid drop approximation upon which classical nucleation theory is based becomes extremely doubtful. This in turn leads one to doubt the validity of a calculation of γ based upon nucleation theory, even if the value derived seems reasonable, since nucleation theory itself may not be applicable to this sytem.

In light of the above arguments, it might seem more appropriate to report the results of nucleation experiments on very refractory species in the manner adopted by Bauer and co-workers.[1,26-28] They present plots for log P_c vs T_c of the conditions which yield avalanche nucleation. P_c is defined as the critical partial pressure of the condensing species (in torr) and T_c is the condensation temperature. Stephens and Bauer[6] have recently completed a study of the nucleation of SiO_x using a shock tube at ambient temperatures between ⌀ 1250 K and ⌀ 4000 K. Figure 5 is a plot of log P_c vs T_c under conditions of avalanche nucleation which combines our data (700 K < T < 1000 K) with that of Stephens and Bauer[6] in the range 1250 K $\leq$ T $\leq$ 2200 K. Their

207

Figure 5. Log P_{SiO} vs. Ambient Temperature. Shown is the Critical

Pressure (P_{SiO}) vs. Condensation Temperature at which avalanche

nucleation was detected in this work (filled circles) and in the shock

tube experiments of Stephens and Bauer[6] for oxygen to silicon ratios

of 3.1 (squares), 1.6 (open circles) and 1.4 (triangles). Also shown

is an exponential regression best fit to our data (correlation

coefficient of .95) extrapolated to that of Stephers and Bauer.[6]

Combined (20,35,50 torr) Data (this work)

☐ O:Si::3.1:1
☐ O:Si::1.6:1 from Stephens and Bauer
○ O:Si::1.6:1 (1981)
△ O:Si::1.4:1

estimated error (this work)

LOG P$_{SiO}$ (torr)

CONDENSATION TEMPERATURE (°K)

data was obtained at calculated O/Si ratios of 3.1, 1.6 and 1.4 respectively and indicates a tendency for nucleation to occur at lower P_c at a given temperature as the ratio O/Si increases. Also shown in Figure 4 is a linear regression fit to equation (9)

$$\ln P_{SiO}(torr) = b \ln T - \ln a \qquad (9)$$

which used only data obtained in this work (700 K < T < 1000 K) and was extrapolated to higher temperatures. We find that $\ln a = 70.52$, $b = 9.66$ with a correlation coefficient (r^2) of 0.95. The agreement of our work with that of Stephens and Bauer seems quite good. This is in spite of the uncertainty in the exact polymorph of silica which actually condenses in either system. Stephens and Bauer report finding amorphous SiO_2 in high O/Si experiments and a combination of Si metal and amorphous SiO_2 in low O/Si runs.[6]

V. CONCLUSIONS

We have demonstrated that controlled, reproducible nucleation experiments involving refractory oxides can be performed in the apparatus described in this report and that the nucleation of SiO is extremely sensitive to the temperature of the ambient gas. We have found that the vapor phase nucleation of SiO in H_2 yields the solid phase SiO_x (where X $\approx$ 1.5) rather than the thermodynamically favored product SiO_2. This is in agreement with the earlier work of Day and Donn.[5]

210

Analysis of our data within the framework of the Becker-Doring or Blander-Katz theories of homogeneous nucleation yield values for the surface free energy, γ, of our condensate of 500 ergs/cm^2 and 650 ergs/cm^2 respectively. This is within the range which could be expected of a silicate compound, the composition of which lies between that of amorphous silica and silicon metal. However, because of the difficulty in the formulation of a realistic definition of the supersaturation ratio, S, for a material which preferentially nucleates into a form which itself is thermodynamically unstable, standard theories of homogeneous nucleation which rely on thermodynamic arguments may not be applicable. In such a case, a kinetic theory of nucleation, such as that proposed by Bauer and Frurip,[26] may be the preferential way to describe the condensation process.

Finally, we find excellent agreement between our results, obtained at relatively low temperatures and high supersaturations, and those of Stephens and Bauer[6] obtained at much higher temperatures. Both experiments demonstrate that the vapor phase nucleation of SiO requires a very high degree of supersaturation.

References

1. Frurip, D. J. and Bauer, S. H., J. Phys. Chem., 81, 1001 (1977).

2. Tabayashi, K. and Bauer, S. H., in Proceedings of the 12th International Symposium on Shock Tubes and Waves, Jerusalem, July 16-19, 1979 (Magnes Press, The Hebrew University, Jerusalem, Israel), 409 (1979).

3. Katz, J. L., Mirabel, P., Sceppa, C. J., Virkler, T. L., J. Chem. Phys., 65, 382 (1976).

4. Becker, C., J. Chem. Phys., 72, 4579 (1980).

5. Day, K. L. and Donn, B. D., Astrophys. J., 222, L45 (1978).

6. Stephens, J. R. and Bauer, S. H., preprint (1981).

7. Hunten, D. M., Turco, R. P., Toon, O. B., J. Atmos. Sci., 37, (6), 1342 (1980).

8. Donn, B., Hecht, J., Khanna, R., Nuth, J., Stranz and Anderson, A. B., Surface Sci., 106, 576 (1981).

9. Hecht, J. and Nuth, J., Astrophys. J. (submitted).

10. Schick, H. L., Chem. Rev., 60, 331 (1960).

11. Van de Hulst, H. C., Light Scattering by Small Particles (Wiley, New York, 1957).

12. Philipp, H. R., J. Phys. Chem. Solids, 32, 1935 (1971).

13. Adamson, A. W., Physical Chemistry of Surfaces, 3rd Edition, (Wiley, New York, 1976) Chapter 8.

14. Blander, M. and Katz, J., J. Stat. Phys., 4, 55 (1972).

15. King, T. B., Trans. Soc. Glass Technol., 35, 241 (1951).

16. Kosakevitch, P., Rev. de Me't., 46, 505 (1949).

17. Brunauer, S., Kantro, D. L. and Weise, C. H., Can. J. Chem., $\underline{34}$, 1483 (1956).

18. Elliott, J. F., Gleiser, M. and Ramakrishna, V., Thermochemistry for Steelmaking (Addison-Wesley, Reading, Mass., 1963).

19. Blander, M. and Katz, J., Geochim. et Cosmochim, Acta, $\underline{31}$, 1025 (1967).

20. Bruce, R. H., in Science of Ceramics, Volume 2, ed. G. H. Stewart (Academic Press, London, 1965), Chapter 24.

21. Ritter, E., Optica Acta, $\underline{9}$, 197 (1962)

22. Ritter, E., Vakuum Technik, $\underline{21}$, 42 (1972)

23. Volmer, M., Kinetik der Phasenbildung (Theodor Steinkopff, Dresden, 1939), Chapter 5.

24. Hirth, J. P. and Pound, G. M., Condensation and Evaporation Nucleation and Growth Kinetics (Pergamon Press, Oxford, 1963), p. 53.

25. Ostwald, W., Lehrb. Allg. Chem. $\underline{2}$, 2 (1896).

26. Freund, H. J. and Bauer, S. H., J. Phys. Chem. $\underline{81}$, 994 (1977).

27. Frurip, D. J. and Bauer, S. H., J. Phys. Chem. $\underline{81}$, 1007 (1977).

28. Bauer, S. H. and Frurip, D. J., J. Phys. Chem. $\underline{81}$, 1015 (1977).

Chapter 6

The Nucleation and Infrared Spectra of Amorphous Mg-SiO Smokes

Binary nucleation processes are expected to be of considerable importance in the chemically complex astrophysical environments in which interstellar grains are likely to form (Donn, 1976; Donn et al, 1981). Unfortunately, theoretical treatment of this problem is much more difficult than for the case of homogeneous nucleation. Consequently, few theories of binary nucleation exist (Wilemski, 1975 a,b; Reiss, 1950; Hirschfelder, 1974) and these have usually been developed to treat nucleation in relatively low temperature systems.

Since most theories of binary nucleation build upon the classical theory of homogeneous nucleation, all of the problems inherent in this framework are intensified. This is especially true for the vapor phase nucleation of highly refractory species (Stephens and Bauer, 1981; Nuth and Donn, 1981a). It is interesting to note that many of the treatments of the formation of grains which have appeared in the astronomical literature (Draine, 1981; Yamamoto and Hasegawa, 1977; DeGuchi, 1980) have been based upon homogeneous nucleation theory.

Few quantitative studies of the binary nucleation of refractory materials have been published (Stephens and Bauer, 1981) although the work of Day and Donn (1978) indicates that considerable supersaturation is necessary before condensation occurs in such

214

systems. In a previous study (Nuth and Donn, 1981a; hereafter Paper I) we reported measurements of the vapor phase nucleation of SiO in H_2 gas as a function of temperature for the range 750K < T < 1000K. We report here measurements of the binary nucleation from the vapor, of a Mg - SiO - H_2 system in the range 750K < T < 1010K.

Section II presents a brief description of the apparatus used in this study as well as an outline of our experimental procedure. Section III presents the experimental data for the nucleation of the Mg-SiO-H_2 system as compared to that for the "homogeneous" nucleation of SiO-H_2 (Paper I). Section IV presents the infrared spectra of representative samples of condensate both as collected and after annealing at 1000K and 1250K. Section V discusses the relevance of this study to the condensation of refractory grains in various astrophysical environments.

II Experimental Apparatus and Procedure

The experimental apparatus used in this study was similar to that reported in Paper I with several relatively minor modifications. Mg was introduced into the furnace system by placing a crucible containing the metal (and a thermocouple) within the furnace. The temperature of the ambient gas therefore controlled the partial pressure of Mg within the furnace. Several methods to independently vary the Mg pressure were tried, but all failed to produce a uniformly mixed vapor and reproducible results (Work to overcome this limitation is in progress).

The Mg partial pressure within the system could be monitored independently by measuring the strength of the Mg 285.2 nm resonance line in absorption. Because the line was saturated under most of the conditions of the experiment only relatively qualitative information could be obtained. This did show however that the partial pressure of Mg within the furnace was reproducibly controlled by the furnace temperature. The actual Mg pressure was calculated empirically using the data in the Handbook of Chemistry and Physics (53rd Edition). This is plotted in Figure 1. As discussed in Paper 1, the partial pressure of SiO in the region of condensation was determined from the thermodynamic relationship given by Schick (1960) combined with a suitable model for the expansion of the SiO vapor from the crucible.

The experimental procedure used in this study differed in two major respects from that reported in Paper I. First, in our previous study, the temperature of the SiO evaporator was held approximately constant while the temperature of the ambient gas was varied to initiate or halt condensation. In this study, because of the dependence of the Mg partial pressure on the temperature of the ambient gas, we attempted to hold the furnace temperature constant and varied the temperature of the SiO crucible. This procedure tends to increase the error in the measurement of the partial pressure of SiO necessary for nucleation since it increases the uncertainty in the temperature of the SiO crucible at the time avalanche nucleation begins.

216

Figure 1. The partial pressure of magnesium as a function of

temperature.
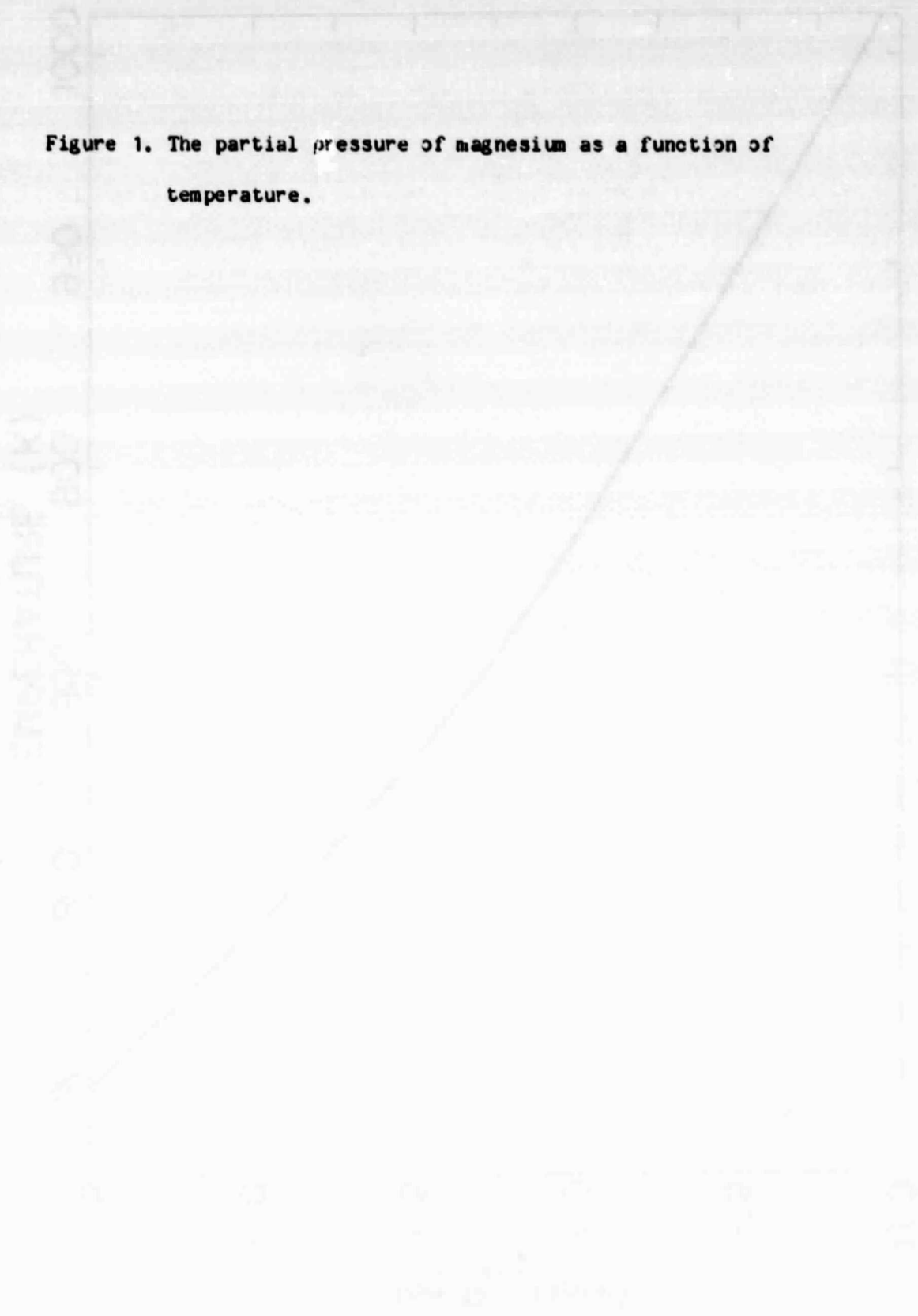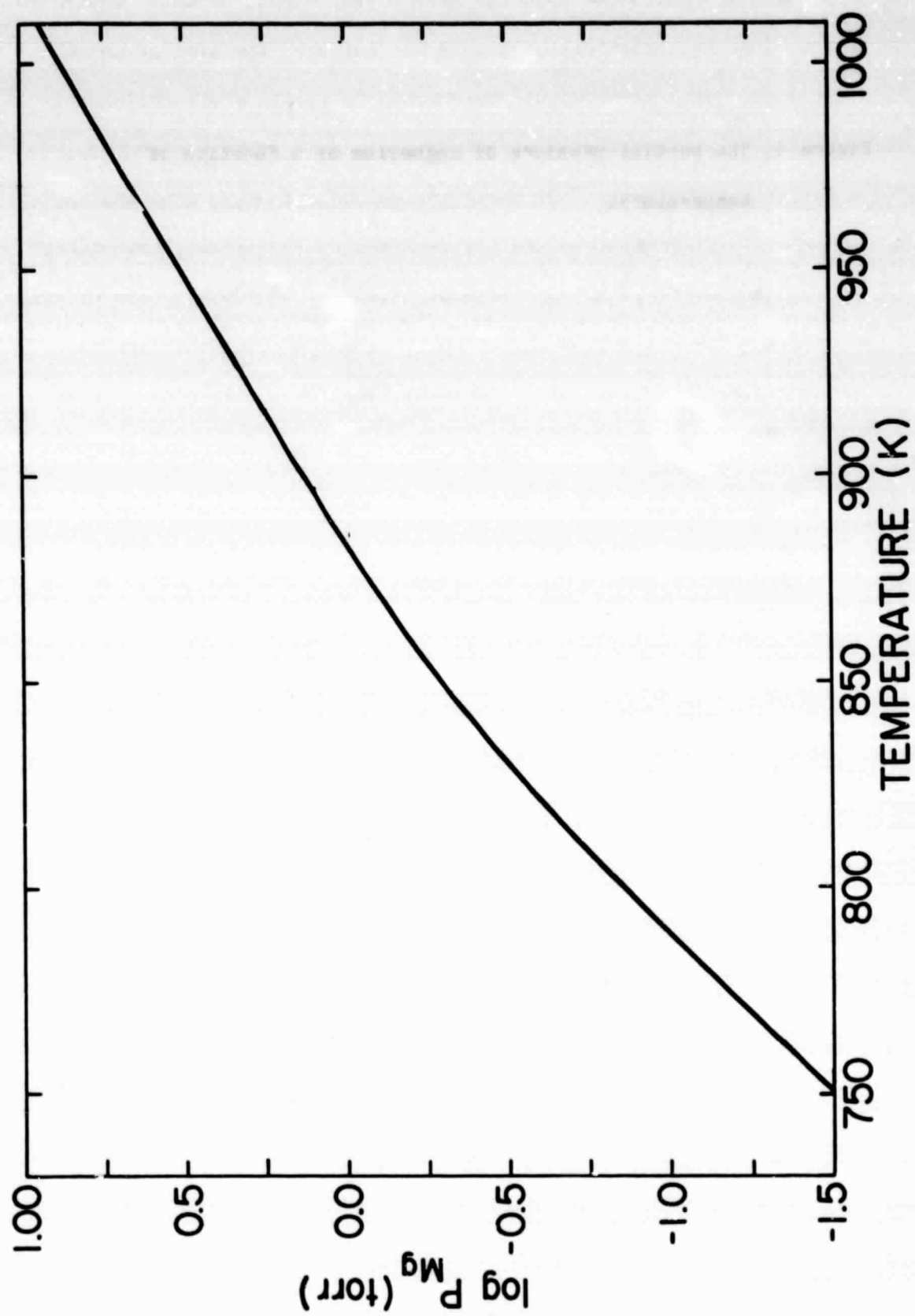
Second, because we used the Xe Arc lamp – Monochromater system to monitor the Mg concentration within the furnace, the time at which nucleation began or ended was determined by eye from the presence or absence of light scattered at 90° to the beam. As in the previous study, light scattered from these grains was extremely blue and 100% polarized. Experiment showed that for the Mg-SiO system, this method was, on the average, as sensitive to the onset of condensation as was monitoring the extinction of the newly formed particles at 200 nm. Unfortunately, this technique certainly was neither as precise nor as quantitative as that used in the previous study (Paper I). All runs were done at a total pressure of 35 torr of H_2.

III Results

Data collected in this study was analyzed using the same correction factors determined from our previous work (see the discussion in section III of Paper I). Figure 2 is a plot of the partial pressure of SiO at which avalanche nucleation occurs as a function of ambient temperature for the condensation of "pure" SiO (2a) and for the Mg-SiO system (2b).

Similarly, Figure 3 is a plot of the supersaturation of SiO (with respect to SiO solid) necessary to initiate avalanche nucleation for the $SiO-H_2$ system (Figure 3a) and for the $Mg-SiO-H_2$ system (Figure 3b). In both of these plots, it is obvious that although the presence of Mg lowers the required SiO partial pressure to induce avalanche nucleation at temperatures less than ~ 900-950K, it appears that Mg is

219

Figure 2a. The partial pressure of SiO at which avalanche nucleation is observed in the $SiO-H_2$ system as a function of the temperature of the ambient gas.

$$P_{SiO} = 2.36 \times 10^{-31} \, T^{9.66}$$

$$(r^2 = 0.95)$$

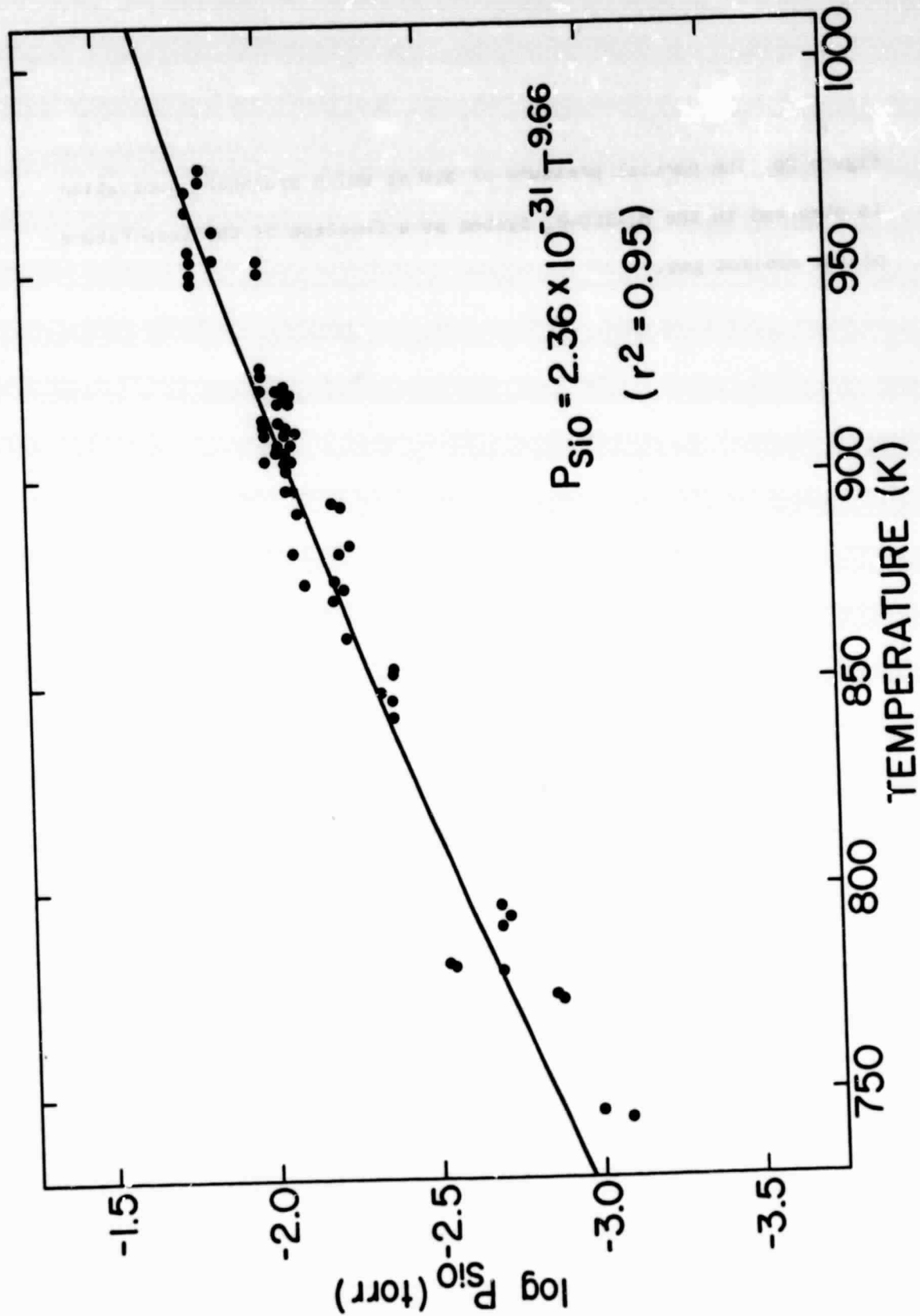log P_{SiO} (torr)

TEMPERATURE (K)

Figure 2b. The partial pressure of SiO at which avalanche nucleation is observed in the $Mg-SiO-H_2$ system as a function of the temperature of the ambient gas.

$P_{SiO} = 2.36 \times 10^{-31} \, T^{9.66}$

TEMPERATURE (K)

1000 950 900 850 800 750

log P_{SiO} (torr)

-1.5 -2.0 -2.5 -3.0 -3.5

Figure 3a. The supersaturation of SiO vapor at which avalanche nucleation is observed in the $SiO-H_2$ system as a function of the temperature of the ambient gas.
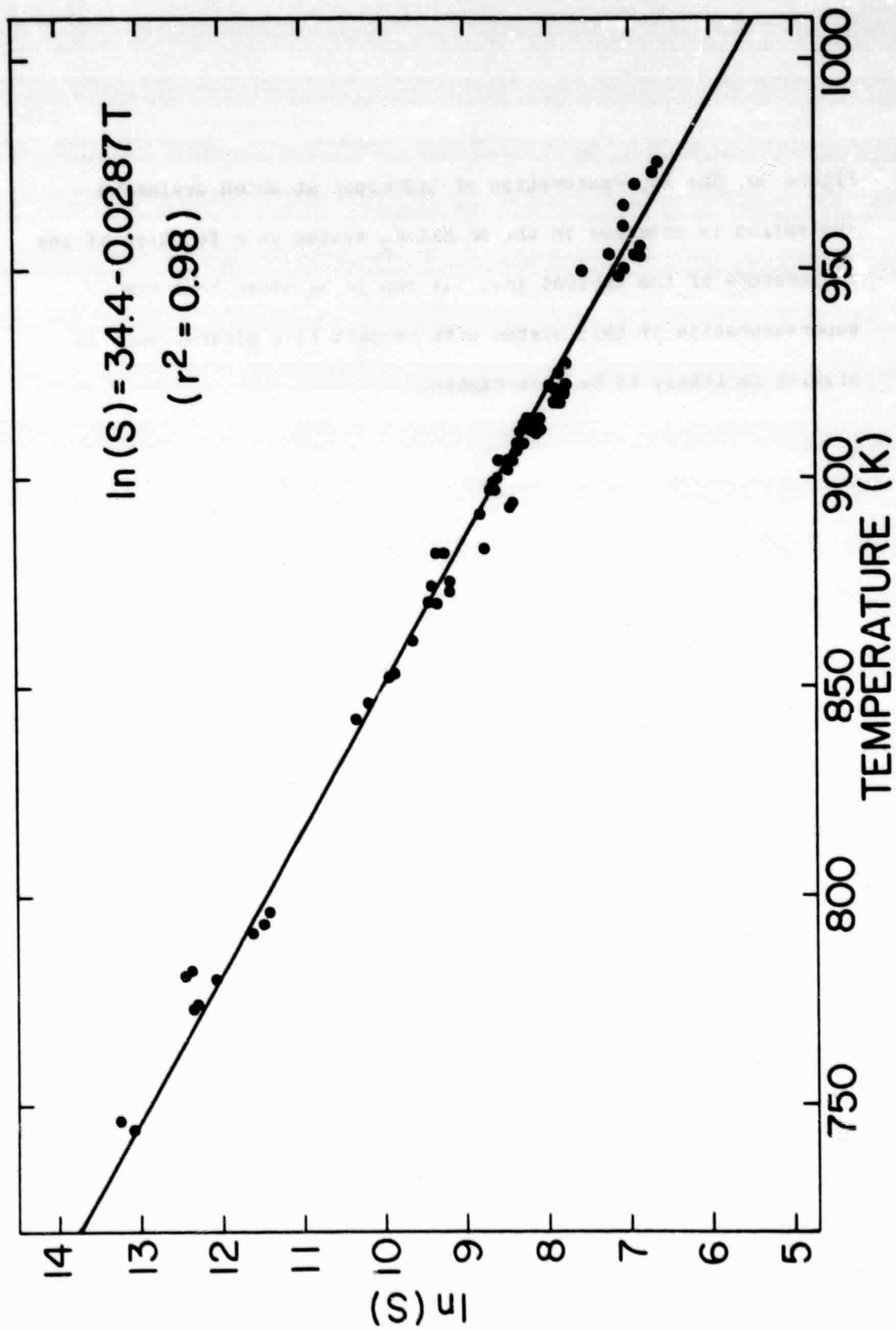
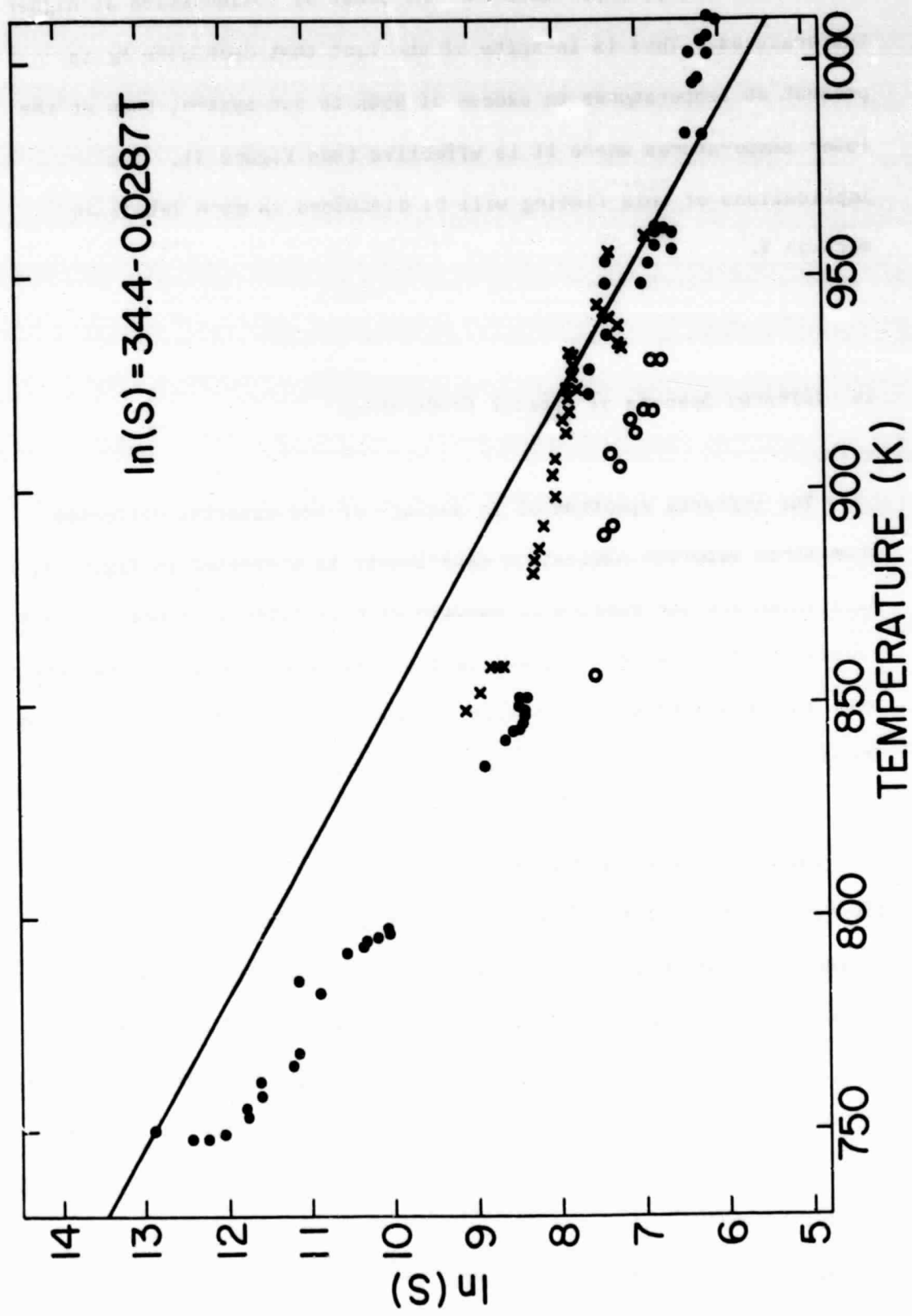$\ln(S) = 34.4 - 0.0287\,T$
$(r^2 = 0.98)$

Figure 3b. The supersaturation of SiO vapor at which avalanche nucleation is observed in the $Mg-SiO-H_2$ system as a function of the temperature of the ambient gas. It should be noted that the supersaturation of this system with respect to a mineral such as olivine is likely to be much higher.

$\ln(S) = 344 - 0.0287 T$

of little, if any, importance for the onset of condensation at higher temperatures. This is in spite of the fact that much more Mg is present at temperatures in excess of 950K in our system, than at the lower temperatures where it is effective (see Figure 1). The implications of this finding will be discussed in more detail in section V.

IV Infrared Spectra of Typical Condensates

The infrared spectrum of an average of the material collected from three seperate nucleation experiments is presented in Figure 4. Also shown are the spectra of samples of this material annealed under vacuum for 1, 2, 4, 8, 16.5 and 30 hours at 1000K. All spectra were obtained by dispersing the sample in finely ground KBr powder and then pressing the mixture at 10,000 psi into a clear disk.

Figure 5 shows the spectrum of the material collecte. when pure SiO vapor was condensed in H_2 gas (Paper I). Also shown in Figure 5 is the spectrum of a sample of Si_2O_3 smoke annealed at 1250K for 30 minutes. It should be noted that the condensation of SiO vapor in 35 torr of H_2 gas at temperatures in excess of 750K produced a mixture of amorphous SiO_2 and Si_2O_3 grains (Paper I). This is obvious from the spectrum of the material since it contains peaks at both 11.4 and 12.5 microns as well as the more familiar peaks near 10 and 20 microns. The peak at 11.4 microns (attributed to Si_2O_3) disappears when the

Figure 4. The infrared spectrum of an average Mg-SiO smoke, as well as the spectra of smoke samples annealed in vacuo at 1000K for 1, 2, 4, 8, 16.5 and 30 hours.

A. Unannealed amorphous magnesium silicate smoke

B. Smoke annealed at 1000K for 1 hour

C. Smoke annealed at 1000K for 2 hours

D. Smoke annealed at 1000K for 4 hours

E. Smoke annealed at 1000K for 8 hours

F. Smoke annealed at 1000K for 16.5 hours

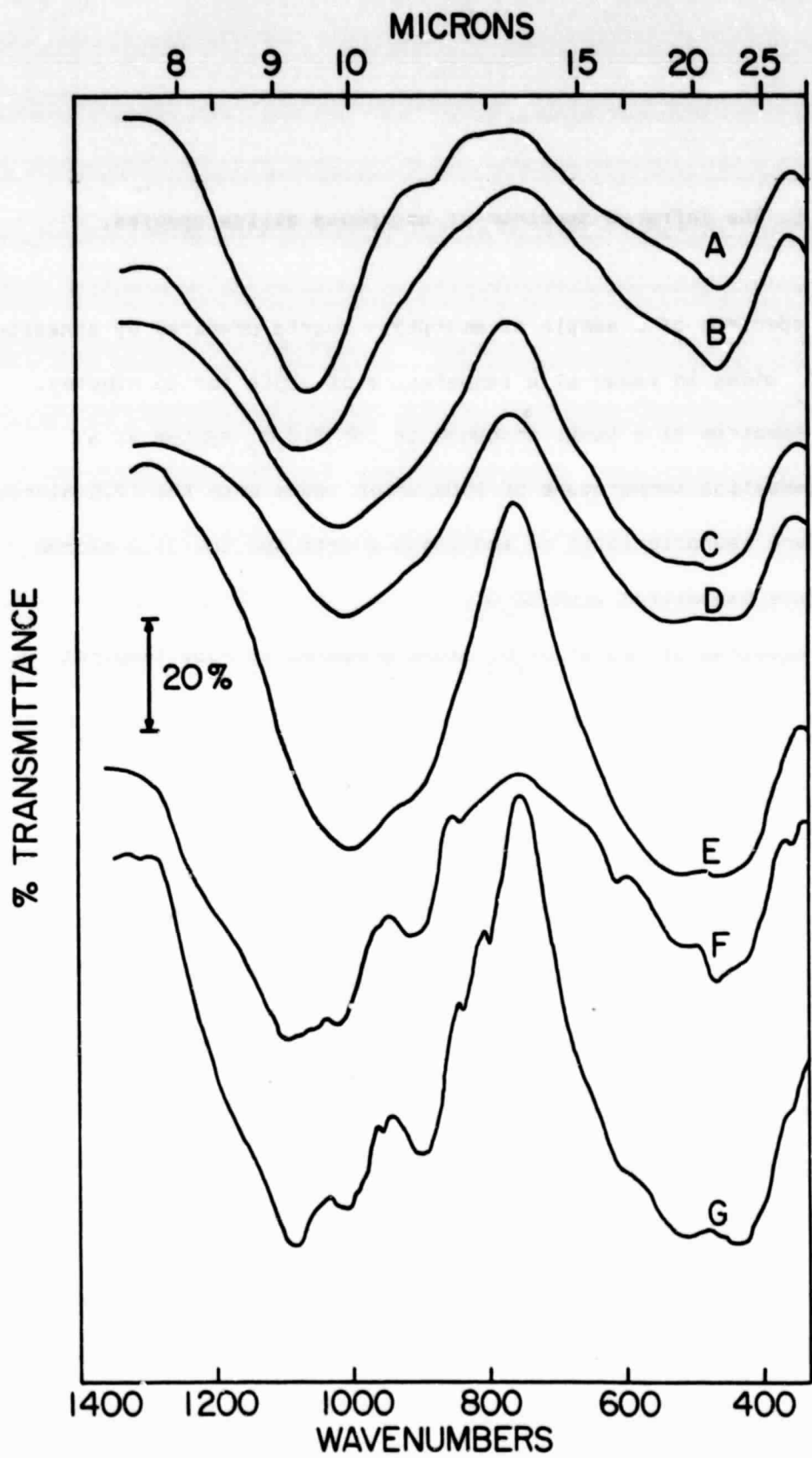G. Smoke annealed at 1000K for 30 hours

Figure 5. The infrared spectrum of amorphous silica species.

A. The spectrum of a sample of amorphous quartz prepared by annealing Si_2O_3 smoke in vacuo at a temperature of 1250K for 30 minutes.

B. The spectrum of a smoke produced in the $SiO-H_2$ system at a condensation temperature of 750K which shows both the 12.5 micron feature characteristic of amorphous quartz and the 11.2 micron feature associated with Si_2O_3.

C. The spectrum of 'pure' Si_2O_3 smoke prepared at room temperature.
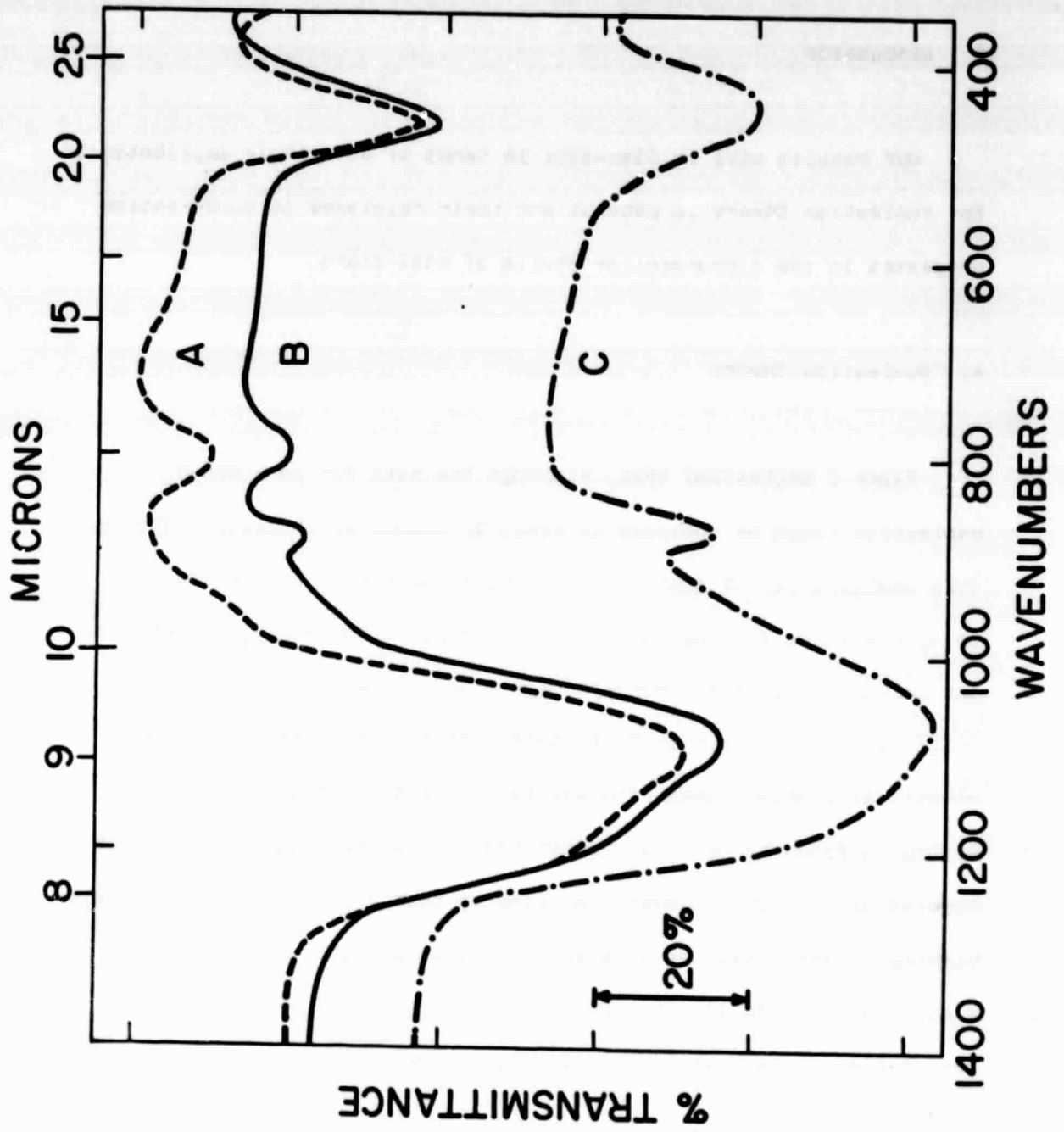
sample is annealed in vacuum for ∼ 30 minutes at 1250K. This is indicative of the transformation of the Si_2O_3 into amorphous quantz.

V   Discussion

Our results will be discussed in terms of both their implications for nucleation theory in general and their relevance to condensation processes in the circumstellar shells of cool stars.

a. Nucleation Theory

Paper I emphasized that, although the data for pure $SiO-H_2$ nucleation could be analy?ed in terms of Classical Nucleation Theory, this analysis led to some logical inconsistencies. For instance, using the value for the surface free energy of the $(SiO)_x$ condensate, one calculates that the monomer, dimer and trimer constitute the critical sized cluster at 750K, 900K, and 950K respectively. An additional problem stems from the fact that the condensate in this system is found to be Si_2O_3 rather than the thermodynamically stable species SiO_2.   This causes a problem in that a logical and physically meaningful definition of supersaturation is difficult to formulate since the usual definition involves the free energy of formation of the stable species, while the application refers to the clusters which actually nucleate.

Because theories of binary nucleation are generally only extentions of Classical Homogeneous Nucleation Theory, we might expect

similar problems to emerge if such theories were applied to our results. Unfortunately, additional problems arise since theories of binary nucleation are really formulated to account for the precipitation of nearly ideal liquid <u>mixtures</u> from vapors of two completely miscible components. In such a system it is typical that <u>both</u> species are at least slightly supersaturated. In our system, although SiO is always supersaturated, the pressure of magnesium never exceeds the equilibrium vapor pressure. In fact, the magnesium concentration most likely remains below the equilibrium value due to delays inherent in the diffusion of the vapor from the source into the region of condensation.

Furthermore, we actually condense an amorphous magnesium silicate (Day and Donn, 1978) rather than a mixture of magnesuium metal and silica. In this sense, it would be more appropriate to use a theory of nucleation developed for systems in which the monomer form of the condensate must first appear via chemical reaction in the vapor. Such a theory has been developed by Katz and Donohue (1982). In order to apply this theoretical treatment to our data we need to know the surface tension of our clusters as well as various reaction rates for the formation of our "monomers" from a magnesium rich, SiO vapor diluted in H_2. Unfortunately we don't know the exact composition of our "critical" clusters. Furthermore, we really don't even know the exact composition of the important vapor phase monomers - i.e. Mg-SiO, Mg-$(SiO)_2$, Mg-SiO-Mg, SiO-Mg, etc. - which condense. Although we do plan to study this problem in the near future using a quadropole mass spectrometer to monitor the pre-nucleation vapor composition as a

235

function of temperature, pressure and initial chemical composition, we can now simply state the qualitative implications of our results.

Inspection of Figures 2 and 3 indicates that the presence of magnesium vapor reduces the concentration of SiO needed to initiate avalanche nucleation for temperatures less than about 925K. This is to be expected if Mg-SiO clusters are important nucleating species. At temperatures in excess of 925K, such clusters apparently become less stable than those involving only SiO, even though the concentration of magnesium in the vapor is 2 or 3 orders of magnititude greater than that of SiO (see Figs. 1 and 2). Nucleation under such conditions is therefore initiated by the precipitation of $(SiO)_x$ from the vapor.

Inspection of the infrared specturm of our "magnesium silicate" (Figure 4) shows substantial differences from that of Si_2O_3 smoke (Figure 5) nucleated from a SiO-H_2 system (Paper I). This indicates that although formation of $(SiO)_x$ clusters may initiate the nucleation process in our Mg-SiO-H_2 system at high temperatures, magnesium is apparently still incorporated into the grains during the growth process.

b. Astrophysical Implications

These results have two major implications with regard to the formation of refractory grains in the regions surrounding cool stars. First, condensation in such sources may be initiated by the formation

236

of $(SiO)_x$ clusters, although the composition of the resultant grains would then be subject to modifications by subsequent reaction with other refractory constituents also present in the gas. Second, it may be possible to observe distinct chemical differences in the infrared spectra of grains newly formed in stellar sources, especially compared to those grains which may have undergone significant reprocessing such as those in molecular clouds. These implications will be discussed in more detail below.

Grain Formation: It has been shown that the vibrational population of SiO molecules in circumstellar regions is characterized by a temperature significantly below the kinetic temperature of the ambient gas (Nuth and Donn, 1981b). It is well known that the rates of gas phase reactions are very sensitive to the vibrational states of the reactants (Polanyi, 1973; Bartozek et al, 1981). It is quite possible, therefore that nucleation in stellar sources could still be initiated by Mg-SiO clusters if such clusters could be further stabilized by radiative cooling. Of course, there is the additional possibility that Fe-SiO or any number of combinations of the more abundant refractory elements might also be important sources of condensation nuclei. This possibility can however be checked by laboratory studies similar to those reported in this work.

Infrared Observations: Figure 6 is the spectrum of OH26.5 + 0.6 from the work of Forrest et al (1978) taken in April/May 1975 and again May/June 1976. Several points should be noted. First, in the spectrum obtained in April/May 1975, it is possible to identify minima

237

Figure 6. The infrared spectrum of OH 26.5 + 0.6 obtained over a two year period after an infrared brightening (Forrest et al.,1978) and which shows features at 11.2, 12.5, 18-19, 20 and 22-23 microns suggestive of the features in Si_2O_3, amorphous quartz and partially annealed Mg-SiO smokes.

OH 26.5 + 0.6

• May / June 1976
• April / May 1975

$\lambda \ (\mu)$

$F_\lambda \ (W/cm^2\mu)$
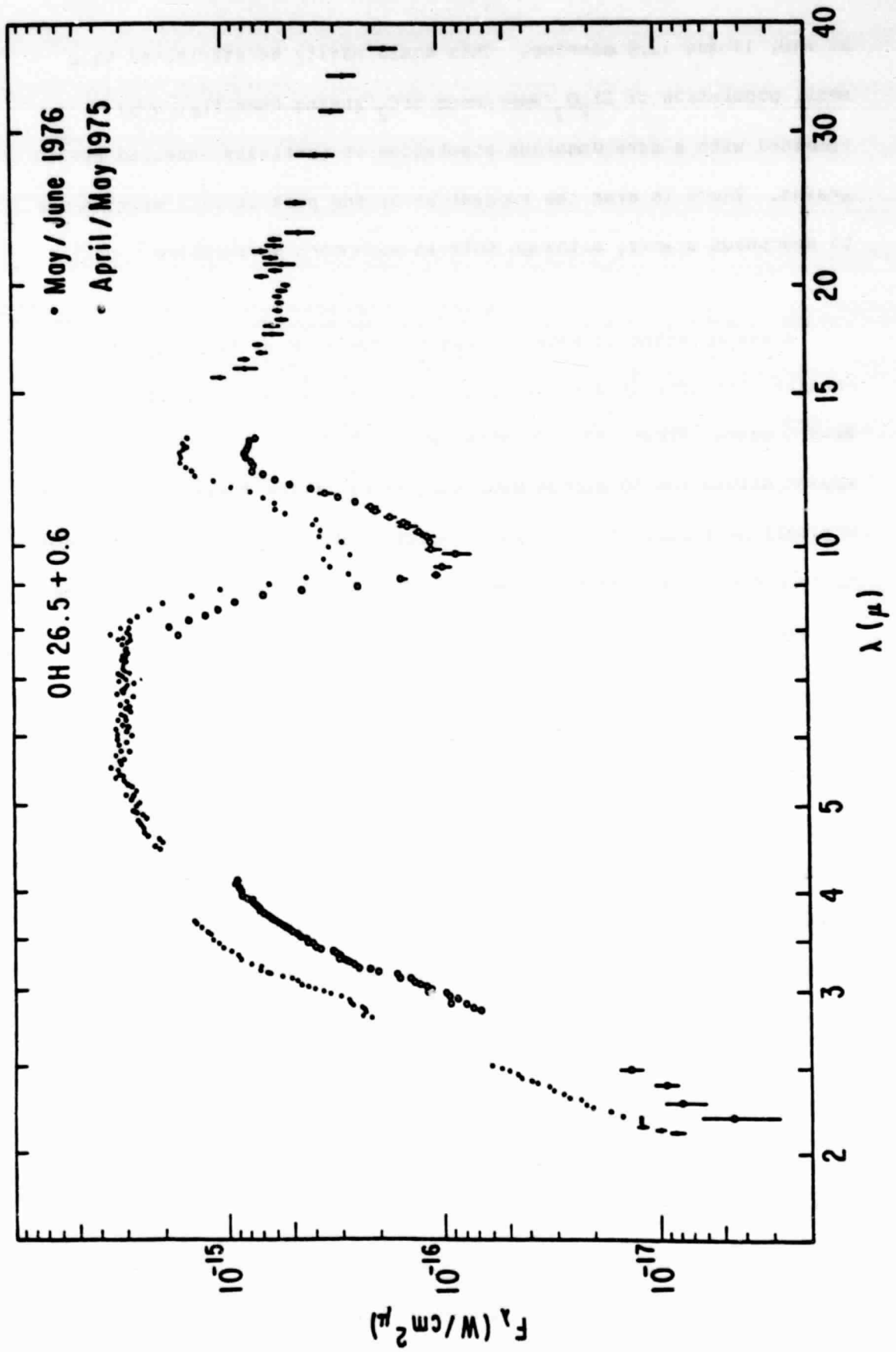
at ~10, 11 and 12.5 microns. This could easily be attributed to a small population of Si_2O_3/amorphous SiO_2 grains (see Figure 5) combined with a more numerous population of partially annealed Mg-SiO grains. There is even the suggestion of the peak at ~9.2 microns due to amorphous quantz, although this is much more speculative.

A second point to note is that the spectrum of this object changes with time in a manner suggestive of the annealing of our Mg-SiO smoke (Figure 4). In other words, definite structure begins to appear within the 10 micron band suggestive of the formation of a more crystalline solid. The irregular scatter in this spectrum is not due to random noise but is real (Merrill, 1981) and due to the pointwise procedure used to obtain the measurements.

The third interesting point is the similarity of the 16-25 micron spectrum of this object to that of our amorphous magnesium silicate. OH26.5 + 0.6 may show weak features at ~18-19, 20 and ~22-23 microns. At least two of these components can be reproduced in the laboratory (Figures 4 and 5). Future experiments using additional condensible species (i.e. Fe or Ni) may allow other residuals within these rather broad features to be better identified.

The previous remarks indicate that much more information about the chemical nature of the grains in circumstellar sources can be obtained from infrared observations than has hitherto been expected. In this regard, high resolution continuous spectra in the 8-13 and 16-25 micron regions of grain forming circumstellar shells could be

240

especially interesting since such material represents new interstellar grains which have undergone little reprocessing or annealing. Comparison with the chemical state of "average" interstellar material might reveal the process by which such fresh grains are annealed, homoginized and mixed to yield the normal population of "silicates" seen in dense clouds.

Even in such homogenized materials it should be noted that some structure within the 10 micron feature is evident in the literature. For instance, the spectrum of the Trapezium shows a peak near 11 microns (Forrest, Gillett and Stein, 1975) while that of the BN-KL complex shows a definite feature at 12.5 microns as well as possible structure within the 10 micron peak itself (Gillett and Forrest, 1973).

VI Conclusions

We have demonstrated that the nucleation barrier in the system $Mg-SiO-H_2$ at temperatures less than $\sim 925K$ is lower than that for $SiO-H_2$ alone. At temperatures in excess of $\sim 925K$ however, nucleation in the $Mg-SiO-H_2$ system is unaffected by the presence of magnesium. This could have interesting applications to the problem of condensation in the atmospheres of cool stars.

We have also demonstrated an interesting correspondence between small residuals seen in the infrared spectra of various astronomical sources (8 microns $< \lambda < 25$ microns) and the spectra of specific

241

laboratory condensed silicates. We suggest that more careful infrared observation of such sources could reveal valuable information about the chemical state of the grains. This could in turn lead to a better understanding of the processes which tranform newly formed dust into the relatively homogeneous material observed in the general interstellar medium.

References

Bartoszek, F. E., Blackwell, B. A., Polanyi, J. C. and Sloan, J. J.,
1981, JCP, $\underline{74}$, 3400.

Day, K. L. and Donn, B., 1978, Ap. J., $\underline{222}$, L45.

Deguchi, S., 1980, Ap. J., $\underline{236}$, 567.

Donn, B., 1976, Mem. Soc. Roy. Sci. Liege, Ser. 6, Tome IX, 499.

Donn, B., Hecht, J., Khanna, R., Nuth, J., Stranz and Anderson, A.,
1981, Surface Sci. $\underline{106}$, 576.

Draine, B. T., 1981, in Physical Processes in Red Giants, I. Iben and
A. Renzini (eds.), (D. Reidel, Boston, 1981) p. 317.

Forrest, W. F., Gillett, F. C., Houck, J. R., McCarthy, J. F.,
Merrill, K. M., Pipher, J. L., Puetter, R. C., Russell, R. W.,
Soifer, B. T. and Willner, S. P., 1978, Ap. J. $\underline{219}$, 114.

Forrest, W. F., Gillett, F. C., and STein, W. A., 1975, Ap. J., $\underline{195}$,
423.

Gillett, F. C. and Forrest, W. F., 1973, Ap. J., $\underline{179}$, 483.

Handbook of Chemistry, (53rd Ed.) 1972-1973, R. C. Weast (Ed. in
Chief), (CRC Press, Cleveland, 1972) p. D-173.

Hirschfelder, J. O., 1974, JCP, $\underline{61}$, 2690.

Katz, J. L. and Donohue, M. D., 1982, J. Coll. Interfac. Sci. (in
press).

Merrill, K. M., 1981, Personal Communications.

Nuth, J., and Donn, B., 1981a, JCP, 1981, (Submitted).

Nuth, J., and Donn, B., 1981b, Ap. J. $\underline{246}$, 925.

Polanyi, J. C., 1973 in <u>Molecules in the Galactic Environment</u>, M.

Gordon and L. Snyder (Eds.), (J. Wiley, and Sons, New York,, 1973)

p. 330.

Reiss, H., 1950, JCP, <u>18</u>, 840.

Schick, H., 1960, Chem. Rev., <u>60</u>, 331.

Stephens, J. R., and Bauer, S. H., 1981, preprint.

Wilemski, G., 1975a, JCP, <u>62</u>, 3763.

Wilemski, G., 1975b, JCP, <u>62</u>, 3772.

Yamamoto, T., and Hasegawa, H., 1977, Prog. Theor. Phys., <u>58</u>, 816.